ADVANCED MASTERS IN STRUCTURAL ANALYSIS
OF MONUMENTS AND HISTORICAL CONSTRUCTIONS

Master's Thesis

Diogo Coutinho

Seismic Analysis and Strengthening of Mallorca Cathedral.

This Masters Course has been funded with support from the European Commission. This publication reflects the views only of the author, and the Commission cannot be held responsible for any use which may be made of the information contained therein.

Spain | 2010

DECLARATION

Name: Diogo Simões do Amaral Coutinho

Email: diogo.coutinho@fe.up.pt

Title of the Msc Dissertation: Seismic Analysis and Strengthening of Mallorca Cathedral

Supervisor: Professor Pere Roca

Year: 2010

I hereby declare that all information in this document has been obtained and presented in accordance with academic rules and ethical conduct. I also declare that, as required by these rules and conduct, I have fully cited and referenced all material and results that are not original to this work.

I hereby declare that the MSc Consortium responsible for the Advanced Masters in Structural Analysis of Monuments and Historical Constructions is allowed to store and make available electronically the present MSc Dissertation.

University: Universitat Politècnica de Catalunya

Date: 13th of July, 2010

Signature: 

ACKNOWLEDGEMENTS

I am grateful to my supervisor, Professor Pere Roca, not only for the conditions he provided me as well as for his support guiding the works carried out in order to produce this thesis. In the same way, I want to thank all the professors that lectured during the coursework in Czech Technical University, in Prague. I express also my gratitude to Giulia Bettiol for her technical support.

I also want to thank the SAHC Consortium for providing me financial support during the whole master course.

I am also thankful to all the friends in Prague and Barcelona, including my colleagues in the Czech Technical University and in Technical University of Catalonia, for all the friendship and support, which greatly contributed to the enriching experience that was to attend this master course during the last year.

I want to thank also my family and friends in Portugal for the constant support and incentive despite the distance.

ABSTRACT

Seismic Analysis and Strengthening of Mallorca Cathedral

Due to the complexity associated with the seismic action, as well as the dynamic properties of the structures, the design of historical buildings only took into account static actions. Depending on the seismicity of the site, the buildings are characterized by more or less constructive details adopted in order to prevent important damages due to seismic action.

Therefore, the seismic analysis of Mallorca Cathedral is carried out in the present work. The typical damages arising from seismic activity in historical buildings are caused by single architectonic parts that are characterized by an autonomous structural behaviour than the rest of the building. These local mechanisms, which are likely to develop during an earthquake, are individualized with respect to Mallorca Cathedral within this thesis.

The seismic analysis of Mallorca Cathedral comprises the individual analysis of each one of the considered local mechanisms. The nonlinear structural behaviour is obtained through limit analysis and the performance point is obtained though the capacity spectrum method. The results obtained for each local mechanism are its safety condition and, in the case of the safety being assured, the damage level that may be expected. A specific procedure developed for the analysis of historical structures that is recommended in the Italian code is used.

The seismic demand of Mallorca Cathedral considered within this thesis corresponds to several spectrums obtained from the European and Spanish codes and the detailed seismic hazard evaluation of the cathedral carried out in a previous work. This evaluation comprised deterministic and probabilistic estimations of the seismic action that may be expected in the site.

In order to reduce the damage level or to assure the safety of the local mechanisms, strengthening solutions are proposed in order to improve the seismic behaviour of Mallorca Cathedral. The main principles and criteria for conservation and restoration of historical structures are respected.

RESUMEN

Análisis Sísmico y Reforzamiento de la Catedral de Mallorca

Debido a la complejidad asociada a la acción sísmica, así como a las propiedades dinámicas de las estructuras, el diseño de edificios históricos sólo ha tenido en cuenta las acciones estáticas. Dependiendo de la sismicidad del sitio, los edificios se caracterizan por detalles constructivos más o menos adoptados para prevenir daños importantes debido a la acción sísmica.

Por consiguiente, en el presente trabajo se realiza el análisis sísmico de la Catedral de Mallorca. Los daños típicos derivados de la actividad sísmica en edificios históricos son causados por elementos arquitectónicos aislados que se caracterizan por un comportamiento estructural autónomo del resto del edificio. Estos mecanismos locales, que son propensos a desarrollarse durante un sismo, se individualizan en la Catedral de Mallorca en el curso de los estudios realizados en esta tesis.

El análisis sísmico de la Catedral de Mallorca incluye el análisis individual de cada uno de los mecanismos locales considerados. El comportamiento estructural no lineal se obtiene mediante análisis límite y el punto de desempeño se obtiene a través del método del espectro de capacidad. Los resultados obtenidos para cada mecanismo local son su condiciones de seguridad y, si la seguridad está garantizada, el nivel de daño que se puede esperar. Se utilizó un procedimiento desarrollado específicamente para el análisis de las estructuras históricas que está presente en la norma Italiana.

La demanda sísmica de la Catedral de Mallorca considerada en este trabajo corresponde a varios espectros obtenidos en la norma Europea y Española, y en una evaluación detallada de la peligrosidad sísmica de la catedral llevada a cado en un trabajo anterior. Esta evaluación incluye estimaciones determinísticas y probabilísticas de la acción sísmica que puede esperarse en el sitio.

Con el fin de reducir el nivel de daño o para garantizar la seguridad de los mecanismos locales, se proponen soluciones de reforzamiento para mejorar el comportamiento sísmico de la Catedral de Mallorca que respeten los principios y criterios fundamentales para la conservación y restauración de estructuras históricas.

RESUMO

Análise Sísmica e Reforço da Catedral de Maiorca

Devido à complexidade associada à acção sísmica, bem como às propriedades dinâmicas das estruturas, o projecto de edifícios históricos considerava somente acções estáticas. Dependendo da sismicidade do local, os edifícios são caracterizados por mais ou menos pormenores construtivos adoptados de forma a prevenir danos importantes devido à acção sísmica.

Assim, neste trabalho é realizada uma análise sísmica da Catedral de Maiorca. Os danos típicos em edifícios históricos decorrentes da actividade sísmica são causados por partes arquitectónicas singulares, caracterizadas por um comportamento estrutural autónomo do resto do edifício. Estes mecanismos locais, com possibilidades de se desenvolverem durante a ocorrência de um sismo, são individualizados na Catedral de Maiorca no decorrer dos estudos realizados nesta tese.

A análise sísmica da Catedral de Maiorca compreende a análise individual de cada um dos mecanismos locais considerados. O comportamento estrutural não linear é obtido através de análise limite e o ponto de desempenho é obtido através do método do espectro de capacidade. Os resultados obtidos de cada mecanismo local são a respectiva condição de segurança e, no caso de a segurança estar assegurada, o nível de dano que pode ser esperado. É utilizado um procedimento especificamente desenvolvido para a análise de estruturas históricas que está presente na norma Italiana.

A acção sísmica esperada para a Catedral de Maiorca considerada nesta tese corresponde a diversos espectros obtidos através das normas Europeia e Espanhola e de uma avaliação detalhada do risco sísmico da catedral que foi realizada num trabalho anterior. Esta avaliação compreende a execução de estimativas determinística e probabilística da acção sísmica que pode ser esperada no local.

De forma a reduzir o nível de dano ou para assegurar a segurança dos mecanismos locais, são propostas solução de reforço com o intuito de melhorar o comportamento sísmico da Catedral de Maiorca. São respeitados os princípios e critérios principais para a conservação e reabilitação de estruturas históricas.

TABLE OF CONTENTS

1. INTRODUCTION

1.1 General aspects

Since many years ago, the protection of the historical buildings towards the action of natural risks has been studied. It is well known that it have always represented the main cause of damage and losses to this kind of cultural heritage. Among these natural risks, earthquakes are the kind of event causing more significant losses.

Because of the complexity associated with the seismic action, as well as the dynamic properties of the structures, only static actions were considered in the design of historical structures. These were built proportional to bear vertical loads and the static horizontal thrusts of arches and vaults.

Till nowadays the scientific community developed several methods to consider the seismic action in the design of new buildings and in the structural analysis of existing ones. These methods may be linear static where lateral forces obtained from seismic spectrums are applied, nonlinear static, or pushover, where a pattern of lateral forces is applied and nonlinear dynamic. The latter is the most powerful method of analysis but, due to its complexity, it is not suitable for the seismic analysis of many buildings.

The aim of the present study is to propose a strengthening solution for Mallorca Cathedral so that the safety and damage expected from a seismic event are within an acceptable level. Mallorca Cathedral is a building which construction started around the year 1300 and it was subjected to some seismic events. The most significant one occurred in 1851 and caused the collapse of the main façade of the building.

In order to carry out a seismic analysis of Mallorca Cathedral, it is important to understand the usual structural response of historical building towards seismic events. Usually, the damages arising by an earthquake include: damage in the towers; separation of the main external walls; cracking of the external walls; among others. The nature of these damages depends on the construction details and on the spectral values and the motion history of the seismic event.

However, it was noted the recurrent damage and collapse mechanisms that were observed usually don’t involve the whole structure but only single architectonic parts, named macroelements, which are characterized by an almost autonomous structural behaviour in comparison with the rest of the building.

In these cases, the common pushover methodologies recently developed are not suitable. Therefore, the main procedure applied in this work for the seismic analysis of Mallorca Cathedral is also a nonlinear static procedure developed specifically for the analysis of historical buildings. The capacity of the each macroelement is obtained through limit analysis.

1.2 Objectives of the thesis

As it was mentioned before, the main objective of this thesis is to propose a strengthening solution for Mallorca Cathedral so that the safety and damage expected from a seismic event are within an acceptable level.

In order to lay-out the strengthening solution, a seismic analysis of Mallorca Cathedral is carried out. To use the aforementioned methodology it is first necessary to individualize the several local mechanisms that may occur during an earthquake. It is intended for each one to get its capacity curve, which relates acceleration with displacement, by kinematic limit analysis. These capacity curves are then intersected with seismic spectrums in order to get the performance point of the local mechanism and the corresponding seismic demands in terms of accelerations and displacements.

The possibility of occurring local mechanisms which complexity doesn't allow the execution of kinematic linear analysis is also considered. In this case, a more general pushover methodology is applied. Due to the need of complex modelling in order to obtain the capacity curve of these macroelements, the results from previous works on the structural analysis of Mallorca Cathedral are used.

For the determination of the seismic demand spectrums, the European code EC8 and the Spanish code NSCE-02 are used. However, the spectrums presented in codes are suitable only to new constructions since they are usually calibrated considering their over strength. Therefore, a suitable method to determine the seismic demand of a site is to perform a seismic hazard study considering the demand given by an envelope of a great number of response spectrums registered in the place where it is intended to evaluate the structure.

There are two types of evaluation of the seismic hazard, which are the deterministic and the probabilistic types. The deterministic approach is based on the fact the historic seismicity of a region is enough in order to obtain the seismic hazard. The probabilistic approach is based on the seismic hazard information of the last century for the whole peninsular region.

Since this seismic hazard study is too complex to carry out within the objectives of this thesis, the results obtained by the seismic hazard study performed in previous studies about Mallorca Cathedral are used.

After the obtainment of the seismic behaviour of the several local mechanisms of Mallorca Cathedral, the strengthening solutions are proposed in order to assure the safety of the mechanisms and to reduce the expected damage, if needed.

1.3 Organization

The thesis is organized in six chapters. After this 1st chapter of introduction, in the 2nd chapter it is discussed the methods of seismic analysis of structures in general, and of historical structures in

particular. It is described specifically the basic assumptions of limit analysis and the nonlinear static procedure that is mainly applied in this thesis.

In the 3rd chapter a description of Mallorca Cathedral is presented. This includes the general structural and architectural description of the building, the description of its history and the significant events that occurred in the past, the description of the construction process and also the damage identification that was carried out by previous studies about Mallorca Cathedral.

In the 4th chapter the previous works which comprised a structural analysis of Mallorca Cathedral are described. This description includes from works carried out in the beginning of the 20th century till works that were done very recently.

In the 5th chapter the seismic analysis of Mallorca Cathedral is carried out. The local mechanisms that are likely to occur during a seismic event, as well as the seismic demand spectrums considered, are described. Also the assumptions made in order to perform the necessary calculations for the seismic analysis are referred. Finally, the results are presented and discussed.

In the 6th chapter the strengthening solutions are proposed. This is done taking into account the results obtained from the seismic analysis. It is presented the philosophy behind the strengthening proposals and the aim of each one of them.

In the 7th chapter the main conclusions that came out from the work developed are presented. These conclusions include comments on the results obtained from the seismic analysis as well as remarks about the strengthening needed for Mallorca Cathedral.

2. SEISMIC ANALYSIS OF HISTORICAL STRUCTURES

2.1 Methods of analysis

The seismic action is the natural phenomenon that causes more damage in structures. The damages are caused by the ground motion that must be considered somehow in the structural design. Nowadays it is not possible to predict exactly not only when is an earthquake going to occur, but also the ground acceleration that it will induce. This prediction can only be made in probabilistic terms. Therefore, the aim of seismic engineering nowadays is to design structures, through the register of past seismic events, so that in the future they will have an acceptable probability of not collapsing.

Since earthquakes are rare actions, the builders experience was different from area to area and from time to time. In areas of high seismicity, where significant earthquakes occur quite often, buildings are characterized by constructive details and reinforcements specifically adopted to protect them from seismic actions. In areas of moderate seismicity, these solutions may be found only in the buildings constructed immediately after a serious earthquake, together with traditional repairing techniques (tie rods, buttresses, scarp walls, foil arches between facing buildings). However, awareness of the importance of these details disappears after two or three generations.

With respect to the structural design, in the past masonry buildings were constructed taking into consideration only static actions. Notions such as dynamic amplification, damping, interaction between the soil and the structure were not simple to manage. Therefore, masonry buildings were proportional to bear vertical loads and the static horizontal thrusts of arches and vaults (Lagomarsino (2006)).

Nowadays, the usual method that is presented in codes to consider the seismic action in the design of new buildings is linear analysis with forces obtained using design spectrums. This simple application of forces without considering the nonlinear behaviour of the materials and its capacity to deform beyond its elastic limit may lead to a significant increase of the forces of the structures. This is the reason why usually these forces are affected by a behaviour coefficient that reduces the forces and increases the displacement.

This type of linear analysis, or equivalent linear analysis, is very simple and easy to apply. However, it is not suitable for the seismic analysis of existing and, particularly, historical buildings since the displacements distribution obtained in the inelastic range is usually very different from the one obtained by linear elastic analysis.

Since rehabilitation of historical structures in seismically vulnerable areas is a matter of growing concern and the main objective is to identify the structures susceptible to damage and also determine its acceptable level of damage, function of the seismic nonlinear response, simplified linear static analyses are found to be inadequate to make such kind of assessment. A continual research by the

structural engineering community has successfully developed a new generation of analysis procedure called performance based structural evaluation (Das (2008)).

The most powerful method for seismic analysis of historical buildings is the dynamic nonlinear analysis. However, this kind of analysis is very difficult to apply due to several aspects. One of them is the difficulty of modelling the deformation of the materials subjected to loading and unloading cycles. Also dynamic nonlinear analysis is computationally too expensive and sometimes the interpretation of the results is too complex. Intending to perform simpler analysis, through the last years several methods have been developed where the nonlinear dynamic behaviour of structures is approximated by the behaviour obtained by the application of static forces to a structure, modelled taking into account the nonlinear relation between forces and displacements.

It is assumed that the curve that represents the forces acting on the structure as a function of the displacement of a chosen control point includes the peak responses that could be obtained by a nonlinear dynamic analysis. This curve is named capacity curve. Through the use of the capacity spectrum method this curve is intersected with a demand seismic spectrum and the resultant point, designated as performance point, represents the seismic demand of the structure.

The capacity curve of a structure can be obtained through, for example, pushover analysis. The basic idea of the pushover analysis is to apply to the structure a pattern of incremental forces or displacements in a way that the response obtained constitutes an approximation of the peak responses that are obtained by nonlinear dynamic analysis. In other words, it is assumed that the response obtained by the application of incremental forces or displacements may represent the result that would by obtained by dynamic analysis. It is expected that pushover analysis provides information of several characteristics of the seismic response of a structure, which would not be possible to obtain through the linear static analysis that have been used for structural seismic design in the last years.

Many methods were presented to apply the nonlinear static pushover techniques to structures. The first ones proposed the modification of the demand spectrum according to the extent of the inelasticity of the seismic response of the structure.

Since these proposals only took into account the response of the fundamental mode of vibration of the structure, methodologies where the seismic performance of a structure is determined as a combination of the response obtained by all the modes that influence the seismic behaviour were proposed later.

In order to take into account the changes of the modal properties of the structure within the inelastic range, several methodologies were recently proposed where the force or displacement pattern applied is uploaded before each load increment step according to the corresponding modal properties of the structure.

Another way to obtain the capacity curve to be used in the capacity spectrum method is the limit analysis. Due to its simplicity and to its wide application in historical structures and structural elements in particular, this is the main analysis used in the seismic assessment of Mallorca Cathedral carried

out in the present study. Therefore, a detailed description of the limit analysis is provided in the next section.

2.2 Limit analysis

2.2.1 Basic assumptions

Limit analysis depicts realistically the collapse and capacity of masonry structures and it constitutes a very reliable and powerful tool for their structural assessment, sometimes in combination with other possible tools. The possibilities of the classic calculations of the limit analysis, based on the theories of plasticity, have been highlighted by Heyman (1966). The theories of limit or conventional plastic analysis can be applied to masonry structures if it is accepted that the material fulfils the following properties:

- Masonry has no tensile strength. In fact, masonry structures present some tensile strength, but due to the weakness of mortar and bond behaviour between mortar and masonry units, the tensile strength can be considered negligible since only low tensile forces can be transmitted.
- Masonry has an infinite compressive strength. Although this is usually realistic to apply, since in many historical masonry buildings the compressive stresses are smaller than the corresponding strength, it should be always confirmed. Some authors who studied this subject found that the crushing failure is likely to happen in some historical structures.
- Sliding between stone blocks is impossible to occur. This is not totally true since in some cases failure is possible to occur due to sliding, but its consideration in limit analysis is very difficult to carry out. Therefore, the assumption of no slide is made.
- Elastic deformations are negligible, but displacements and rotations are possible due to the cracking.

If these properties are fulfilled in a masonry construction, it can be demonstrated three fundamental theorems that constitute the basics for the analysis or calculations of masonry structures: lower bound theorem, upper bound theorem and uniqueness theorem.

2.2.2 Lower bound theorem

A masonry structure is safe if it is possible to find a statically admissible state of equilibrium compatible with the loads. This occurs when a thrust line can be determined in equilibrium with the external loads that falls within the boundaries of the structures (Figure 2.1). The load applied is a lower bound of the actual ultimate load.

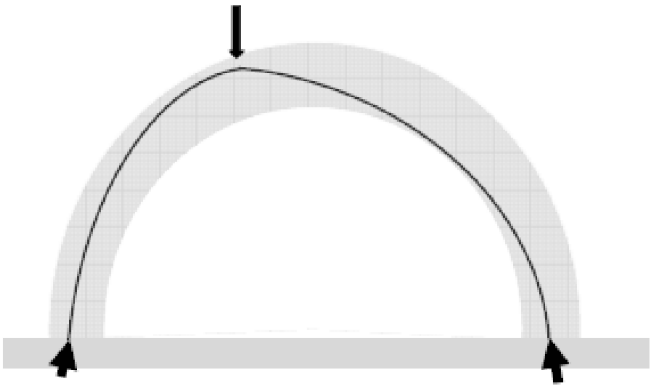

Figure 2.1 – Thrust line within a masonry structure.

2.2.3 Upper bound theorem

The upper bound theorem states that if a kinematically admissible mechanism can be found, for which the work developed by external forces is positive or zero, the arch will collapse. In another words, if a mechanism is assumed (by arbitrarily placing a sufficient number of hinges), the load which results from equalizing the work of the external forces to zero is an upper bound of the actual ultimate load (Figure 2.2).

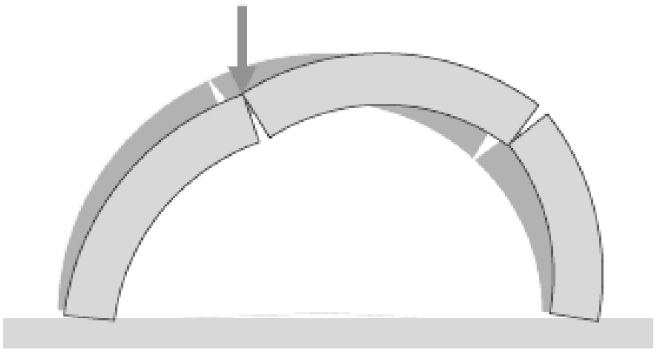

Figure 2.2 – Kinematic mechanism of an arch.

2.2.4 Uniqueness theorem

The uniqueness theorem states that, ,if a both statically and kinematically admissible collapsing mechanism is possible to be found, a limit condition is reached meaning that the structure will be about to collapse.

In other words, if a solution for the thrust line within the boundaries of the masonry structure is found and it is tangent to it in a number of points equal to the number of hinges that are needed to form an instable mechanism, then the applied load is the true ultimate load and the mechanism represents the collapse mechanism (Figure 2.3).

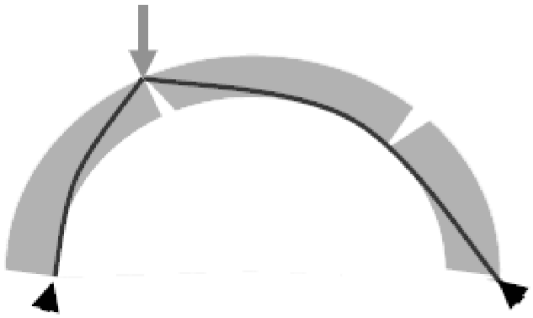

Figure 2.3 – Collapse mechanism of an arch.

2.2.5 Application of limit analysis

From engineering point view, static limit analysis can be useful in some cases. However, in the case of the building presented in Figure 2.4, the thrust line has no significant meaning. If kinematically admissible mechanisms like the ones of Figure 2.4 are considered, it is possible to find the safety factor against horizontal loads, corresponding to the mechanism which leads to the smallest value of this factor. Therefore only kinematic limit analysis can be combined with the capacity spectrum method.

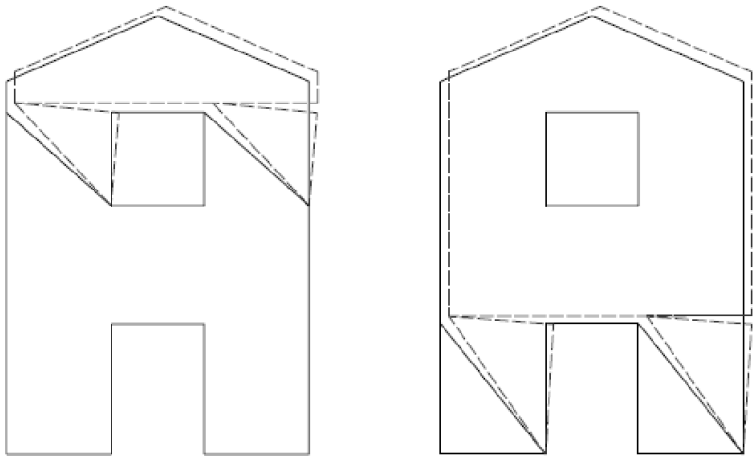

Figure 2.4 – Collapse mechanisms of a building wall.

Since the masonry structure is considered to be made of rigid blocks, only few geometrical parameters and technological details are needed. In order to determine a capacity curve of the structure, an incremental nonlinear limit analysis may be performed, in order to evaluate the displacement capacity of the masonry structure, by an approximate approach that makes use of the capacity spectrum method.

2.3 Seismic behaviour of historical structures

There are several types of damages in churches caused by earthquakes. The most frequent are: damage in the towers (sometimes including its fall), separation of the main external walls by rotation with respect to the foundation, cracking of the external walls produced by shear forces and by the existing large openings, flattening of vertical elements (columns and walls) due to high axial loading and damages elements that are not located on the main structure.

The nature of the former damages depends on many things like the presence or not of connectors that restrain the walls, the deterioration state, the type of soil or the characteristics of the seismic action. The spectral values as well as the motion history along a seismic event are also of great importance to the performance of the structure. These aspects depend very much on the proximity to the fault, on the presence of soft soil and on the topography of the place.

Going deep into damage observation, recurrent damage and collapse mechanisms have been observed, which usually don't involve the whole structure but only single architectonic parts, named macroelements, which are characterized by an almost autonomous structural behaviour in comparison with the rest of the building. Therefore, the concept of macroelement allows analyzing the most vulnerable parts of the structure which are characterized by the activation of the partial collapse mechanisms (Martinez (2007)).

In Lagomarsino (1998), the author proposed the possible collapse mechanisms in churches through the observation of the structural behaviour during past earthquakes. These collapse mechanisms are presented in Figure 2.5.

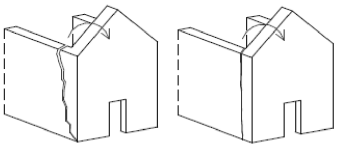

(a) Façade overturning

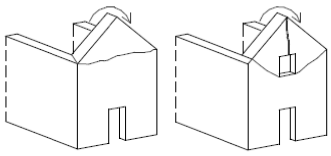

(b) Overturning of the upper part of the façade

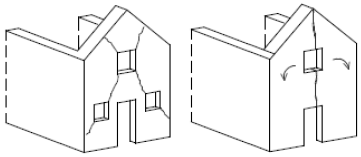

(c) In plane mechanism

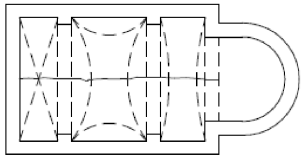

(d) Transversal vibration of the nave

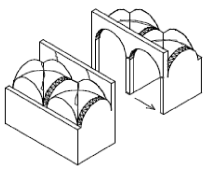

(e) Longitudinal response of the nave

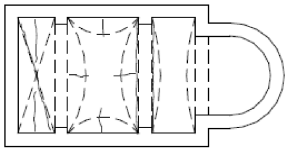

(f) Dome of the central nave

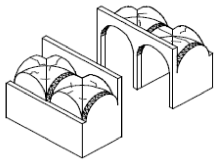

(g) Dome of lateral naves

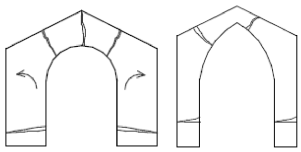

(h) Triumphal arches

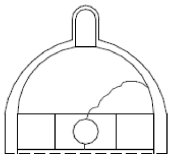

(i) Vault or cimborio

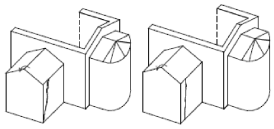

(j) Overturning of extreme walls

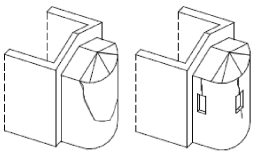

(k) Apse overturning

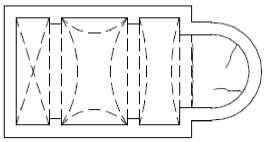

(l) Dome of the apse

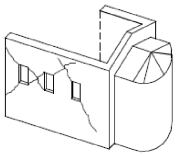

(m) Shear mechanisms in walls

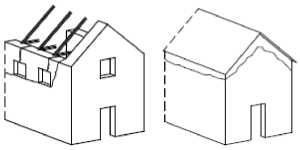

(n) Roofing system

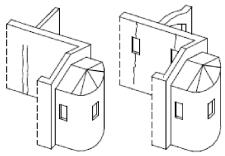

(o) Absence of continuity in walls

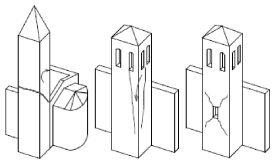

(p) Mechanism in the tower

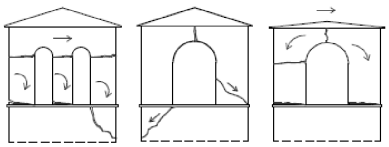

(q) Upper part of the tower

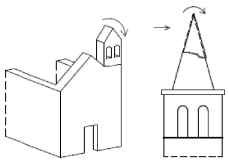

(r) Mechanisms in the pinnacles or statue

Figure 2.5 – Macroelements for churches proposed by Lagomarsino (1998).

2.4 Capacity spectrum method

2.4.1 General description

The capacity spectrum method was developed by Freeman (1998) and Fajfar (1999). Through a graphical procedure schematized on Figure 2.6, the capacity of a structure is compared with the demand of the soil movement due to a seismic event. The graphical representation turns possible a visual evaluation of how the structure will act when subjected to an earthquake.

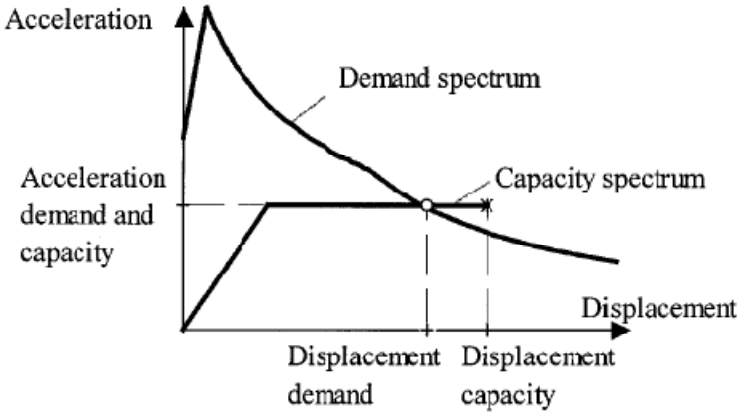

Figure 2.6 – Capacity spectrum method (Fajfar (1999)).

The capacity of the structure is represented by a curve relating force as a function of displacement, obtained through a static nonlinear analysis, which may be a pushover analysis or a limit analysis. The base shear force and the displacements are converted in spectral accelerations and spectral displacements of an equivalent single degree of freedom system. These values define the capacity spectrum. The demand of the earthquake is represented by an elastic seismic spectrum that is then modified in order to take into account the inelastic response of the structure. In the case of Freeman (1998), this modification is carried out by considering an over-damped spectrum and in the case of Fajfar (1999) it is carried out considering a ductility factor.

The seismic demand is represented by a curve in the ADRS (Acceleration-Displacement Response Spectra) format, where the spectral accelerations are computed as a function of the spectral displacements, with the natural periods of vibration represented by radial lines.

The point corresponding to the intersection of the capacity spectrum with the demand spectrum is the performance point of the structure and provides the safety condition of the structure subjected to the design earthquake as well as the damage level.

However, as stated by Lagomarsino (2006), these procedures which take into account the reduction of the elastic spectrum to obtain the inelastic demand are not suitable in the case of rocking mechanisms like almost all the mechanisms that are analyzed in this study. Therefore, in this work, the main procedure used is presented on the Italian code (2009) and it is based on the capacity spectrum method, with the capacity curve being obtained through limit analysis and the performance point being obtained through the estimation of a secant natural period of the structure.

2.4.2 Capacity curve

The capacity curve is a function of a building's lateral load resistance versus its characteristic lateral displacement. In the case of limit analysis, it is determined for the different local mechanisms that are possible to be developed during an earthquake. Therefore, the first step is to define the local mechanisms that will be under consideration during the study of an historical building.

The loads applied to each macroelement are the weights of the blocks, the vertical loads carried by them (the weights of the floors, roof and other wall elements not considered in the structural model), the system of horizontal forces proportional to vertical loads if they are not being effectively transmitted to other parts of the building, the internal forces and the external forces. The horizontal forces generated by a horizontal acceleration are determined as being proportional to the vertical forces through the coefficient α.

For each local mechanism considered, it has to be determined the coefficient α_0 that corresponds to the loose of equilibrium and to the formation of the local mechanism. In order to accomplish that, a virtual rotation θ_k is applied to the macroelement. As a function of this rotation and of the geometry of the macroelement, it is determined the displacement on the direction of the applied forces. Then it is applied the principal of virtual work as in Equation (1), in terms of displacements, equalizing the total work done by the external and internal forces applied to the system in correspondence with the virtual motion.

$$\alpha_0 \cdot \left(\sum_{i=1}^{n} P_i \cdot \delta_{x,i} + \sum_{j=n+1}^{n+m} P_j \cdot \delta_{x,j} \right) - \sum_{i=1}^{n} P_i \cdot \delta_{y,i} - \sum_{h=1}^{o} F_h \cdot \delta_h = L_{fi} \qquad (1)$$

In Equation (1):

- ***n*** is total number of the dead loads applied to the different rigid blocks;
- ***m*** is the number of weight forces not directly acting on the blocks, but which masses, due to the effect of the seismic action, generate horizontal forces on the rigid blocks as they are not transmitted to other parts of the building;
- ***o*** is the number of the external forces applied to the rigid blocks but not related to the masses;
- $\boldsymbol{P_i}$ is the generic weight force;
- $\boldsymbol{P_j}$ is the generic weight force not directly applied on the rigid blocks, but which mass, due to the effect of the seismic action, generate horizontal forces on the rigid blocks as they are not transmitted to other parts of the building;
- $\boldsymbol{\delta_{x,i}}$ is the virtual horizontal displacement of the point of application of the weight P_i, assuming the positive direction as the one through which the seismic action activates the mechanism;
- $\boldsymbol{\delta_{x,j}}$ is the virtual horizontal displacement of the point of application of the weight P_j, taken as above;
- $\boldsymbol{\delta_{y,i}}$ is the virtual vertical displacement of the point of application of the weight P_i, taken as positive if directed upwards;
- $\boldsymbol{F_h}$ is the generic external force, in absolute value, applied to the block;

- $\boldsymbol{\delta_h}$ is the virtual displacement of the point where the force F_h is applied in the same direction, though with positive sign if discordant;
- $\boldsymbol{L_{fi}}$ is the work done by internal forces.

The loose of equilibrium does not correspond to the ultimate condition of the structure, because the structure has capacity to support several horizontal actions even after the mechanism activation.

The displacement capacity of the structure until the collapse of the local mechanism considered is identified through the horizontal multiplier α of the load determined varying the configuration of the kinematic system, representative of the evolution of the mechanism and described through the displacement d_k of a control point of the system.

The analysis, through a graphical or an analytical procedure, must be carried out up to the configuration where the multiplier α is equal to zero, corresponding to the displacement $d_{k,0}$.

This means that with the principle of virtual work, Equation (1), it is obtained an equation to determine the rotation $\theta_{k,0}$, if it is imposed α equal to zero. Once the rotation $\theta_{k,0}$ is determined, the displacement $d_{k,0}$ is obtained (Figure 2.7).

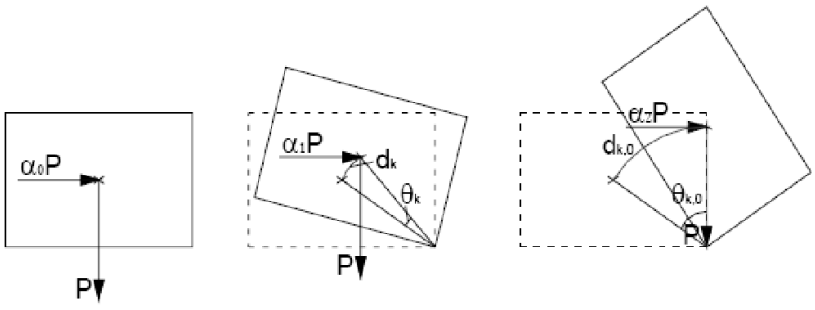

Figure 2.7 – Evolution of a kinematic mechanism.

The evolution of the kinematic mechanism may be determined by points if the actions (self weight, external or internal actions) are constant during the evolution of the kinematic mechanism. In this case, the obtained curve is linear and, in a simplified way, it is sufficient the evaluation of the displacement $d_{k,0}$ for which the multiplier α is equal to zero. The curve assumes the expression expressed on Equation (2).

$$\alpha = \alpha_0 \cdot \left(\frac{1 - d_k}{d_{k,0}} \right) \tag{2}$$

The latter is illustrated by the graphic of Figure 2.8.

If it is considered the progressive variation of external forces with the evolution of the kinematic mechanism, for example in the case of the lengthening of a tie, the curve is piecewise linear, having

abrupt changes corresponding to displacements for which significant events occur like the yielding of the tie or its collapse (Figure 2.9).

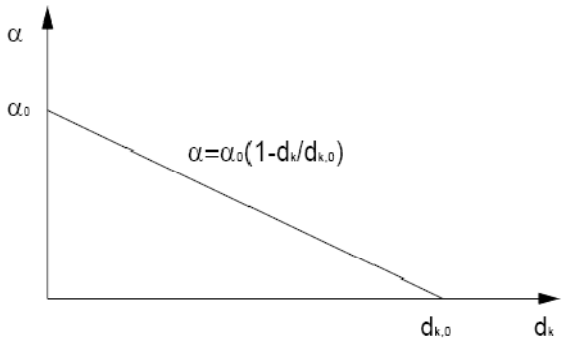

Figure 2.8 – Capacity curve.

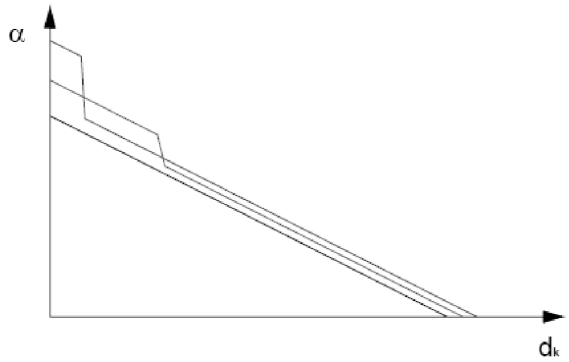

Figure 2.9 – Examples of capacity curves.

Knowing the evolution of the load horizontal multiplier α as a function of the displacement d_k of the control point of the structure, the capacity curve of the equivalent system is defined as the relation between the spectral acceleration a^* and the spectral displacement d^*.

The participation mass of the kinematic mechanism M^* is determined considering the virtual displacements of the points of applications of the several weights associated to the kinematic mechanism. The participation mass is calculated through Equation (3), where $n+m$ is the number of weights P_i applied to the macroelement which mass, due to the effect of the seismic action, generates horizontal force in the rigid blocks and $\delta_{x,i}$ is the virtual displacement of the point of application of the weight P_i.

$$M^* = \frac{\left(\sum_{i=1}^{n+m} P_i \cdot \delta_{x,i}\right)^2}{g \cdot \sum_{i=!}^{n+m} P_i \cdot \delta_{x,i}^2} \tag{3}$$

The spectral seismic acceleration a^* is obtained by multiplying the gravity acceleration by the multiplier α and dividing it by the product between the fraction of the participation mass of the kinematic and a confidence facto. The spectral acceleration corresponding to the activation of the kinematic mechanism is obtained through Equation (4), where e^* is the fraction of the participation mass and is determined through Equation (5) and *FC* is the confidence factor which is equal to 1.35.

$$a_0^* = \frac{\alpha_0 \cdot \sum_{i=1}^{n+m} P_i}{M^* \cdot FC} = \frac{\alpha_0 \cdot g}{e^* \cdot FC} \tag{4}$$

$$e^* = \frac{g \cdot M^*}{\sum_{i=1}^{n+m} P_i} \tag{5}$$

Knowing the displacement of the control point d_k, it is defined the spectral displacement d^* of the equivalent system with reference to the virtual displacements evaluated on its initial configuration, as expressed by Equation (6), where n, m and P_i are taken as above and $\delta_{x,k}$ is the virtual displacement of the point k, taken as the reference for the determination of the displacement d_k.

$$d^* = d_k \cdot \frac{\sum_{i=1}^{n+m} P_i \cdot \delta_{x,i}^2}{\delta_{x,k} \cdot \sum_{i=1}^{n+m} P_i \cdot \delta_{x,i}} \tag{6}$$

In the case of the curve presenting a linear evolution, meaning that the actions are constant, the capacity curve assumes the expression expressed in Equation (7), where d_0^* is the equivalent spectral displacement corresponding to the displacement $d_{k,0}$.

$$a^* = a_0^* \cdot \left(\frac{1 - d^*}{d_0^*} \right) \tag{7}$$

In the case that the external forces are variable, the curve is assumed as being piecewise linear.

As defined in the Italian code (2009), the resistance and capacity related to the Ultimate Limit State (SLV – *Stato limite di salvaguardia della vita*) is evaluated on the point of the capacity curve that corresponds to the spectral ultimate displacement d_u^*. As it was verified on experimental dynamic testing carried out by several authors, this displacement is defined as 40% of the displacement for which the spectral acceleration a^* is equal to zero assessed on a curve in which it is considered only the actions which presence is verified until the collapse. However, if the displacement corresponding

to a situation of local incompatibility with the stability of the elements is smaller, this displacement should be taken as the ultimate displacement. The latter kind of situations may occur for example due to the slipping of a tie.

2.4.3 Safety verification

- **Kinematic linear analysis**

For the safety verification, the Italian code (2009) recommends to carry out a preliminary simplified linear analysis with a structural factor *q*. In the case that in this analysis the safety is verified, we can considered the local mechanism safe, otherwise a kinematic nonlinear analysis must be performed.

In the case of an isolated macroelement or a part of the building supported on the soil, its safety is verified if the spectral acceleration a_0^* is higher than the soil acceleration, which is equal to the elastic spectrum evaluated for a period equal to zero, divided by the structural factor *q* that may be assumed equal to 2. This is expressed by the inequality of Equation (8), where a_g is the design ground acceleration function of the probability of being exceeded during a reference period and *S* is a soil parameter that may be taken equal to 1 for the seismic demands considered in this work.

$$a_0^* \geq \frac{a_g \cdot S}{q} \tag{8}$$

In the case of a part of the construction at a certain height in the building, the acceleration is generally amplified with respect to the acceleration of the soil. The safety of the macroelement is verified if the inequality of Equation (9) is verified. In this equation, $S_e(T_1)$ is the elastic spectral response calculated for a period T_1 that corresponds to the first mode of vibration of the whole structure in the direction considered. The parameter $\psi(Z)$ is the first mode of vibration in the direction considered, that in the absence of an accurate evaluation may be taken as equal to Z/H_{TOT}, being H_{TOT} the height of the structure with respect to the foundation and *Z* the height, with respect to the foundation of the building, of the barycentre of the bond line between the studied macroelement and the rest of the structure. The parameter γ is the corresponding coefficient of modal participation that in the absence of an accurate evaluation may be taken as equal to $3N/(2N+1)$, being *N* the number of floors of the building that in this case is 1.

$$a_0^* \geq \frac{S_e(T_1) \cdot \psi(Z) \cdot \gamma}{q} \tag{9}$$

Thus, the safety of the kinematic mechanism is assured through the kinematic linear analysis if the spectral acceleration a_0^* is higher than the maximum of demand accelerations calculated in Equation (8) and Equation (9).

- **Kinematic nonlinear analysis**

In a kinematic nonlinear analysis, the verification consists on the comparison between the the ultimate displacement d_u^* of the mechanism and the displacement demand obtained by the displacement spectrum in correspondence with the secant period T_s. This period corresponds to the displacement d_s^* that is equal to $0.4 \cdot d_u^*$ and the corresponding a_s^* in the capacity curve. The obtainment of the seismic demand in this way is illustrated in Figure 2.10.

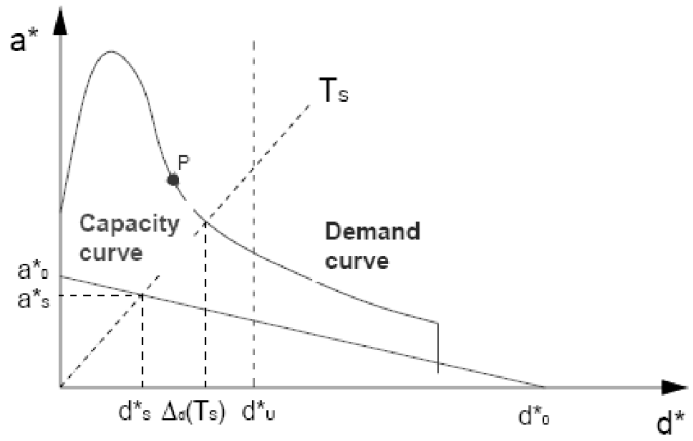

Figure 2.10 – Secant period T_s.

The calculation of T_s is then carried out through the Equation (10).

$$T_s = 2 \cdot \pi \cdot \sqrt{\frac{d_s^*}{a_s^*}} \tag{10}$$

This procedure was introduced in order to take into consideration the fact that in the mechanisms where the rigid overturning is prevalent, the structure shows a nonlinear behaviour where there are small values of hysteretic damping and limited degradation. In this case the determination of the seismic demand for values of period smaller than the one correspondent to d_u^* should bring to not overestimate it.

For a macroelement supported on the soil, the safety is verified if the inequality expressed on the Equation (11) is satisfied, where $S_{de}(T_s)$ is the elastic spectral response in terms of displacements corresponding to the period T_s.

$$d_u^* \geq S_{De}(T_s) \tag{11}$$

In the macroelement studied is at a certain height of the building, it must be considered the response spectrum in terms of displacements of the building at the height which the kinematic mechanism is developed. It is considered that the safety is assured if the condition expressed on the Equation (12) is satisfied, where $S_e(T_1)$, $\psi(Z)$ and γ are taken as above.

$$d_u^* \geq S_{De}(T_1) \cdot \psi(Z) \cdot \gamma \cdot \frac{\left(\frac{T_s}{T_1}\right)^2}{\sqrt{\left(1-\frac{T_s}{T_1}\right)^2 + 0.02 \cdot \frac{T_s}{T_1}}} \quad (12)$$

Thus, the safety of the kinematic mechanism can be assured through the kinematic nonlinear analysis if the ultimate displacement d_u^* is higher than the maximum of the demand displacements calculated in Equation (11) and Equation (12).

2.4.4 Damage levels

With the method presented above, it is possible to state if the safety of the possible local mechanisms is assured or not. However, if the collapse is not expected to occur, it is important to evaluate the damage level that can be expected for the several possible local mechanisms.

Knowing the value of the performance point and its corresponding spectral displacement, it is possible to know the damage level expected comparing this value with defined thresholds values. These thresholds values are the spectral displacements that limit a range of values associated to a certain damage level.

Different proposals have been carried out for these thresholds values, but in this study the values proposed by Lagomarsino et al. (2003) are going to be used, since they were proposed specifically for the case of historical buildings based on the European macroseismic scale. The thresholds between two different damage levels are defined as follows:

- **Limit state 1** (no damage) is defined by a fraction of the acceleration that activates the mechanism, being defined by $\alpha=0.7 \cdot a_0^*$;
- **Limit state 2** (slight damage) is defined by the acceleration that activates the mechanism , being defined by $\alpha=a_0^*$;
- **Limit state 3** (moderate damage) is defined by $d^*=1/8 \cdot d_0^*$;
- **Limit state 4** (extensive damage) is defined by $d^*=1/4 \cdot d_0^*$;
- **Limit state 5** (complete damage) is defined by $d^*=1/2 \cdot d_0^*$.

These limits are shown in Figure 2.11.

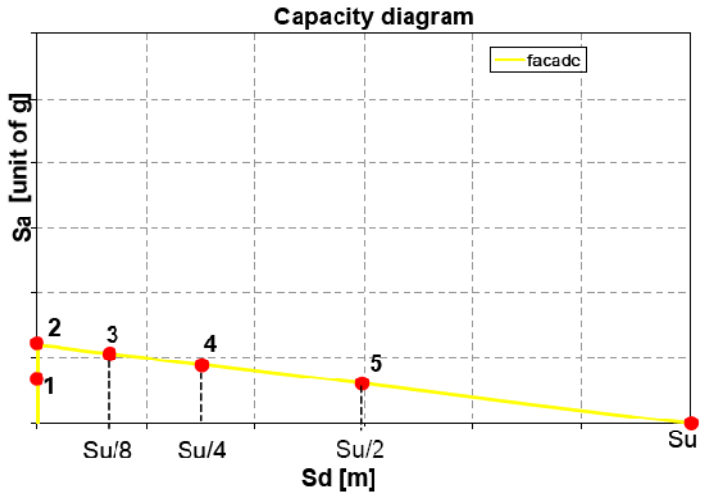

Figure 2.11 – Capacity curves with the definition of the damage limit states (Lagomarsino et al. (2003)).

The damage levels are defined as presented in Table 2.1.

Table 2.1 – Level of damage.

Damage level	Description
D0	No damage
D1	No damage to slight damage
D2	Slight to moderate damage
D3	Moderate to extensive damage
D4	Extensive to complete damage
D5	Complete damage

3. MALLORCA CATHEDRAL

3.1 Description of the building

The Mallorca Cathedral (Figure 3.1), popularly known as “La Seu”, is located in the city of Palma de Mallorca which is the capital of the Spanish island Mallorca, belonging by its turn to the Baleares islands, located in the Mediterranean Sea. Designed in a French-gothic style, Mallorca Cathedral is one of the well known cathedrals in Spain for its architecture. In comparison to other cathedrals, like for example Santa Maria del Mar in Barcelona that was built within 53 years, Mallorca Cathedral was built over a large period spanning around 300 years (1300 to 1601) being later subjected to significant repairs and constructions (Das (2008), Martinez (2007), Rodriguez (2009), González et al. (2008)).

The building is characterized by some major features, such as the search for spaciousness, the high lateral naves (although not so high as to take the role of flying arches), the lateral chapels between buttresses and the extremely slender and solid octagonal piers. In a way, the builders managed to synthesize Northern and Southern Gothic architecture to produce a vast and diaphanous space.

(a) External view (b) View from the interior

Figure 3.1 – Mallorca Cathedral.

In Figure 3.2 and Figure 3.3 a plan and an elevation of the Cathedral are presented. It is possible to distinguish two parts of the structure. The first is the largest body formed by the main nave limited by the West façade and the second is located at East and composed by the choir and surrounding chapels.

The first body of the cathedral comprises the central nave and the lateral ones surrounded by a series of lateral chapels built in between the buttresses. The second body had been built in previous historical stage and it included the Royal chapel (a single nave Gothic construction) and Trinity chapel (the first element built in the complex). It is not known if the building was meant to have the present arrangement or if it is the result of decisions to extend to other parts taken after another part was completed. Remains of unused capitals and nervure springing at the end of the Royal Chapel suggest

that the decision of building an imposing body of larger dimensions was actually taken after the completion of the Eastern part of the building.

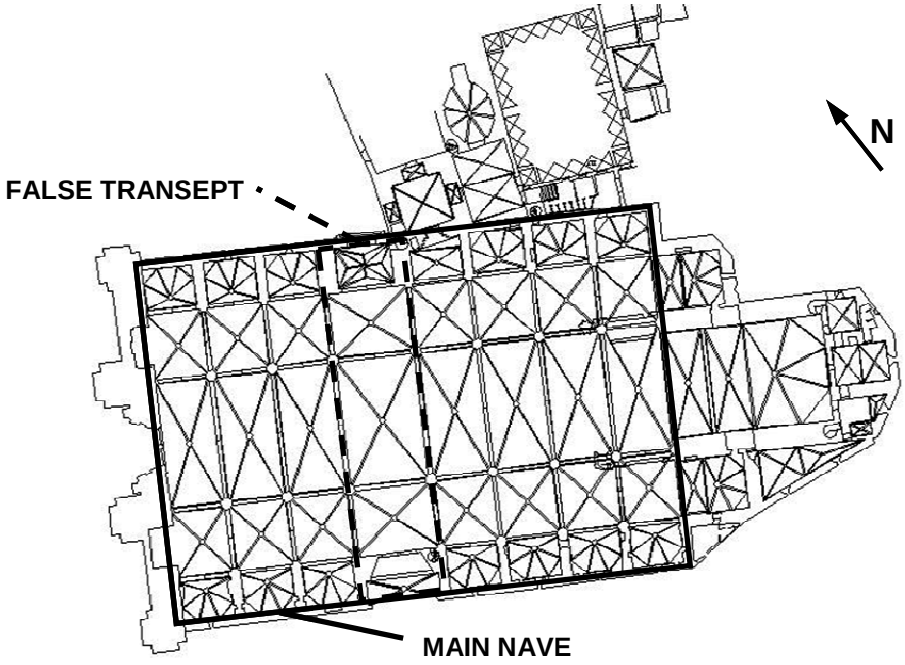

Figure 3.2 – Plan of Mallorca Cathedral.

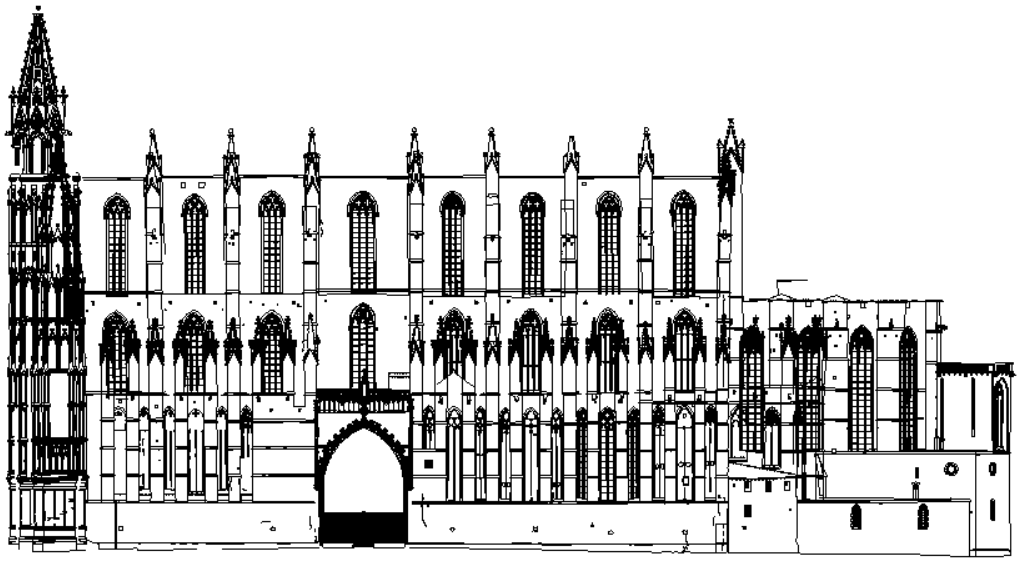

Figure 3.3 – Elevation from South of Mallorca Cathedral.

The cathedral has the global dimensions of 120m in length and 55m in width. The central nave has longitudinally 77m and it is composed by seven bays. It spans 19.9m and its height reaches 43.9m at the vaults keystone. About the lateral naves, they span 8.75m and a height equal to 29.4m. The vaults in the latter are quadrangular with the dimension equal to the nave span, while in the central nave they are rectangular with a dimension equal to the last vaults and the other one equal to the central nave

span (Figure 3.4). A false transept 11.7m wide (33% bigger than the other bays) connects the main doors located in the North and South sides of the building, named Almoina and Mirador respectively. The octagonal piers have a free height to the springing of the lateral vaults equal to 22.7m and their octagonal transverse section has a circumscribed diameter around 1.6 and 1.7m, being though extremely slender, as it was before mentioned (Figure 3.5).

Figure 3.4 – Main nave vaults.

Figure 3.5 – Piers.

The vaults are complemented with some sort of filling material up to the level of the terrace. A lightweight pottery fill was probably removed from the central vaults during the 18th century while the lateral vaults are still filled with pottery.

Another interesting characteristic in Mallorca Cathedral is the existence of a double battery of flying arches (Figure 3.6), which is not common in Spanish cathedrals. While the function of the under flying arches is totally justified, that is to transfer the lateral thrust offered by the central vault towards the buttresses, the upper battery doesn't seem to have a structural purpose, since the building roofing doesn't transmit forces due to the wind (main purpose of the upper flying arches in the Northern European churches), working only as a drainage channel. Another possible reason for the existence of the upper battery of the flying arches is to provide vertical stability along with the additional weights over the arches and the keystones in the vaults of the central nave. These additional weights consist in triangular walls connected to the arch and stone pyramids with square base over the keystones or central zone of the vaults.

Because of the strong solar exposition of the buildings located in Palma de Mallorca, since it is in the Mediterranean Sea, the windows are very narrow (Figure 3.7). However, the number of windows is very high, which is not possible to be observed in the French Gothic cathedrals.

It is also the cathedral with the world's largest Gothic rose window (Figure 3.8), with a diameter equal to 11.5m. This rose window is characterized by the existence of a big star of 6 tips (David's star) inscribed in it.

Figure 3.6 – Flying arches.

Figure 3.7 – Windows.

Figure 3.8 – Rose window.

3.2 Historical issues

According to the legend, the construction of the Mallorca Cathedral was decided in one night of 1229. When Jaume I was on his way to recapture the island of Mallorca, his fleet was struck by a strong storm. He promised to the Virgin Mary that if he survived, he would erect a church is her honour.

In the place where the Mallorca Cathedral was built, previously had existed an Arab mosque, which was being demolished while the construction of the Cathedral advanced, until its complete demolition in 1378.

From the starting of construction in fourteenth century to present century the cathedral has been altered in several occasions. For example, the present outlook of the main West façade was not originally built in this way. After the 1851 earthquake it was repaired and came out in a showy

Renaissance style. Also several internal alterations including the change of the colour of the window glasses had been incorporated by the famous architect Gaudi between 1904 and 1914.

The history of the construction, alterations and significant events taken place in the history of Mallorca Cathedral are not fully documented in the historical period. Although several attempts have been made by the researchers in the present century to investigate the historical aspects and related events, still there is not a unique opinion about who the constructors of the building were and what the different stages that followed its construction were. However, it is possible to define five periods or stages of the construction process (Das (2008), Martinez (2007), Rodriguez (2009)).

- **First period: The royal construction (1300-1368)**

The beginning of the construction occurs around the year 1300, when the king Jaume II (1276-1311) left an important legacy in his testament to support the cost of the Trinity chapel, which mission was to host the royal tombs in the crypt. The first architect who was in charge of the project was Ponç des Coll.

In 1311 began the construction works of the next body of the cathedral apse, the presbytery known as the Royal chapel. This stage was concluded when the construction of the latter chapel ended, around the year 1370.

- **Second period: The naves (1368-1601)**

As it was before mentioned, there is a theory based on the principles of its construction that indicates that the cathedral was originally planned to have only one nave with the same width as the Royal chapel. However, it is thought than in 1368, the architect Jaume Mates conceived the actual three naves of the cathedral.

Around the year 1400, the constructions works were in the door of the Mirador. In 1498 the door of the Almoina was built and in 1601 the West façade was finished with a remarkable Renaissance style. During this stage, it is supposed that an arch of the central nave fell in April of 1490 causing serious damage.

- **Third period (1601-1851)**

This stage encompasses since the end of the construction of the West façade to the beginning of its replacement. It comprises several episodes related to pathologies of the vaults.

In 1639, several experts stated that the major vault near the façade should be dismantled and replaced since it presented several cracks. It was the first report of damage in the structure of the cathedral, and it is supposed to be the result of the lack of longitudinal bracing. As stated by Gonzalez and Roca (2000), this was due the inefficient role that the main façade was performing in this aspect.

In 1655, the greater arch of the main nave and the first flying buttress were considered that they had to be remade. In 1659 it is known that an arch fell, but there is no specification of which one it was.

In the end of March of 1660, there was an earthquake in Palma de Mallorca which caused the fall of two arches near the façade. This event can be also related to the origin of the out-of-plumb of the façade, which was reported to have a deformation of 80cm 19 years later.

In 1698, the vault of the second bay collapsed and right after its reconstruction, it fell again in 1699. After this event the architect recommended the reconstruction of a set of the vaults in the nave which was carried out in the 18th century. After this, also in the 18th century, several proposals have been made to prop up six flying buttresses and also to demolish the façade because of the out-of-plum deformation. The latter was finally decided to be done in a report with the date of 28th of March of 1851, when the deformation was about 1.3m in a total height equal to 60m. However, in the 15th of May of 1851, Palma de Mallorca was struck by an earthquake of intensity between VII and VIII, which caused the collapse of the already degraded façade. The earthquake didn't have greater effect on the rest of the building.

- **Fourth period: The reconstruction (1851-1888)**

In the summer of 1851 the construction works started in order to demolish what was left from the West main façade and they lasted for six months. The next step was taken in August of the next year when the architect Bautista Peyronnet was designated to carry out the reconstruction of the main façade. The restoration project was finally presented in 1854. In the place of the old façade (Figure 3.9-a), he laid-out a very different neo-Gothic façade (Figure 3.9-b). The sections of the buttresses of the new façade were significantly increased. The reformation finished in 1888, although four years the construction works were almost concluded.

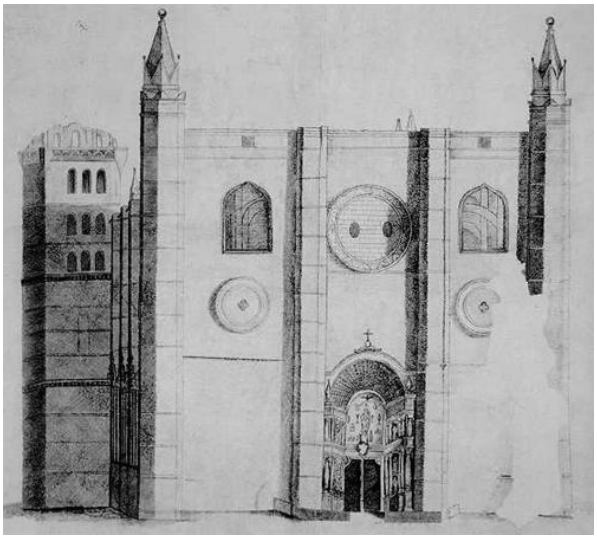

(a) Old façade

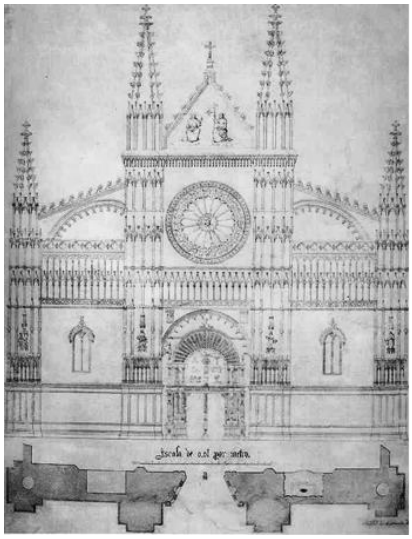

(b) Project to the reconstruction of the façade

Figure 3.9 – West façade (Martinez (2007)).

- **Fifth period: Reforms (1888-2006)**

This last stage comprises several interventions, like the reformation carried out by the Catalan architect Antoni Gaudi between 1904 and 1914, in association with other architects. From then on, several restoration and conservation works have been carried out. In 2006 the restoration of the towers of the West façade was concluded (Figure 3.10).

Figure 3.10 – Actual view of the West façade.

3.3 Construction process

The construction process of the Mallorca Cathedral was reported by González et al. (2008), where it was also identified the damage present in the building and where a structural analysis was carried out.

As it was before mentioned, the historical process leading to the final lay-out of the cathedral is not very well known. However, research on the historical books carried out by González et al. (2008) has provided significant hints on the construction process.

It is known that it was built with limestone from the local quarries of Santanyi. The construction of the nave progressed, bay after bay, from the presbytery towards the façade (the last part to be built). The construction of the chapels was ahead because of the funding provided by noble families or corporations willing them as pantheons or gremial chapels.

It has been possible, at least for one of the bays (the fourth one), to identify the process leading to its complete construction. Once again, it started with the lateral chapels, followed by the piers, then one lateral vault, then the other and finally the central one. In the case of this bay, the construction of the vault lasted 7 years. It should be noted that during a period of about 5 years, the lateral vaults were already pushing against the pier while the lateral vault was not yet there to counteract their thrust.

From a theoretical point view, structures based on the balance of arch thrusts, as Gothic cathedrals, attain full stability only at their final and complete configuration. Moreover, adequate equilibrium

requires (again, theoretically) the simultaneous activation of all the arches and vaults by first building the entire system and then removing all the centring almost at once. This is not obviously the case of Mallorca Cathedral (as it is not either the case of most similar constructions). Conversely, real construction processes involved intermediate stages where equilibrium was reached only thanks to auxiliary devices or, in a more hazardous way, by relying in the capacity of the incomplete structure. The order in which the structural members were built was essential to make the entire construction viable or to limit the construction difficulties.

As mentioned, the construction of Mallorca Cathedral followed a path involving the subsequent construction of the bays. The lateral vaults were built before the construction of the central ones. In this case, historical research has not provided, so far, any hint on the way the structures were stabilized while the central vault was not yet built. Several possibilities were considered by González et al. (2008).

First, the lateral vaults could have been stabilized by means of previously built transverse arches. If so, the almost 20m span arches would have needed some stabilizing extra weight to resist the thrust of the lateral vaults without experiencing inward deformation or collapse. Extra weight actually exists, although its original purpose might be different. Second, they could have been stabilized by means of auxiliary devices such as steel or timber ties across the lateral arches or struts across the central one. Third, they could have been built without any stabilizing element, the partial structure being (precariously) stable by itself thanks mainly to the available tensile strength.

Whatever the method, there was some hazard and chance for damage and deformation. This is consistent with the fact that the lateral deformations at the piers are very variable (almost “random”) although large in average, and suggests that the outcome was very sensitive to the skills and methods used by different builders. Moreover, maybe not only one stabilization procedure was used. Maybe different approaches (as the three ones mentioned) have been used during the certainly long and irregular construction process.

The longitudinal stability at intermediate stages is even more challenging as the piers had to face the unbalanced longitudinal thrust of both the lateral and central vaults. According to the historical information available, a previous construction of all the clerestory arches (as a way to stabilize the bays at intermediate stages) should be clearly disregarded. The use of possible temporary devices (temporary ties or buttressing walls) appears as a likely possibility,

3.4 Damage identification

Study on the building also carried out by González et al. (2008) revealed that the building has structural problems in terms of deformations and structural cracks that demand for more structural studies to understand the cause and future consequences. Very recently some of the minor damages have been repaired, therefore now it is not possible to find all those minor damages behind the repairs. The damages found are of three different types:

- *Cracking in piers*: Cracks exist in few piers of Mallorca Cathedral. They tend to concentrate close to the corners of the octagonal section (the less confined parts) and in some cases shape full wedges are partially or totally detached from the core of the pier.
- *Cracking in walls and façade*: Cracking, mostly developed along the mortar joints, can be also recognized in the exterior or clerestory walls. It can be linked to the out-of-plumbing experienced by the façade.
- *Deformation*: The deformation of the overall structure is perceptible. The piers show significant lateral deformation, reaching, in some cases, up to 30cm that is 1/100 of the height at the springing of the lateral vaults. Remarkably and as it was before mentioned, both the magnitude and the shape of the deformation vary very significantly (almost randomly) among the different bays, or even between the two halves of a single bay. The possibility of these deformations being mostly a consequence of errors and hazards experienced during the construction cannot be disregarded. The same applies to possible soil settlements estimated as a difference between architecturally related vertical references (such as opposite imposts, capitals or ach springing), which unevenness might be due, at least in part, to construction inaccuracies.

4. PREVIOUS STRUCTURAL ANALYSIS OF MALLORCA CATHEDRAL

4.1 Introduction

Till the present date, several studies with structural purposes have been carried out in Mallorca Cathedral, due to the great interest that exists towards the building. These studies had the aim to understand the structural behaviour of the cathedral and to assess its safety that became questionable to researchers from time to time in the analysis history. They constitute an invaluable starting point to understand the structural behaviour of the building.

Compared to its life period, and despite the amount of studies carried out, the history of analysis on Mallorca Cathedral is relatively new. However, it should be highlighted that the studies had a pioneer nature and that significantly contributed to the development and the practical application of structural analysis tools to complex structures.

In the present chapter it is presented from the earlier studies, the ones that used rigorous hand calculations (static graphic method), to the more recent ones that used modern computer codes.

4.2 Rubió i Bellver (1912)

The architect Joan Rubió I Bellver was disciple and collaborated with Antonio Gaudi in several works, which comprised the last big intervention in Mallorca Cathedral, from 1904 to 1914. Due to this last collaboration, Rubió I Bellver (1912) carried out a thrust line analysis by the static graphic method, which was a pioneer study. The static graphic analysis only considered the system composed by vaults and arches as well as the typical transversal bay subjected to self weight. After a laborious process, he obtained a thrust line that was totally contained within the thickness of the several structural members. The thrust line of the equilibrium solution appeared almost tangential to the perimeter of the pillar at the junction of the springing of the lateral vault (Figure 4.1).

Rubió I Bellver (1912) noted that his solution was consistent with the displacement of the pillars. He also noted that these structural vertical elements are not in the right place and that the damage could have been avoided if they were displaced out 45cm without changing the span of the arch.

According to Rubió I Bellver (1912), the pillars are subjected to both compression and flexural forces. Also, he concluded that the under battery of the flying arches have optimal shapes and weights. However, the upper battery generates thrust towards the central vault, forcing the placement of the extra weight that exists over the keystones of the vaults and the arches. Rubió I Bellver (1912) suggested that maybe the structure would have a better behaviour if these upper flying arches didn't exist.

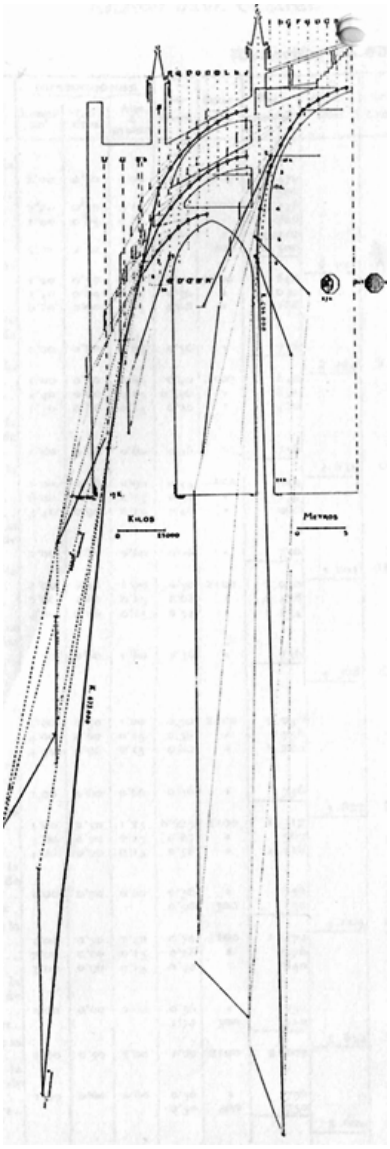

Figure 4.1 – Static graphic analysis by Rubió I Bellver (1912).

At the point of maximum pressure in the principal arches, a compression equal to 3.1MPa was reached, whereas in the pillars the maximum compression reached 4.5MPa. Both the values are small but near to the resistance of the material.

4.3 Mark (1982)

During the decade of 1970, Mark performed several studies applying the photo-elasticity method to historical structures. This method was initially introduced for complex mechanical analysis of components of airplanes and reinforced concrete structural elements. Later, Mark (1982) performed a comparison between Mallorca Cathedral and the French cathedrals Chartres and Bourges.

It was implemented a flat model on epoxy plastic plate describing the section of the structure. Scaled load equivalent to gravity and wind load were applied to the model and simultaneously the model was

heated at 50ºC. The material started to deform and the deformation remained even after removal of load. Then the model was observed through polar scope. The pattern of light interprets the qualitative distribution of internal forces. Figure 4.2 below shows the distribution of internal forces obtained by the photo-elastic model of Mallorca Cathedral.

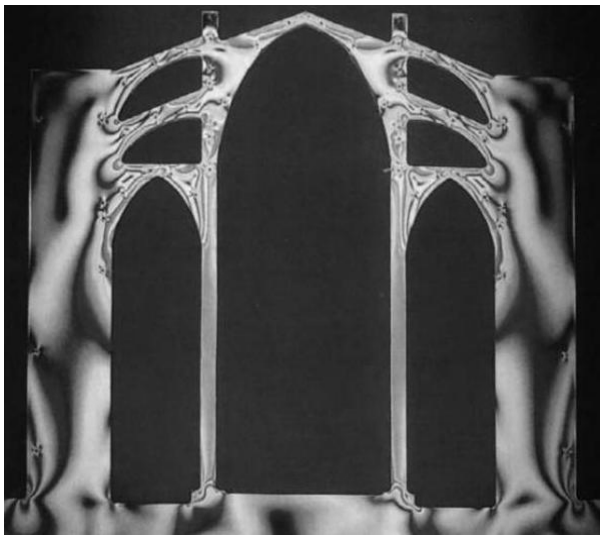

Figure 4.2 – Photo-elastic analysis by Mark (1982).

The results obtained by Mark (1982) are different from the ones obtained by Rubió I Bellvner (1912), leading to the conclusion that subjected only to the self weight, the Mallorca Cathedral's pillars have only compression stresses with a maximum value equal to 2.2MPa (Figure 4.2), while the latter obtained a value of 4.5MPa. This value is increased with 2.7MPa when the wind load is considered, with a design value equal to 130km/h.

It's then clear that there is flexural moment on the upper battery of the flying arches, which leaded to the shoring of some of these elements.

4.4 Maynou (2001)

By means of computer programming, Maynou (2001) carried out a more recent analysis in order to study the thrust lines. Several possible thrusts lines within the geometry of the structure were obtained (Figure 4.3), which presented a good agreement with the results obtained by Rubió i Bellver (1912).

He concluded that without taking into account the displacement of the pillars it is possible to obtain acceptable thrust lines, which it is not in agreement with Rubió i Bellver (1912). However, despising the displacement of the pillars the number of possible thrust lines is lower.

About the extra weight over the keystones of the vaults and the arches, this study is in agreement with Rubió i Bellver (1912), since it was concluded that its placement was justified to provide stability to the structure, since without the mentioned weights, less possible thrust lines were found.

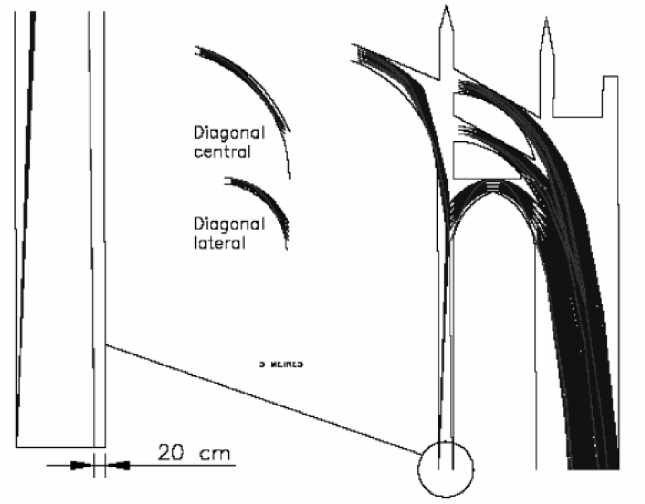

Figure 4.3 – Thrust line analysis by Maynou (2001).

It was also noted that the under battery of the flying arches were correctly positioned since the thrust line crosses it in its upper section in the central zone. The latter is also in accordance with Rubió i Bellver (1912).

However both studies disagree in the length that the pillars should be displaced out to avoid their displacements, since Maynou (2001) provides a value of 31cm, that is different from the 45cm proposed by Rubió i Bellver (1912).

4.5 Salas (2002)

Salas (2002) carried out a structural analysis of Mallorca Cathedral using two different methods and made a comparison between both results. One of the methods is the well known finite element method with an isotropic damage model and the other one is a generalized matrix formulation. The latter is a method to analyze 3D structures with curve geometry and elements with variable section.

Using both methods, the gravity load had to be multiplied by a factor around 1.7 to achieve the collapse of the structure. Figure 4.4 shows the collapse mechanism of the structure in this load condition.

The model based on the generalized matrix formulation resulted to be more versatile than the finite element method identifying damage in the structure and predicting collapse mechanisms.

It was also understood the justification of the extra weight over the keystones of the vaults and the arches to stabilize the structure, as it assures the safety of the structure since without these elements the analysis indicates that the structure is not capable of supporting its own self weight, being obtained a factor for the self weight equal to 0.9. Figure 4.5 and Figure 4.6 shows the collapse mechanism in this particular condition.

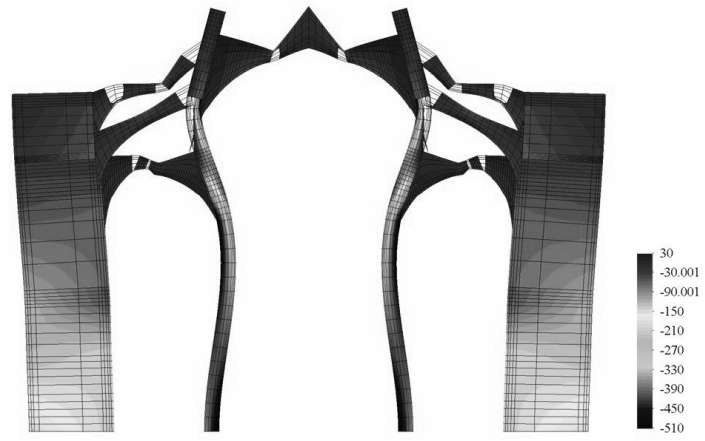

Figure 4.4 – Collapse mechanism of the generalized matrix formulation model corresponding to a gravity load factor of 1.7 (Salas (2002)).

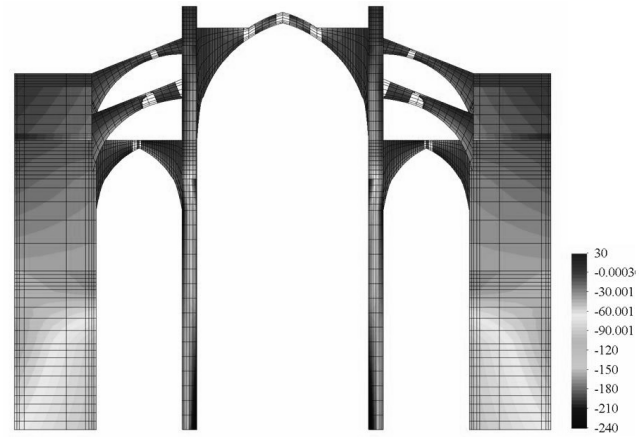

Figure 4.5 – Stresses of the generalized matrix formulation model without the extra weights corresponding to a gravity load factor of 0.9 (Salas (2002)).

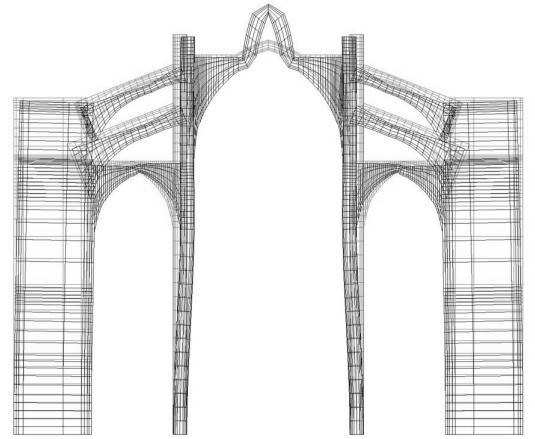

Figure 4.6 – Deformed shape of the generalized matrix formulation model without the extra weights corresponding to a gravity load factor of 0.9 (Salas (2002)).

Neglecting the weight and the stiffness of the upper battery of the flying arches, the models provided a gravity load factor equal to 0.7. In Figure 4.7 it is showed the collapse mechanism corresponding to this situation. It is remarkable the clear understand of the structural system by who introduced this upper battery of flying arches.

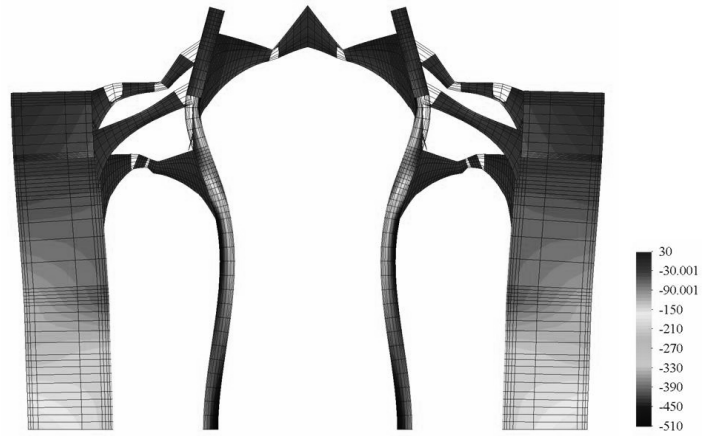

Figure 4.7 – Stresses of the generalized matrix formulation model corresponding to a gravity load factor of 1.7 and neglecting the upper battery of flying arches (Salas (2002)).

However, if along with the upper battery of flying arches the extra weights are also neglected, the system not only is stable, but also it has to reach a gravity load factor equal to 1.6 in order to collapse.

The structure resists to a seismic design acceleration equal to 0.12g, which is equivalent to a return period of 1000 years, according to Salas (2002). About the wind, the structure reached a pressure equal to 1.45kN/m^2. In both cases, the resulting condition of the structure is very severe and seems to be near collapse. The collapse mechanisms are similar (Figure 4.8) and it was also possible to verify that both the lateral loads resulted in similar formation of cracks.

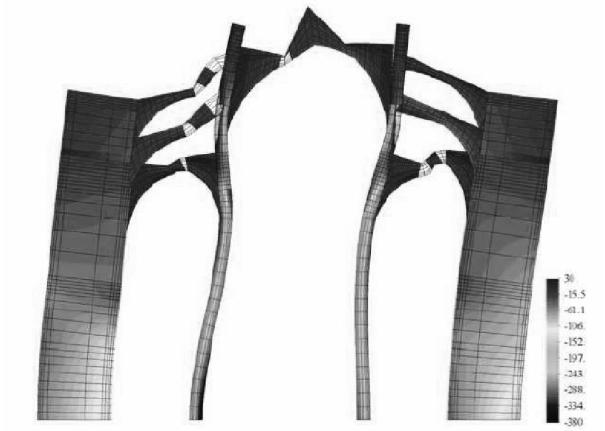

Figure 4.8 – Distribution of normal stresses, cracking and deformation of the generalized matrix formulation model corresponding to a wind pressure of 1.45kN/m^2 (Salas (2002)).

4.6 Clemente (2006)

More recently, Clemente (2006) presented an analysis of the typical bays of Mallorca Cathedral applying a nonlinear 3D finite element model, built through the geometry created before by Casarin and Magagna (2001). Clemente (2006) used both a distributed damage model and a localized damage model. An important material parameter for the modelling is the fracture energy that in the study carried out by Clemente (2006) was considered infinite. This consideration may overestimate the results since the softening is a very important phenomenon in the case of masonry.

A first nonlinear localized damage model was built in order to analyze the bay under instantaneous gravity loading. The deformed shaped obtained showed displacements of the pillars towards the central part of the building whereas the buttress displaced towards the exterior part of the structure (Figure 4.9). Both tendencies coincide qualitatively with real condition observed in the structure. However, the maximum displacement obtained for the pillar was 0.76cm while the real state of the structure showed that the displacements in the pillar vary from 4cm to 16cm.

The same model was used for simulating the construction process in two phases in order to understand the effect of sequence loading. The first phase of the construction considered is the construction of the lateral vaults, so the model is the one represented in Figure 4.10. Analysis of the first phase shows that horizontal displacement of the upper part of the pillar reached to 3cm, which is four times higher than the displacement obtained in the previous case. The latter confirmed the deformation of the pillar during the construction of the structure. In the second phase of the analysis the value for the displacement of the pillar obtained was 1.84cm which is still much higher than the previous case.

Figure 4.9 – Deformed shape of the typical bay corresponding to the instantaneous gravity load obtained by (Clemente (2006)).

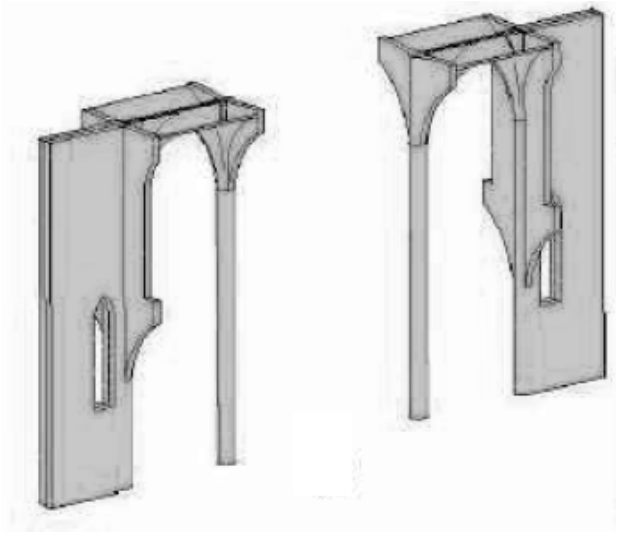

Figure 4.10 – First phase of the construction process simulated by (Clemente (2006)).

Also the effect of the creep of material due to long term loading was analyzed. A three step sequential analysis was performed in this case, being the first two steps done in order to simulate the construction process like in the previous model and the third one was done in order to observe the increase of deformation as a result of creep of material. There was a good agreement with the horizontal displacement in the real structure and the displacement obtained by the model.

The same analysis was carried out again, this time using a large displacement formulation instead of small displacement formulation as it was used before. With the large deformation formulation, it is not only taken into account the material non linearity, but also the geometrical non linearity. Clemente (2006) showed that due to the effect of creep, damage progress gradually in the lateral vault, inner face of the pillar and in the clerestory towards the collapse (Figure 4.11).

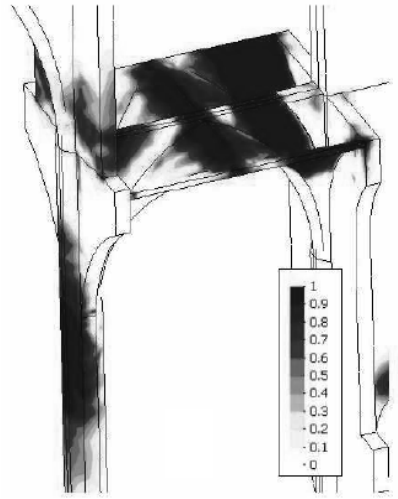

Figure 4.11 – Distribution of tension in collapse due to creep effect (Clemente (2006)).

Also complete 2D and 3D models were built considering both distributed and localized damage model. Two load cases, namely gravity and horizontal seismic load in the terms of gravity, were applied in consecutive phases. The models with distributed damage yielded a seismic collapse load factor equal to 0.1 of the gravity load. The deformed shape and the tension damage can be observed in Figure 4.12. The result obtained with localized damage generated higher collapse load.

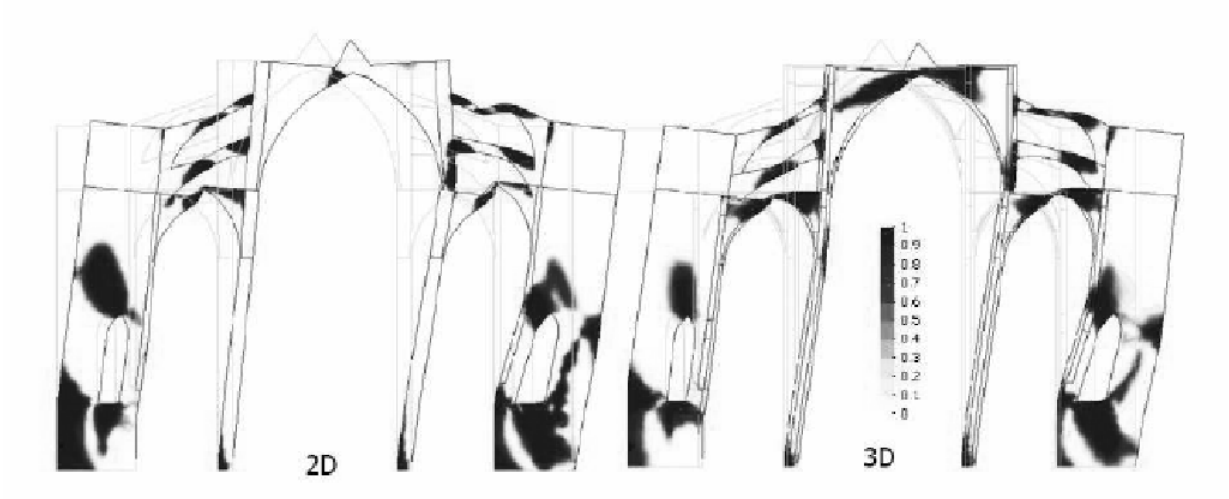

Figure 4.12 – Collapse mechanism and tension damage obtained with seismic analysis (Clemente (2006)).

4.7 Martinez (2007)

Martinez (2007) developed a methodology for the assessment of the seismic vulnerability of historical constructions, considering the seismic risk of the location and analytical models calibrated through the attainment of dynamic properties of the soil and the structure. In order to develop this methodology, the tasks carried out by Martinez (2007) were:

- to obtain the dynamic properties of Mallorca Cathedral:
- to develop a detailed finite element model of the cathedral with the calibration done through the dynamic properties obtained;
- to characterize the soil of the cathedral through dynamic methods (Figure 4.13);
- to assess the seismic vulnerability of the cathedral applying simplified methods based of vulnerability indexes;
- to carry out a deterministic and probabilistic study of the seismic risk in order to obtain the demand spectrums for the cathedral;
- to determine its seismic vulnerability as a function of the damage expected by the structural model through the capacity spectrum method;

- to obtain fragility curves for the different macroelements that compose the Mallorca Cathedral.

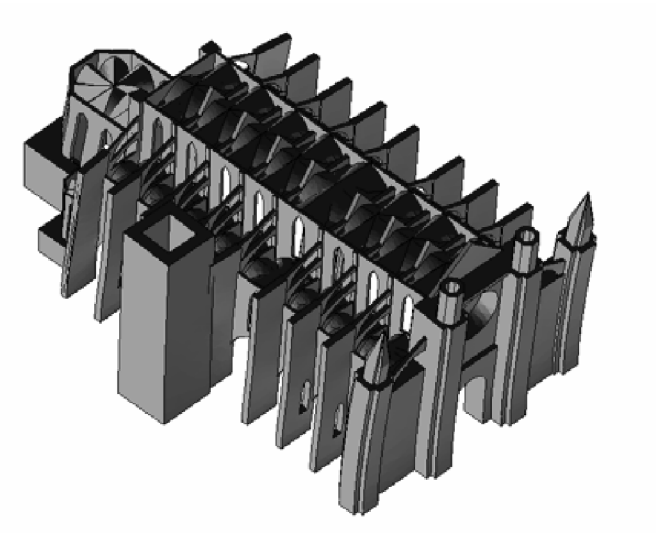

Figure 4.13 – First mode of vibration obtained by the modelling carried out by Martinez (2007).

According to Martinez (2007), an accurate approach for the seismic design is to consider the demand given by an envelope of a great number of response spectrums registered in the place where it is intended to evaluate the structure. However, this definition has a lack of practical application when it is not possible to count with a great amount of accelerometric registers and that's why the design spectrums are usually built through seismic hazard studies.

Martinez (2007) used two types of analysis for the evaluation of the seismic hazard: the deterministic and the probabilistic.

The deterministic is based on the assumption that the historic seismicity of a region is enough in order to obtain the seismic hazard. Therefore, Martinez (2007) established a possible seismic scenario based on the earthquakes that occurred in the past. In Table 4.1 is presented this deterministic scenario considered.

Table 4.1 – Earthquakes used for the deterministic scenario by Martinez (2007).

Date	Latitude N	Longitude E	I0	ML	Epicentral distance (km)
02/02/1428	42° 18'	2° 20'	IX-X	6.4	304.5
25/05/1448	41° 38'	2° 24'	VII-VIII	5.4	230.1
15/05/1851	39° 36'	2° 48'	VIII	5.4	13
21/05/2003	36° 48.6'	3° 49.8'	-	6.7	324.7

After obtaining the maximum probable magnitudes and the epicentral distances of the earthquakes, it was necessary to analyze the effect of those events in the site of study. Therefore, it is common to use attenuation relations elaborated from seismic information of the site. Several semi-empirical attenuation relations have been proposed. Martinez (2007) used the ones proposed by Ambraseys et

al. (1996) that were developed based on a catalogue made to Europe and adjacent areas in terms of magnitude, epicentral distance and local geology. With these relations, the spectrums obtained were the ones presented in Figure 4.14.

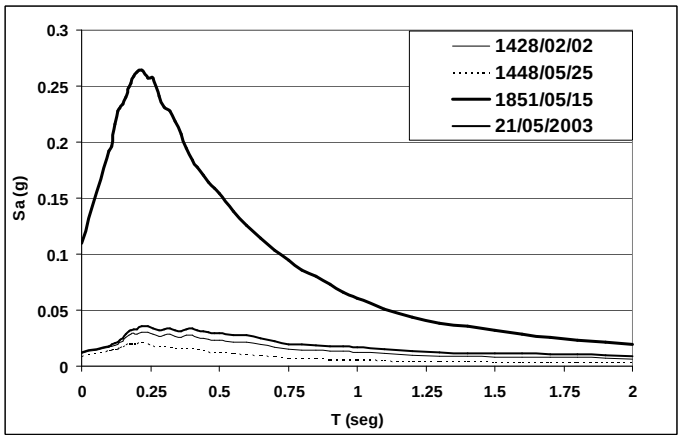

Figure 4.14 – Deterministic scenario spectrums according to Martinez (2007).

Due to the significant uncertainties that still exist with respect to the dynamic properties of Mallorca Cathedral, the softening of the site spectrums was carried out. The criteria established in the European code EC8 (1998) were used.

Knowing the maximum acceleration of the ground associated to the vibration period equal to zero and the maximum acceleration of the site spectrum, Martinez (2007) obtained the elastic response spectrum the Figure 4.15, considering a soil type B.

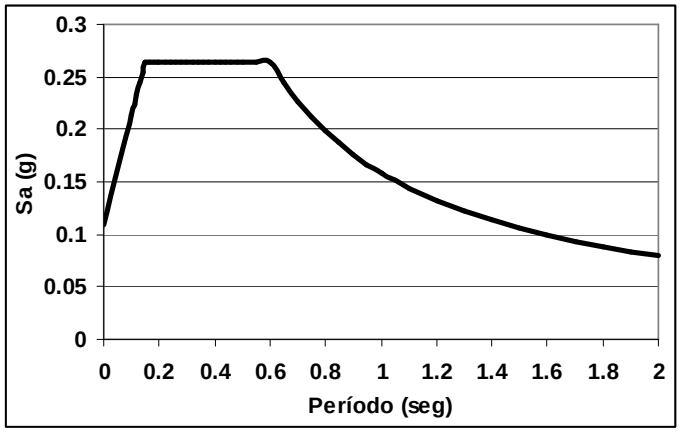

Figure 4.15 – Spectral acceleration spectrum considering the deterministic scenario (Martinez (2007)).

For the probabilistic estimation of the seismic hazard for the Mallorca Cathedral in terms of spectral values of acceleration, Martinez (2007) used the information provided by GSHAP (Global Seismic Hazard Assessment Program). Like in the previous case, the attenuation relation proposed by Ambraseys et al. (1996) was used, so that the response spectrum presented on Figure 4.16 was

obtained. It corresponds to a firm or rock soil, with a 5% of the critical damping and for return periods (Tr) of 475 and 975 years.

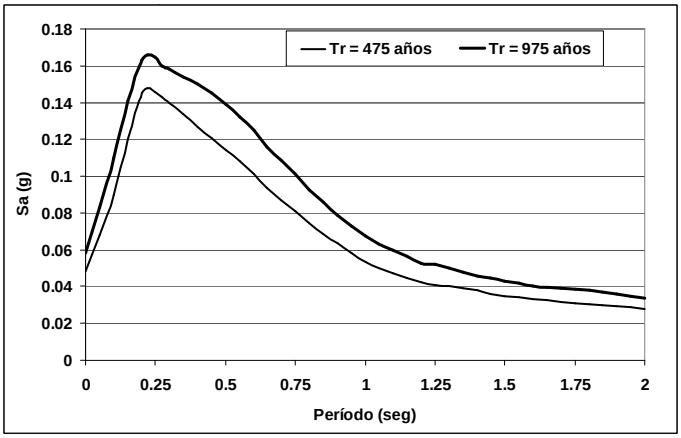

Figure 4.16 – Response spectrums of uniform hazard on firm soil for return periods equal to 475 and 975 years according to Martinez (2007).

Since these results correspond to a firm soil, Martinez (2007) carried out an implementation of viable alternatives to estimate the amplification site effects in a practical way. Through the application of the unidimensional theory of propagation of seismic waves within a soil mass, Martinez (2007) obtained the accelerometric registers and the response spectrums for Mallorca Cathedral on soft soil, with 5% of critical damping and return periods of 475 and 975 years presented on Figure 4.17 and Figure 4.18, respectively.

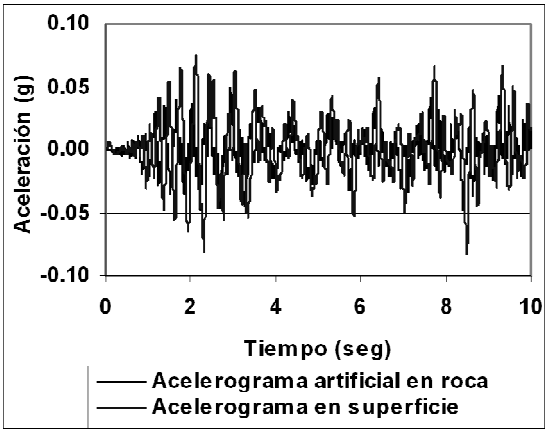

(a) Accelerometric register

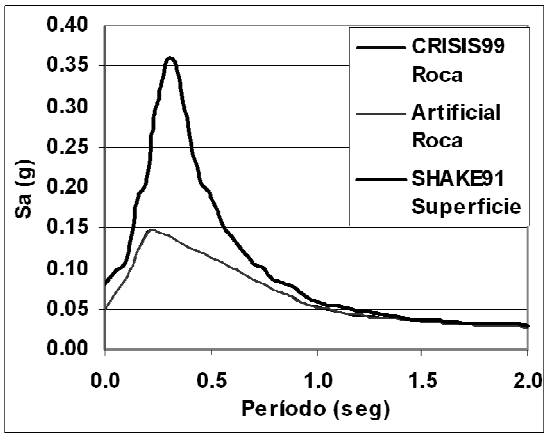

(b) Site spectrums

Figure 4.17 – Probabilistic estimation of seismic hazard for Mallorca Cathedral with a return period of 475 years obtained by Martinez (2007).

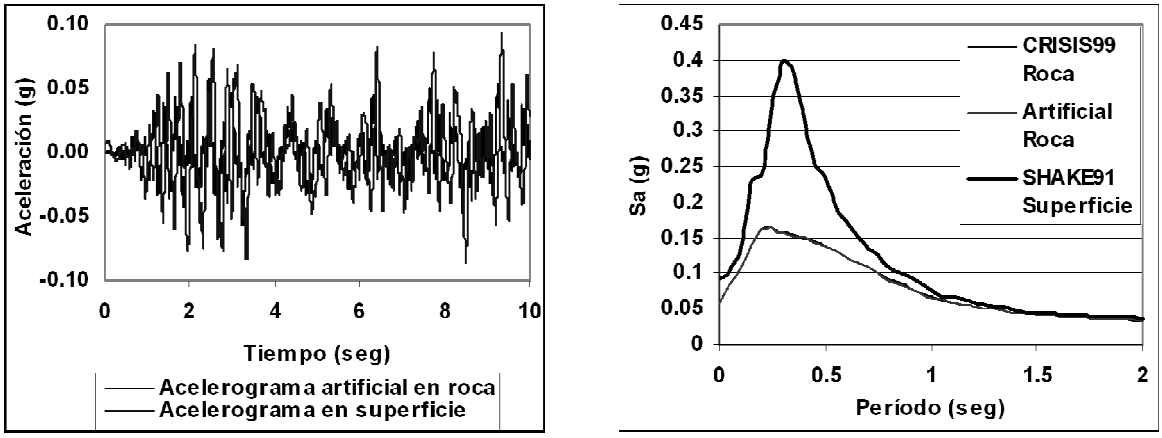

(a) Accelerometric register (b) Site spectrums

Figure 4.18 – Probabilistic estimation of seismic hazard for Mallorca Cathedral with a return period of 975 years obtained by Martinez (2007).

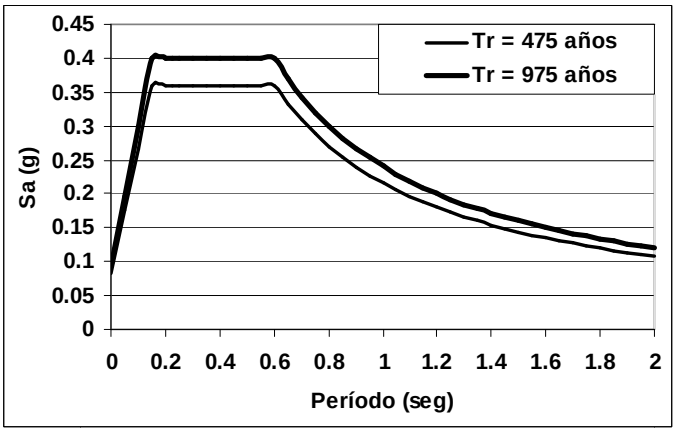

Figure 4.19 – Spectral acceleration spectrum considering the probabilistic scenario and return periods of 475 and 975 years (Martinez (2007)).

Considering these demand spectrums, one of the main conclusions taken by Martinez (2007) with the results obtained for the Mallorca Cathedral was that the most vulnerable direction of the building is the longitudinal. This is due to the abrupt changes of stiffness in the plan and in the height of the building and also due to the existence of few resistant elements to the seismic shear forces. It was also concluded that within the transversal direction of the building, the macroelements corresponding to the transept present the lowest seismic performance.

Martinez (2007) emphasized that in general terms, Mallorca Cathedral has an acceptable seismic resistance capacity to the demand levels considered. However, this conclusion doesn't imply that local damage in walls, vaults or pillars should not be expected.

4.8 Das (2008)

Das (2008) presented structural analysis of historical masonry constructions as well as the challenges in this field with a study of Mallorca Cathedral where the consequence of the past construction and alterations were analyzed. The aim was to find the safety both for gravity load and lateral seismic load.

The analyses were performed for a 3D model of a single bay similar as the one used by Clemente (2006) (Figure 4.20). In contrast to the infinite fracture energy used by the latter, in Das (2008) very low fracture energy was used. A model with modified modulus of elasticity reproduced well the dynamic properties of the structure, near to the properties obtained in field experiment and obtained in the global model prepared by Martinez (2007).

Analysis of the structure for gravity load considering both linear and nonlinear material was found to have a good agreement with Clemente (2006), being the differences due to the improved modulus of elasticity. Gravity load applied till collapse resulted in a load factor of 1.62 which was smaller than the one from Clemente (2006) but close to that obtained by Salas (2002).

(a) Transversal section (b) Isometric view

Figure 4.20 – Geometry of the bay of Mallorca Cathedral (Das (2008)).

Seismic load analysis performed by applying step by step increment load proportional to mass yielded collapse load factor of 0.056. When the force was applied according to first mode the load factor obtained was 0.0874.

Finally the capacity spectrum method had been applied to find the displacement demand corresponding to a demand earthquake. Intersection of the demand spectrum corresponding to an earthquake of peak ground acceleration of 0.048g with a return period of 475 years showed that the structure has a good seismic resistance.

4.9 Cuzzilla (2008)

Cuzzila (2008) applied the limit analysis and the capacity spectrum method to three Gothic churches, which included Mallorca Cathedral, in order to have a better understanding of the seismic behaviour of Gothic structures. The safety factor and the level of damages expected was studied in these churches, resulting from the seismic action present in both in the EC 8 and the Spanish seismic code NCSE-02 (2002).

Cuzzila (2008) divided Mallorca Cathedral's West façade in five different macroelements and for each a proper collapse mechanism has been studied (Figure 4.21). He concluded that Mallorca Cathedral's West façade is substantial safe under seismic action.

He also studied the transversal action applied on the structure applying the capacity spectrum method with the curves obtained by another authors. For this action, it was possible to conclude that moderate damage may be expected for the seismic action recommended both in European and Spanish codes. The damage level has been taken from Lagomarsino et al. (2003).

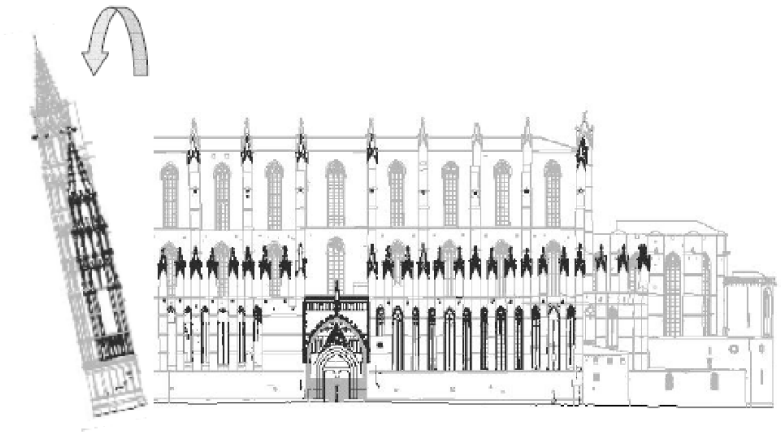

Figure 4.21 – Example of a collapse mechanism of Mallorca Cathedral (Cuzzila (2008)).

The results obtained by Cuzzila (2008) are summarized in Table 4.2.

He also stated that it is possible to increase the safety level or reduce the possible damages due to seismic action on the structures studied. However, taking into account the state of conservation of the structure and the costs to realize a proper strengthening system, this kind of intervention was considered useless for the case of Mallorca Cathedral.

About the method, Cuzzila (2008) concluded that reasonable results can be obtained by limit analysis and capacity spectrum method. These methods are useful to have a realistic idea about the seismic behaviour of a structure, using a simple approach considering the safety factor and the damage level.

Table 4.2 – Results obtained for Mallorca Cathedral (Cuzzila (2008)).

Mechanism	Typology	NCSE02		EC8	
		Safety Factor	Damage level	Safety Factor	Damage level
1	whole façade	8.68	D0	8.16	D0
2	central whole façade	7.58	D0	7.38	D0
3	upper façade with rose window	5.86	D0	5.77	D0
3 mode	upper façade with rose window	5.86	D0	5.01	D0
4	upper façade without rose window	7.06	D0	7.3	D0
4 mode	upper façade without rose window	5.88	D0	5.54	D0
5	tower	6	D0	5.58	D0
6 - Martinez	typical transept	5.9	D1	5.51	D1
6 - Vacas	transept	3.32	D1	2.9	D1

4.10 Vacas (2009)

Vacas (2009) also carried out a study which main objectives were to apply the capacity spectrum method to the macroelements of the main façades and the typical bays of several churches, comprising the Mallorca Cathedral, and to justify the damage that the several previous earthquakes had caused. It was also his purpose to recommend interventions in order to avoid severe damages in future earthquakes.

In Vacas (2009), the macroelements of the main façade (Figure 4.22) and of the typical bay were modelled (Figure 4.23). The seismic action was considered according to the Spanish code NSCE-02. It was defined as elastic over-damped response spectrum in order to take into account the significant amount of energy dissipation that can be produced during the evolution of a kinematic mechanism in the case of monumental buildings.

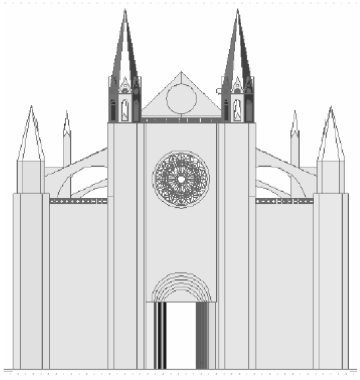

Figure 4.22 – Model of the West façade (Vacas (2009)).

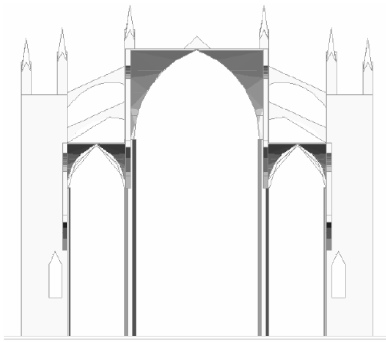

Figure 4.23 – Model of the single bay (Vacas (2009)).

It was concluded that the West façade of the Mallorca Cathedral presents a good structural behaviour when subjected to seismic action. Among the studied mechanisms, the expected damages are light to moderate. However, a higher level of damage can be expected on the upper part of the façade, but without causing its collapse.

Due to the too complex kinematic mechanism, the typical bay was not analyzed in Vacas (2009) work. However, he proposed a collapse mechanism without calculating it.

4.11 Rodriguez (2009)

Rodriguez (2009) also applied the capacity spectrum method to Mallorca Cathedral, but to have a better understanding of the seismic behaviour of the East façade. Rodriguez (2009) studied the safety factor and the same level damages as Rodriguez (2009) did.

Four collapse mechanisms of the East façade of Mallorca Cathedral were considered and the seismic action was determined according to EC 8, the Spanish seismic code NSCE-02 and also according to the deterministic and probabilistic scenarios determined by Martinez (2007) (Figure 4.24).

After this comparison and noticing the higher demand of the deterministic and probabilistic scenarios, it was stated that conventional codes, mostly oriented to modern structures, may not be adequate for the study of ancient structures and may lead to inaccurate results. A better approach is to take into account possible evidence coming from history, the inspection of the structure in its present condition, monitoring and structural analysis. It was also stated that the results obtained from this approach may contribute to a better understanding of the real condition of the structure and its real needs for seismic upgrading.

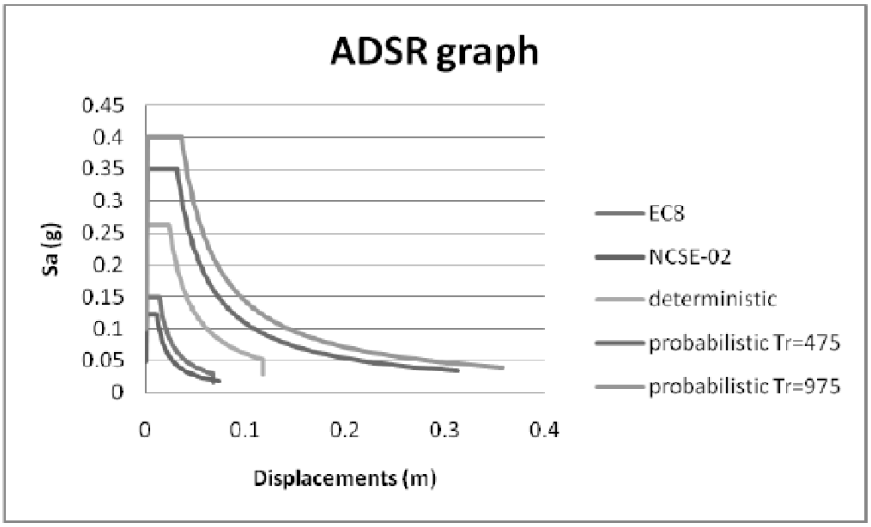

Figure 4.24 – Comparison between the ADSR graphics (Rodriguez (2009)).

Considering the probabilistic scenarios, damage was expected to occur in two mechanisms of the East façade which leaded to the conclusion that strengthening is needed. Therefore, a strengthening solution with tie rods was recommended.

5. SEISMIC ANALYSIS

5.1 Local mechanisms

For the seismic analysis of Mallorca Cathedral, the local mechanisms that are likely to collapse or to cause severe damage are studied. Fourteen mechanisms are chosen, mainly located in the West and East façade. The façades are likely to present significant damage, or even its collapse, during an earthquake, since they are only supported and supporting actions from one of their sides. Thus it is more likely for them, or parts of them, to overturn, when compared to other elements of the building. Apart from the mechanisms on the façade, it is also studied two mechanisms due to the horizontal action on the transversal direction on the building. For this last study, the macroelements considered are a single typical bay and the cathedral transept.

Following, the mechanisms are presented along with the geometry model that was developed based on the photogrametry provided by Gonzalez and Roca (2000). The geometric model was built so that the weights of the several macroelements could be measured.

- **Mechanism 1**

The mechanism 1 corresponds to the overturning of the whole West façade. Since in 1851 the façade had collapsed and was totally rebuilt after, it leads to the conclusion that maybe the interlocking between this element and the rest of the building is not totally efficient. Therefore, during a seismic event, the structural response of this element may be independent of the rest of the building. The mechanism is schematized through the geometrical model on Figure 5.1.

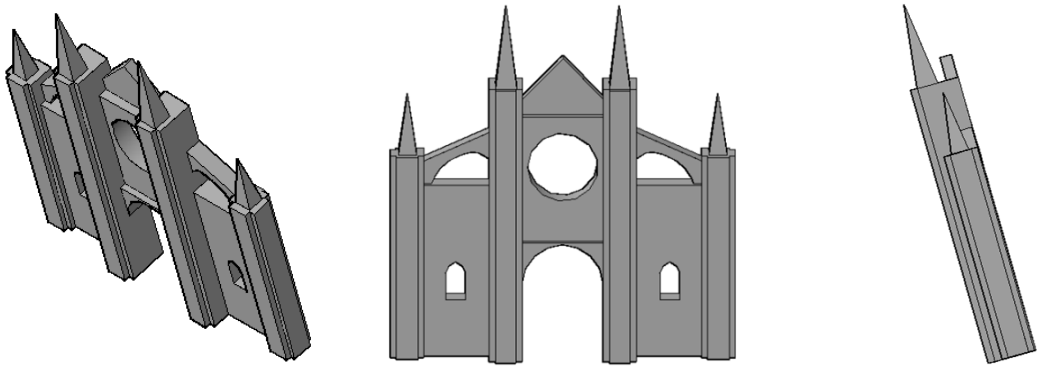

(a) Isometric view (b) Front view (c) Lateral view

Figure 5.1 – Mechanism 1.

- **Mechanism 2**

The mechanism 2 corresponds to overturning of the central of the West façade. Since the central buttresses get the thrust from the central and the lateral vaults, the detachment of this part may occur

if an earthquake in the longitudinal direction of the building occurs. The mechanism is schematized through the geometrical model on Figure 5.2.

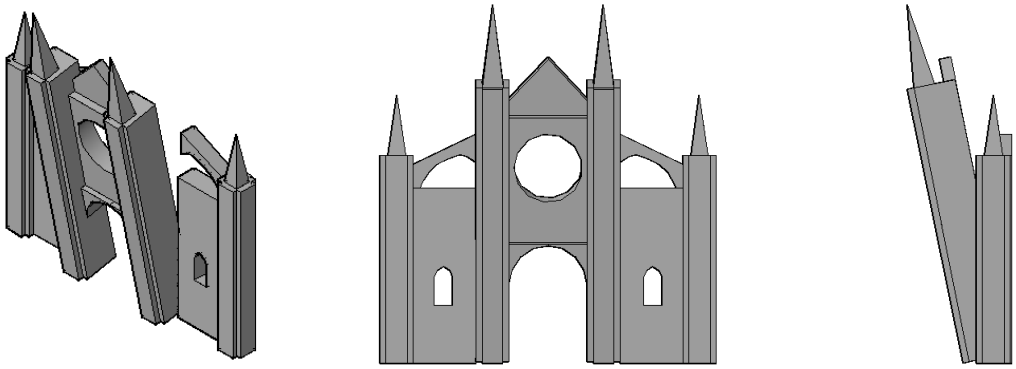

(a) Isometric view (b) Front view (c) Lateral view

Figure 5.2 – Mechanism 2.

- **Mechanism 3**

The mechanism 3 corresponds to the overturning of the upper part of the West façade, which includes the rose window, as schematized in Figure 5.3. Since the surrounding parts are stiffer, the macroelement considered in this mechanism may have an independent seismic response if the interlocking between both parts is not efficient.

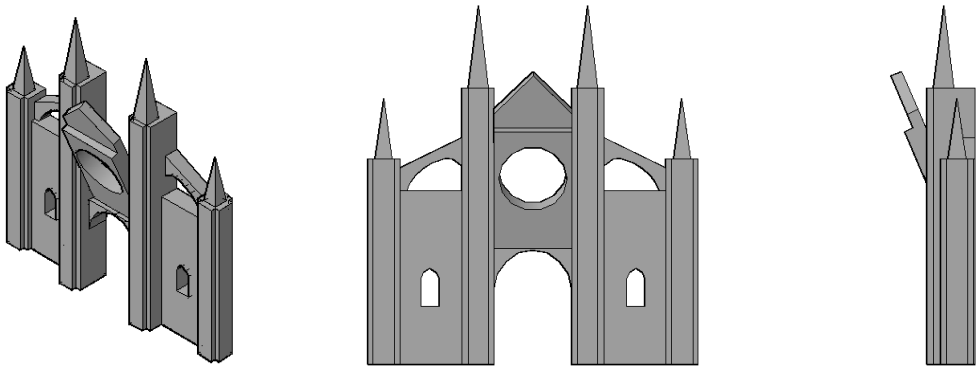

(a) Isometric view (b) Front view (c) Lateral view

Figure 5.3 – Mechanism 3.

- **Mechanism 4**

The mechanism 4 corresponds to the overturning of the upper part of the West façade, limited at middle height of the rose as schematized in Figure 5.4. This seems to be a mechanism that is likely to occur because of the small contact area between this and the under part. The interlocking with the the central towers may not be efficient because of the same reasons explained above.

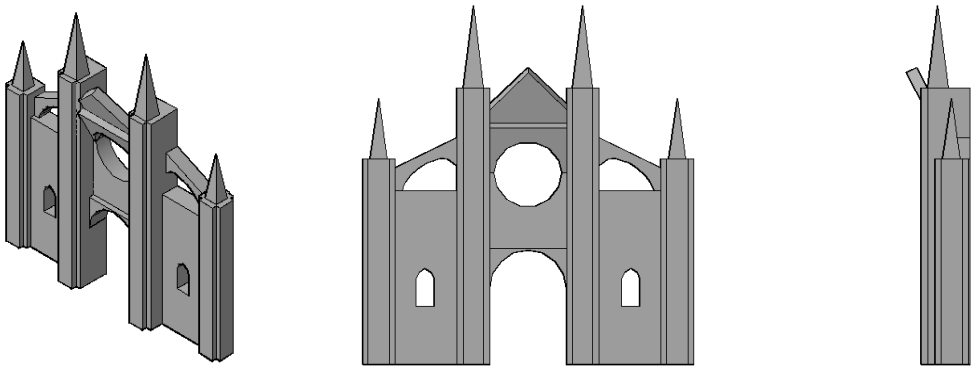

(a) Isometric view (b) Front view (c) Lateral view

Figure 5.4 – Mechanism 4.

- **Mechanism 5**

The mechanism 5 corresponds to the overturning of the upper part of the central part of the West façade, over the rose window as schematized in Figure 5.5.

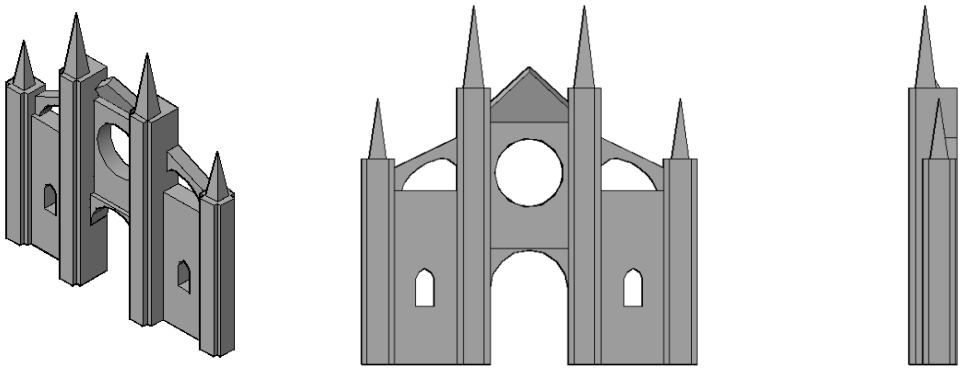

(a) Isometric view (b) Front view (c) Lateral view

Figure 5.5 – Mechanism 5.

This part of the façade is intrinsically vulnerable because of its configuration. This may be understood better by the observation of the photographs presented on Figure 5.6.

Figure 5.6 – Photographs of mechanism 5 (photograph on the right taken from Vacas (2009)).

- **Mechanism 6**

The mechanism 6 corresponds to the overturning of a central buttress. Similarly to the mechanism 2, the thrusts from the vaults may cause the detachment of this element. The mechanism is schematized on Figure 5.7.

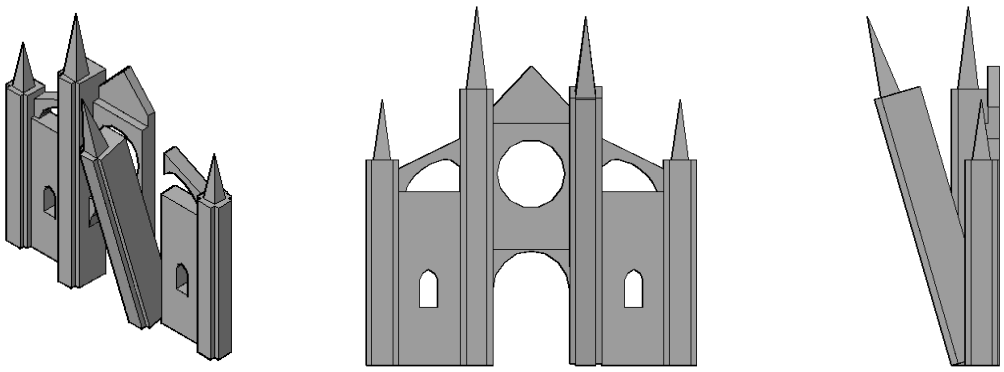

(a) Isometric view (b) Front view (c) Lateral view

Figure 5.7 – Mechanism 6.

- **Mechanism 7**

The mechanism 7 corresponds to the overturning of a lateral buttress of the West façade in the longitudinal direction. Since this macroelement is only connected to a flying arch and the wall under it, it may overturn in this direction if an earthquake occurs. The mechanism is schematized in Figure 5.8.

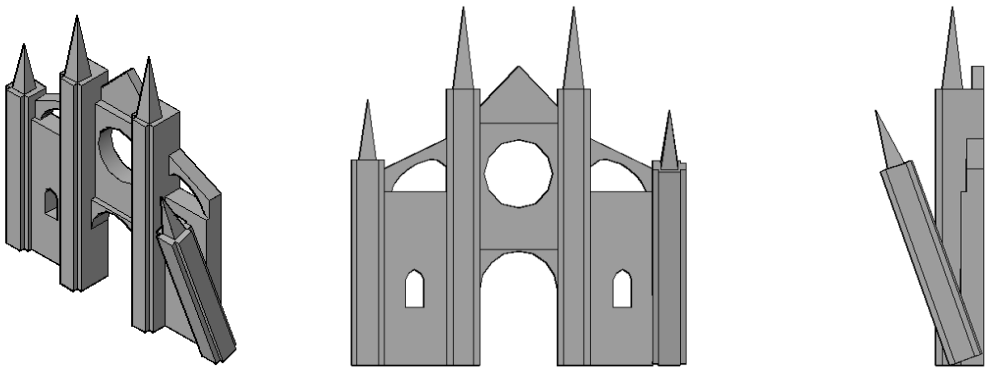

(a) Isometric view (b) Front view (c) Lateral view

Figure 5.8 – Mechanism 7.

- **Mechanism 8**

The mechanism 8 corresponds to the transversal overturning of a lateral buttress of the West façader. The same that was stated for mechanism 7 is applied here. This mechanism corresponds to the possibility of great ground motions due to the earthquake occurring in the transversal direction of the building. The mechanism is presented on the Figure 5.9.

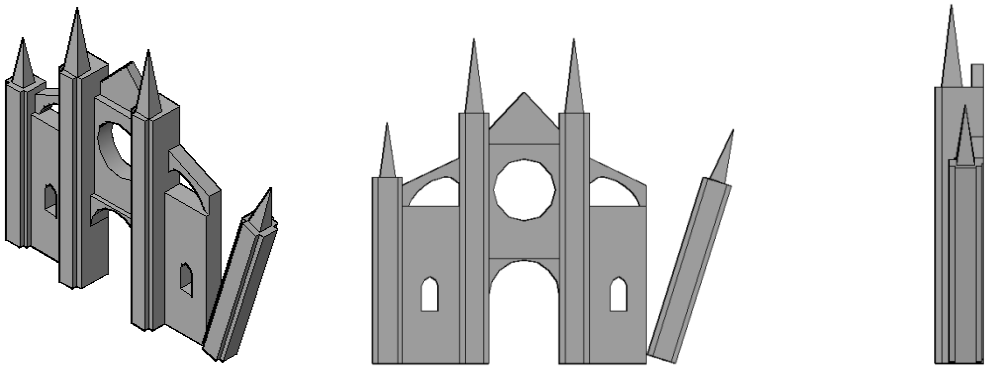

(a) Isometric view (b) Front view (c) Lateral view

Figure 5.9 – Mechanism 8.

- **Mechanism 9**

The mechanism 9 corresponds to the transversal action on a typical bay of the building.

Because of the presence of flying arches, the calculation of the kinematic of the bay is too complex, although Vacas (2009) proposed a possible failure mode (Figure 5.10) where it is necessary the formation of 26 hinges for the formation of the mechanism.

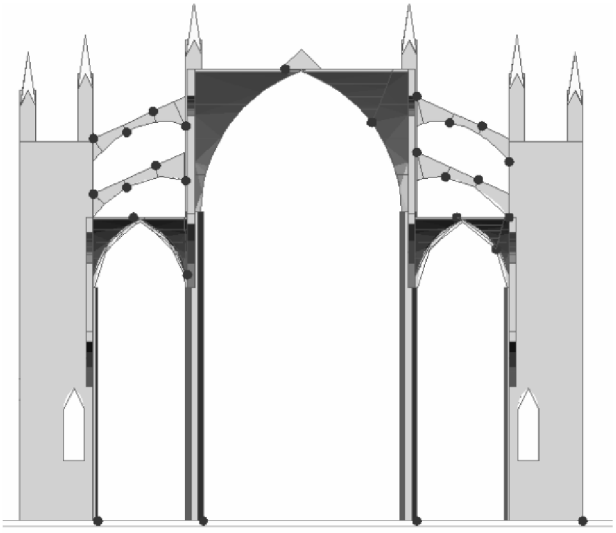

Figure 5.10 – Failure mode proposed for a typical bay by Vacas (2009).

Because of its complexity, the kinematic calculation was not carried out by Vacas (2009). In the present study, the transversal action on a typical bay will be studied through a pushover analysis using the finite element modelling (Figure 5.11) and the results for the capacity curve of the corresponding macroelement obtained by Martinez (2007).

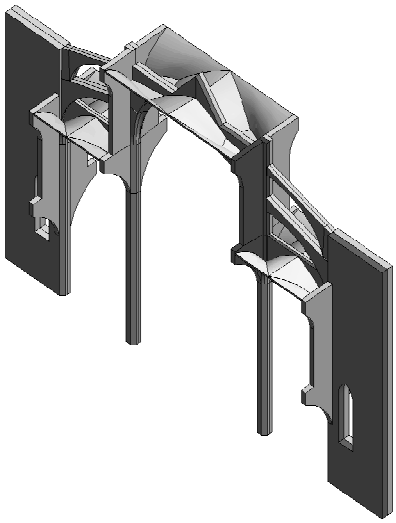

Figure 5.11 – Modelling of the macroelement corresponding to a typical bay by Martinez (2007).

- **Mechanism 10**

In the same way as in the mechanism 9, the transversal action of the transept will be analyzed through a pushover analysis using also the modelling carried out by Martinez (2007) and the corresponding results for the capacity curve. The modelling is presented on Figure 5.12.

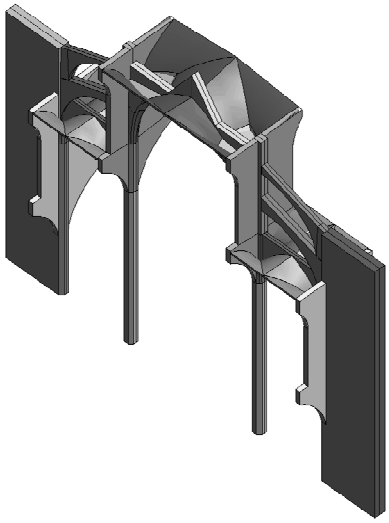

Figure 5.12 – Modelling of the macroelement corresponding to the transept by Martinez (2007).

- **Mechanism 11**

The mechanism 11 corresponds to the overturning of the whole upper part of the East façade. Under this part the structure is equilibrated by the Royal and the other chapels located there. Therefore, in the case of great ground motions due to an earthquake on the longitudinal direction of the building, the under part is not expected to overturn. This mechanism is schematized on Figure 5.13.

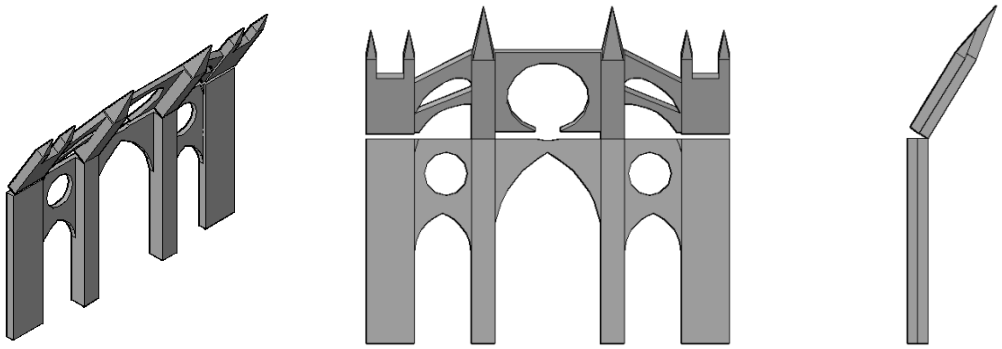

(a) Isometric view (b) Front view (c) Lateral view

Figure 5.13 – Mechanism 11.

- **Mechanism 12**

The mechanism 12 corresponds to the overturning of the upper part of the buttresses of the East façade. This mechanism accounts with the possibility that the buttress may have an independent seismic response than the rest of the façade because of the higher stiffness and the possible bad interlocking with adjacent elements. Like stated for the mechanism 11, it is likely that the under part will not overturn since it if confined by the chapels. The mechanism is schematized in Figure 5.14.

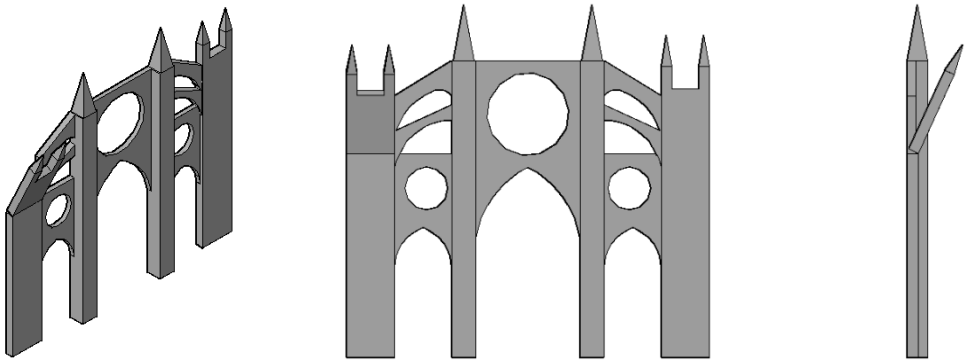

(a) Isometric view (b) Front view (c) Lateral view

Figure 5.14 – Mechanism 12.

- **Mechanism 13**

The mechanism 13 corresponds to the overturning in the transversal direction of the building of a buttress of the East façade. This possibility of a local collapse is due to the aforementioned possible independent seismic response of the buttress and because of the thrust from the vaults on the transversal direction of the building. The mechanism is schematized on Figure 5.15.

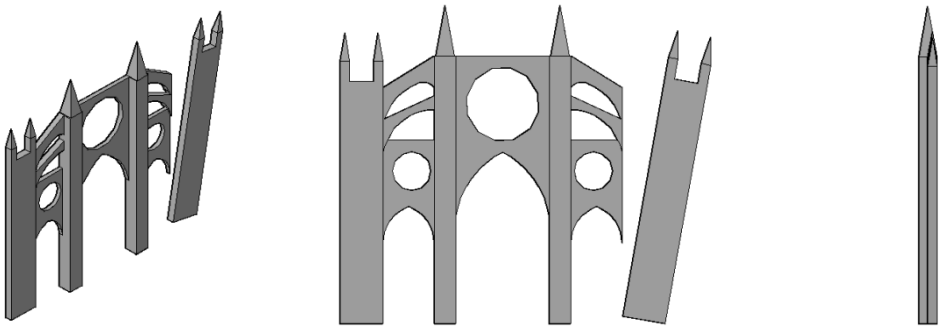

(a) Isometric view (b) Front view (c) Lateral view

Figure 5.15 – Mechanism 13.

- **Mechanism 14**

The mechanism 14 corresponds to the overturning of the central upper part of the East façade. Since the seismic response of this and the buttresses may be independent, it seems reasonable to consider this mechanism. It is schematized of Figure 5.16.

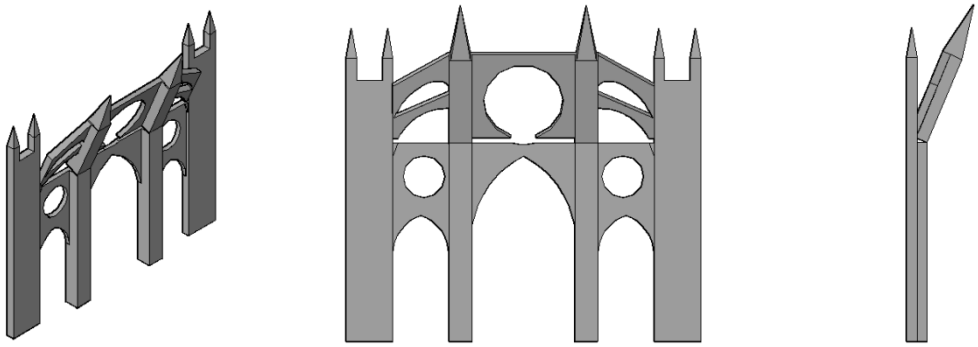

(a) Isometric view (b) Front view (c) Lateral view

Figure 5.16 – Mechanism 14.

5.2 Seismic demand spectrum

To evaluate the seismic demand of the Mallorca Cathedral, four different approaches will be used. One is to use the response spectrum presented in the Spanish code NSCE-02 (2002). Another is to use the EC8 (1998). The other two approaches are the use of the determinist and a probabilistic estimation carried out by Martinez (2007) for Mallorca Cathedral, which determination is detailed in section 4.7.

- **NSCE-02**

In the case of Palma de Mallorca, the maximum acceleration in firm soil, called basic seismic acceleration, a_b, is equal to 0.04g, according to NSCE-02. Applying the specifications of the code to obtain the design seismic acceleration, a_c, it is obtained the Equation (13). In this equation a_b is taken

as above. The parameter ρ is the coefficient of risk, function of the acceptable probability that a_b is exceeded in the life period for which the construction is projected, and it is equal to 1.0 in the case of normal importance constructions and equal to 1.3 in the case of special importance constructions (in this study the value 1.3 will be adopted). The parameter *S* is the soil amplification coefficient that in the case of this study is equal to *C*/1.25, being *C* the soil coefficient that depends on the geotechnical characteristic of the soil and in this case is equal to 1.6, according to Martinez (2007).

$$a_c = S \cdot \rho \cdot a_b \tag{13}$$

Thus, a design seismic acceleration equal to 0.067g is obtained. This value corresponds to a vibration period equal to zero or, in other words, corresponds to the soil period considering in an approximate way the site effects. However, to design purposes it is necessary to know the value of the design elastic spectrum which is obtained as the maximum value of the elastic response spectrum with 5% of the critical damping, defined by the values presented from Equation (14) to Equation (16). In these equations $\alpha(T)$ is the value of the normalized elastic response spectrum, *T* is the fundamental period of the structure in seconds, *K* is the contribution coefficient taken as 1.0 in this study, *C* is taken as above and T_A and T_B are characteristic periods of the response spectrum equal to $K \cdot C/10$ and to $K \cdot C/2.5$, respectively.

If $T < T_A$: $$\alpha(T) = 1 + 1.5 \cdot T/T_A \tag{14}$$

If $T_A \leq T \leq T_B$: $$\alpha(T) = 2.5 \tag{15}$$

If $T > T_B$: $$\alpha(T) = K \cdot C/T \tag{16}$$

Multiplying the design seismic acceleration a_c by the value of the normalized elastic response spectrum $\alpha(T)$, the response spectrum recommended in the Spanish code for Palma de Mallorca is obtained and presented in Figure 5.17.

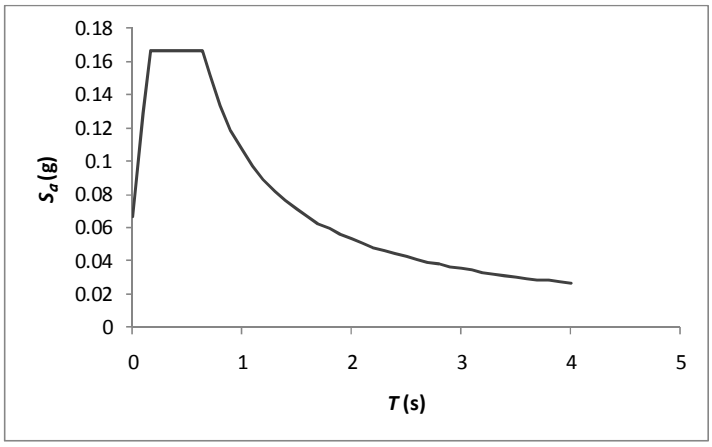

Figure 5.17 – Spectral acceleration spectrum according to NSCE-02.

It is necessary to convert this response spectrum with the spectral acceleration as function of the period to a ADRS demand spectrum, with the spectral accelerations defined as function of spectral displacements. This conversion is obtained with the relation expressed in Equation (17).

$$Sd = Sa \cdot \left(\frac{T^2}{4 \cdot \pi^2} \right) \tag{17}$$

The graph in the ADRS format is presented in Figure 5.18.

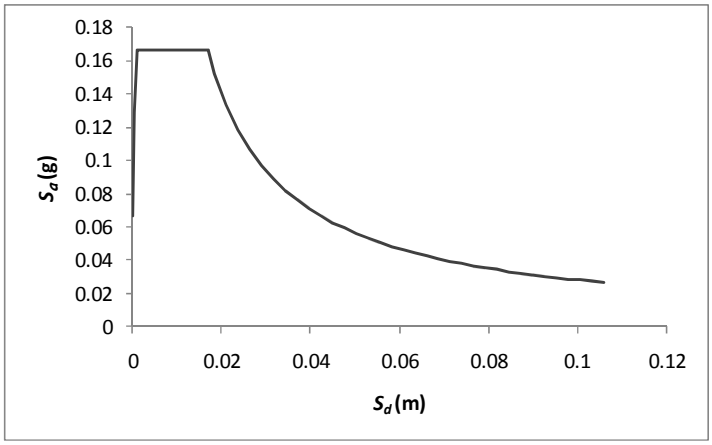

Figure 5.18 – ADRS spectrum according to NSCE-02.

- **EC8**

According to EC8, the values of the spectral values depend of the type of the soil in which the construction is located. The expressions for the calculation of the elastic spectrum are presented from Equation (18) to Equation (21)

$0 \le T \le T_B$ $$S_e(T) = a_g \cdot S \cdot \left[1 + \frac{T}{T_B} \cdot (\eta \cdot 2.5 - 1)\right] \quad (18)$$

$T_B \le T \le T_C$ $$S_e(T) = a_g \cdot S \cdot \eta \cdot \beta_0 \quad (19)$$

$T_C \le T \le T_D$ $$S_e(T) = a_g \cdot S \cdot \eta \cdot \beta_0 \cdot \left(\frac{T_C}{T}\right)^{k_1} \quad (20)$$

$T_D \le T \le 4s$ $$S_e(T) = a_g \cdot S \cdot \eta \cdot \beta_0 \cdot \left(\frac{T_C}{T_D}\right)^{k_1} \cdot \left(\frac{T_D}{T}\right)^{k_2} \quad (21)$$

From Equation (18) to Equation (21):

- $S_e(T)$ is the elastic response spectrum;
- T is the vibration period of a linear single degree of freedom system;
- a_g is the design ground acceleration;
- β_0 is the amplification factor of the spectral acceleration for a damping of 5%;
- T_B and T_C are the limits of the branch with constant acceleration;
- T_D is the value defining the beginning of the constant displacement response range of the spectrum;
- k_1 and k_2 are the exponents that define the shape of the spectrum for a period higher than T_C and T_D, respectively;
- S is the soil parameter;
- η is the damping correction factor with a reference value of 1 for 5% viscous damping, like the case assumed in the present study.

Considering a soil type B according to EC8, as proposed by Martinez (2007), the parameters for the calculation of the elastic response spectrum are presented in Table 5.1. The design ground acceleration assumed is 0.06g.

Table 5.1 – Parameter that define the elastic spectrum according to EC8.

Soil type	S	β_0	k_1	k_2	T_B (s)	T_C (s)	T_D (s)
B	1	2.5	1	2	0.15	0.6	3

Thus, the spectral acceleration spectrum and the ADRS spectrum for Palma de Mallorca, considering the design ground acceleration equal to 0.06g, are presented in Figure 5.19 and Figure 5.20, respectively.

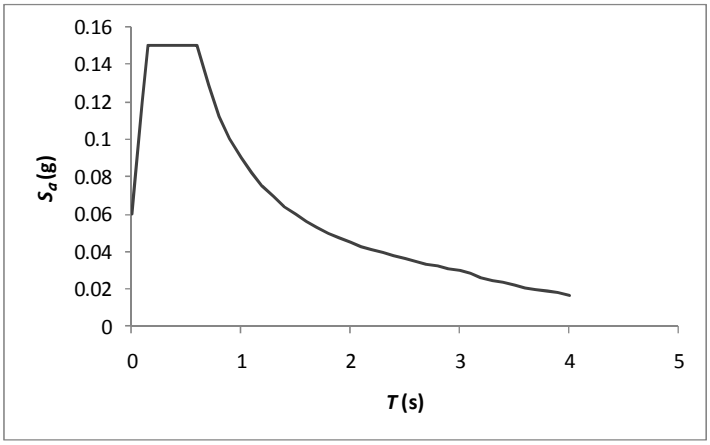

Figure 5.19 – Spectral acceleration spectrum according to EC8.

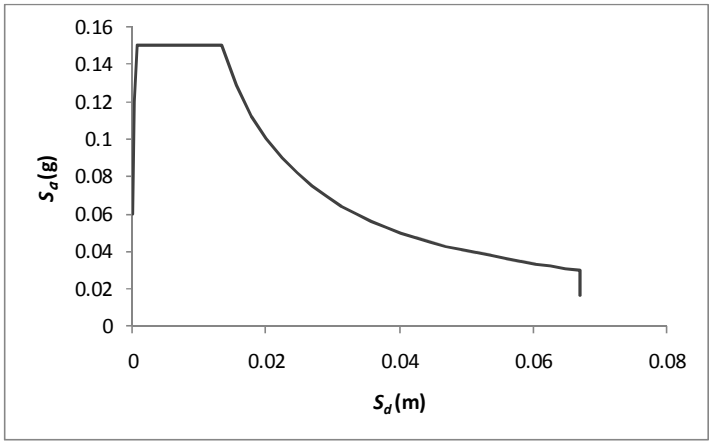

Figure 5.20 – ADRS spectrum according to EC8.

- **Deterministic analysis**

Based on the deterministic estimation of the seismic hazard for Mallorca Cathedral by Martinez (2007), in terms of spectral values of acceleration, the ADRS spectrum shown in Figure 5.21 is used in the present study. Its elaboration is detailed on section 4.7.

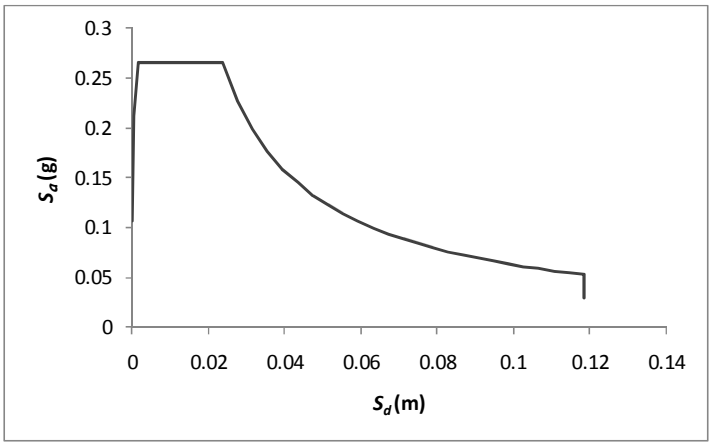

Figure 5.21 – ADRS spectrum considering the deterministic scenario.

- **Probabilistic analysis**

The probabilistic analysis was carried out based on the probabilistic estimation of the seismic hazard for Mallorca Cathedral by Martinez (2007), in terms of spectral values of acceleration. For a return period of 475 years, the ADRS spectrum used in the present work is in Figure 5.22. For a return period of 975 years, the ADRS spectrum used in the present work is shown in Figure 5.23. Their elaboration is detailed on section 4.7.

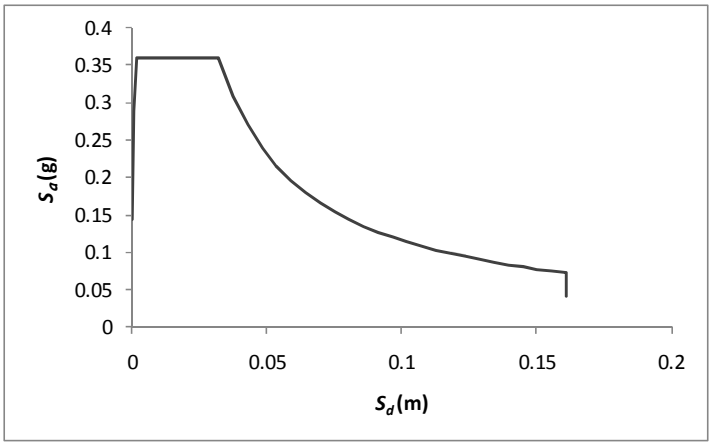

Figure 5.22 – ADRS spectrum considering the probabilistic scenario and a return period of 475 years.

The comparison between the different seismic demands considered for Mallorca Cathedral is presented in Figure 5.24 in the ADRS format.

It is remarkable that the spectrums obtained by the Spanish and European codes are similar between each other. The ones obtained by the probabilistic and the deterministic approach are more demanding. The most demanding spectrum is the one corresponding to the probabilistic approach for a return period of 975 years.

These results highlight that not always the response spectrums recommended by codes are suitable, especially for historical buildings, where the over strength of the new buildings are considered. Also, it

must be used a return period of 975 years instead of the 475 years assumed by the codes, because of the higher life periods of these buildings.

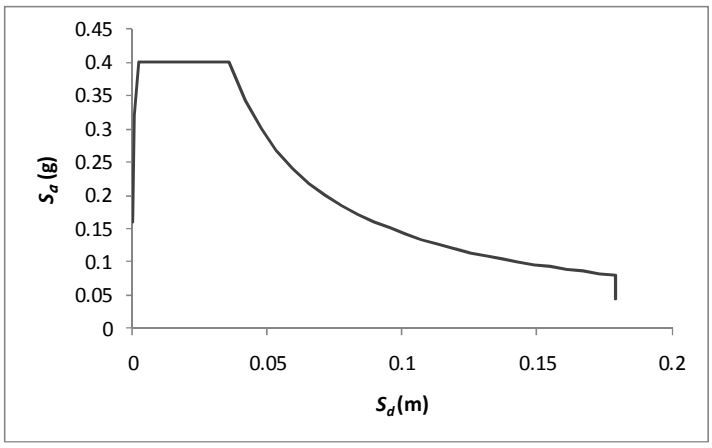

Figure 5.23 – ADRS spectrum considering the probabilistic scenario and a return period of 975 years.

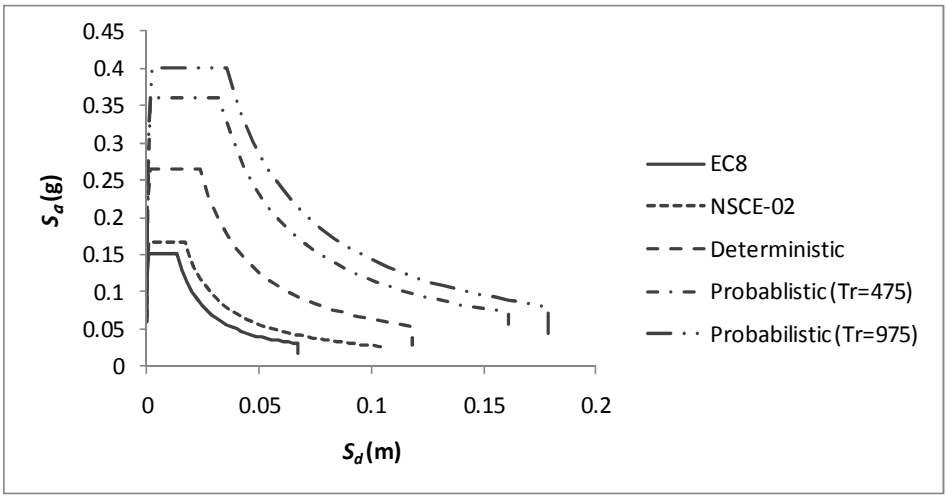

Figure 5.24 – Comparison between the different seismic demands for Mallorca Cathedral.

5.3 Calculation assumptions

5.3.1 Definition of the point of rotation of the overturning mechanisms

The overturning mechanisms are assumed to have as the point a rotation a hinge that is located on the edge of the rigid block in the side towards it is overturning. In this edge, due to the overturning, there is concentration of compression stresses leading to the plasticization.

The distance between this edge and the point of rotation, designated as distance *t*, is evaluated assuming a uniform distribution of the compressive stresses. Therefore the point of rotation is located in the centre of the section subjected to compressive stresses. The kinematic mechanism occurs when the compressive strength of the rigid block is attained, assuming that there is no tension resistance.

The distance t is then calculated by the expression on Equation (22), where w_i is the weight of the block i or another vertical force applied on the macroelement, b is the width of contact between the macroelement and the soil or the structure where it is supported and σ_c is the uniform compressive stress on this area of contact.

$$t = \frac{\sum_i w_i}{2 \cdot b \cdot \sigma_c} \tag{22}$$

The uniform compressive stress σ_c is assumed to be equal to the compressive resistance of the rigid block, which is equal to 2MPa (value taken from Martinez (2007)). The width b is taken as the maximum width of the rigid block where the overturning is being considered.

5.3.2 Thrust of the vaults

The thrust of the vaults supported by the rigid blocks that cause the considered possible local mechanisms is calculated through the use of the table proposed by Ungewitter (1901). Knowing the length and width of the vaulting bay, its rise from springing to crown and the thickness and material of the vault webs, it is possible to estimate the weight of the ribs, bosses and vault fill. With these quantities is also possible to estimate the vault thrust and its line of action. These estimations were made in Ungewitter (1901) and are presented on Table 5.2, which is a reduced form of Ungewitter (1901) tables presented in Heyman (1995). In this table, V_0 and H_0 stand for the vertical and horizontal thrust, respectively, and h is the distance from the crown of the vault to the point of application of the horizontal thrust.

Table 5.2 – Thrusts from quadripartite vaults taken from Ungewitter (1901).

Height/span f/s	1:8		1:3		1:2		2:3		5:6 to 1:1	
kN/m²	V_o	H_o	V_o	H_o	V_o	H_o	V_o	H_o	V_o	H_o
a. $\frac{1}{2}$ lightweight brick	2.0	3.6–4.0	2.3	1.6–1.8	2.6	1.1–1.2	2.9	0.9–1.0	3.4	0.8–0.9
b. $\frac{1}{2}$ strong brick	2.7	5.0–5.5	3.1	2.2–2.4	3.5	1.4–1.6	3.8	1.1–1.3	4.5	1.0–1.1
c. $\frac{3}{4}$ strong brick	3.7	7.0–7.5	4.2	3.0–3.3	4.8	1.9–2.2	5.3	1.6–1.8	6.5	1.5–1.6
d. 200 mm sandstone	5.0	9.5–10.0	5.7	4.2–4.5	7.0	2.8–3.2	7.5	2.2–2.5	9.0	2.1–2.3
e. 300 mm rubble	8.5	16–17	10.0	7.1–7.5	12.0	4.8–5.5	13.0	4.0–4.3	15.0	3.5–3.7
lever arm h/f		0.90		0.85–0.75		0.80–0.70		0.80–0.72		0.80–0.75

The rise to span ratio of the vault is an important parameter and it takes five values in Table 5.2, from the very low rise of 1/8th of the span, through a rise equal to half the span, to a rise of twice this value. The horizontal and vertical weights include allowances for the ribs, bosses and vaults fills.

Ungewitter quotes results for five thicknesses and materials of the vault that are:

- 1/2 lightweight brick (125mm);

- 1/2 strong brick (125mm) or 3/2 lightweight (190mm);
- 3/4 strong brick (190mm) or 1 lightweight (250mm);
- 1 strong brick (250mm) or 200mm sandstone;
- 300mm rubble vault.

There are four different types of vaults supported by the façades: the central and lateral ones in the West and in the East façade. Following, it is shown the calculation of its thrusts. All the horizontal forces are calculated in the longitudinal direction of the building, except for the horizontal force calculated for the lateral vaults on the East façade. In the latter it is only needed to know the horizontal force on the transversal direction of the building because this thrust only has influence on the mechanism 13 that corresponds to an overturning in the same direction. All the vaults are calculated assuming that they are composed by a layer of 200mm of sandstone.

- **Central vault on the West façade**

In Table 5.3 the geometrical properties of the central vault supported by the West façade are presented.

Table 5.3 – Geometrical properties of the central vault on the West façade.

Span *s* (m)	Width *b* (m)	Rise *f* (m)
8.0	19.3	12.5

Being the height to span ration equal to 1.57, the values corresponding to the ratio 1:1 are used. Therefore, the vertical weight V_0 is equal to 9kN/m^2 and the horizontal weight H_0 is equal to 2.3kN/m^2. This values result is a vertical thrust equal to 346.4kN and a horizontal thrust equal to 88.5kN, corresponding to each point of support of the vault (if the macroelement considered for a mechanism is supporting one of the edges of the vault, or in other words two supports, these values have to be multiplied by 2).

Assuming the ratio *h*/*f* equal to 0.75 and knowing that this vault is supported at a height equal to 30.2m (obtained by the photogrametry provided by Gonzalez and Roca (2000)), the horizontal forces are applied at a height equal to 33.4m.

- **Lateral vaults on the West façade**

In Table 5.4 the geometrical properties of the lateral vaults supported by the West façade are presented.

Table 5.4 – Geometrical properties of the lateral vaults on the West façade.

Span *s* (m)	Width *b* (m)	Rise *f* (m)
8.0	9.6	7.6

Being the height to span ratio equal to 0.95, the values corresponding to the ratio 1:1 are used. Therefore, the vertical weight V_0 is equal to 9kN/m^2 and the horizontal weight H_0 is equal to 2.3kN/m^2. This values result is a vertical thrust equal to 172.8kN and a horizontal thrust equal to 44.2kN, corresponding to each point of support of the vault.

Assuming the ratio *h*/*f* equal to 0.75 and knowing that this vault is supported at a height equal to 22.8m, the horizontal forces are applied at a height equal to 24.7m.

- **Central vault on the East façade**

In Table 5.5 the geometrical properties of the central vault supported by the East façade are presented.

Table 5.5 – Geometrical properties of the central vault on the East façade.

Span *s* (m)	Width *b* (m)	Height *f* (m)
8.1	21.3	13.1

Being the height to span ratio equal to 1.62, the values corresponding to the ratio 1:1 are used. Therefore, the vertical weight V_0 is equal to 9kN/m^2 and the horizontal weight H_0 is equal to 2.3kN/m^2. This values result is a vertical thrust equal to 389.1kN and a horizontal thrust equal to 99.4kN, corresponding to each point of support of the vault.

Assuming the ratio *h*/*f* equal to 0.75 and knowing that this vault is supported at a height equal to 0.72m measured from the height at which the longitudinal overturning mechanisms considered on this façade are supported, the horizontal forces are applied at a height equal to 4.0m.

- **Lateral vaults on the East façade**

In Table 5.6 the geometrical properties of the lateral vaults supported by the East façade are presented.

Table 5.6 – Geometrical properties of the lateral vaults on the East façade.

Span *s* (m)	Width *b* (m)	Rise *f* (m)
12.8	8.1	7.9

Being the height to span ratio equal to 0.61, the values corresponding to the ratio 2:3 are used. Therefore, the vertical weight V_0 is equal to 7.5kN/m^2 and the horizontal weight H_0 is equal to 2.5kN/m^2. This values result is a vertical thrust equal to 195.0kN and a horizontal thrust (being it applied on the transversal direction of the building) equal to 65.0kN, corresponding to each point of support of the vault.

Assuming the ratio *h*/*f* equal to 0.72 and knowing that this vault is supported at a height equal to 22.2m measured from the soil, the horizontal forces are applied at a height equal to 24.4m.

5.4 Results

In this section a summary of the results obtained for Mallorca Cathedral are presented. First a kinematic linear analysis was performed for each mechanism. If the safety is verified according to this analysis, it is not necessary to perform a kinematic nonlinear analysis. However, the latter was also applied to all the mechanisms considered in this work in order to understand the seismic nonlinear response of each local mechanism and to obtain the level of damage that can be expected from the seismic demand presented before.

In this section only the main results are presented. The detailed calculations are presented in Annex A.

- **Kinematic linear analysis**

In Table 5.7 it is summarised the results obtained through the kinematic linear analysis presented before.

Table 5.7 – Summary of the results obtained by kinematic linear analysis.

Mechanism	EC8			NSCE-02			Deterministic		
	a_0^* (m/s^2)	$a_{0\,min}^*$ (m/s^2)	Safety	a_0^* (m/s^2)	$a_{0\,min}^*$ (m/s^2)	Safety	a_0^* (m/s^2)	$a_{0\,min}^*$ (m/s^2)	Safety
1	1.43	0.29	**Verified**	1.43	0.33	**Verified**	1.43	0.52	**Verified**
2	0.99	0.29	**Verified**	0.99	0.33	**Verified**	0.99	0.52	**Verified**
3	0.91	0.29	**Verified**	0.91	0.33	**Verified**	0.91	0.52	**Verified**
4	1.62	0.29	**Verified**	1.62	0.33	**Verified**	1.62	0.52	**Verified**
5	1.95	0.29	**Verified**	1.95	0.33	**Verified**	1.95	0.52	**Verified**
6	0.64	0.29	**Verified**	0.64	0.33	**Verified**	0.64	0.52	**Verified**
7	0.76	0.29	**Verified**	0.76	0.33	**Verified**	0.76	0.52	**Verified**
8	0.76	0.29	**Verified**	0.76	0.33	**Verified**	0.76	0.52	**Verified**
9	–	–	–	–	–	–	–	–	–
10	–	–	–	–	–	–	–	–	–
11	2.11	0.29	**Verified**	2.11	0.33	**Verified**	2.11	0.52	**Verified**
12	0.82	0.29	**Verified**	0.82	0.33	**Verified**	0.82	0.52	**Verified**
13	0.69	0.29	**Verified**	0.69	0.33	**Verified**	0.69	0.52	**Verified**
14	1.93	0.29	**Verified**	1.93	0.33	**Verified**	1.93	0.52	**Verified**

Mechanism	Probabilistic Tr=475			Probabilistic Tr=975		
	a_0^* (m/s^2)	$a_{0\,min}^*$ (m/s^2)	Safety	a_0^* (m/s^2)	$a_{0\,min}^*$ (m/s^2)	Safety
1	1.43	0.71	**Verified**	1.43	0.78	**Verified**
2	0.99	0.71	**Verified**	0.99	0.78	**Verified**
3	0.91	0.71	**Verified**	0.91	0.78	**Verified**
4	1.62	0.71	**Verified**	1.62	0.78	**Verified**
5	1.95	0.71	**Verified**	1.95	0.78	**Verified**
6	0.64	0.71	**Not verified**	0.64	0.78	**Not verified**
7	0.76	0.71	**Verified**	0.76	0.78	**Not verified**
8	0.76	0.71	**Verified**	0.76	0.78	**Not verified**
9	–	–	–	–	–	–
10	–	–	–	–	–	–
11	2.11	0.71	**Verified**	2.11	0.78	**Verified**
12	0.82	0.71	**Verified**	0.82	0.78	**Verified**
13	0.69	0.71	**Not verified**	0.69	0.78	**Not verified**
14	1.93	0.71	**Verified**	1.93	0.78	**Verified**

Since the capacity curves of the mechanisms 9 and 10 were obtained through a pushover analysis, by Martinez (2007), the kinematic linear analysis is not applicable to these cases.

According to this preliminary simple analysis, the safety of the mechanisms is not assured for mechanisms 6, 7, 8 and 13 when the most demand seismic action is considered, that is the one estimated through a probabilistic analysis for a return period equal to 975 years.

It is remarkable that these four mechanisms are the only ones which the overturning rigid block is composed by the whole tower or buttress of the façades. This is due to the higher vertical distance from the rotation point to the point of application of the horizontal forces originated by a horizontal acceleration. This distance is higher in these cases because the rotation point of these mechanisms is located at the foundation. Because of it, the horizontal forces produce a higher destabilizing moment and, consequently, the horizontal acceleration that activates the mechanisms is lower.

However, to have a clearer understanding of the seismic response and the safety of these and all the others mechanisms, a kinematic nonlinear analysis must be performed.

- **Kinematic nonlinear analysis**

In Table 5.8 it is summarised the results obtained through the kinematic nonlinear analysis presented before.

The most remarkable conclusion after observing Table 5.8 is that the safety is assured for all the local mechanisms considered in Mallorca Cathedral, even if the seismic demand obtained from the deterministic and probabilistic approach estimated by Martinez (2007) is considered.Although through the kinematic linear analysis the safety was not assured for all the mechanisms, it is possible to notice that if the nonlinear behaviour of the mechanisms is considered, they are not expected to collapse in the case of a seismic event.

However, if a nonlinear response is considered, there is the possibility that the considered local mechanisms may cause some damage in the building. It is possible to notice that except in the cases of the mechanisms 5 and 12, all the damage levels according to Lagomarsino et al. (2003) are between the no damage limit state and the moderate damage limit state. In the cases where the capacity curve is obtained by limit analysis (all expect mechanisms 9 and 10), it is not possible to distinguish the damage levels below the moderate damage limit state, because the elastic behaviour of these mechanisms is not known.

It is also important to remark that if the design seismic demands obtained from the European and Spanish codes are used, it is not expected that significant damage occurs in none of the local mechanisms considered.

However, higher levels of damage may be expected if the deterministic or probabilistic estimations are considered in mechanisms 5 and 12. In order to reduce the damage due seismic activity, it the

possibility of strengthening the structure of the building so that the local mechanisms cause a lower level damage when subjected to an earthquake is studying in the following section.

Table 5.8 – Summary of the results obtained by kinematic nonlinear analysis.

Mechanism	EC8				NSCE-02				Deterministic			
	d_u^* (m)	$d_{u\,min}^*$ (m)	Safety	Level of damage	d_u^* (m)	$d_{u\,min}^*$ (m)	Safety	Level of damage	d_u^* (m)	$d_{u\,min}^*$ (m)	Safety	Level of damage
1	1.736	0.067	**Verified**	**D2 or lower**	1.736	0.126	**Verified**	**D2 or lower**	1.736	0.119	**Verified**	**D2 or lower**
2	1.461	0.067	**Verified**	**D2 or lower**	1.461	0.139	**Verified**	**D2 or lower**	1.461	0.119	**Verified**	**D2 or lower**
3	0.662	0.067	**Verified**	**D2 or lower**	0.662	0.098	**Verified**	**D2 or lower**	0.662	0.119	**Verified**	**D2 or lower**
4	0.791	0.067	**Verified**	**D2 or lower**	0.791	0.080	**Verified**	**D2 or lower**	0.791	0.119	**Verified**	**D2 or lower**
5	0.374	0.083	**Verified**	**D2 or lower**	0.374	0.098	**Verified**	**D2 or lower**	0.374	0.147	**Verified**	**D3**
6	0.875	0.067	**Verified**	**D2 or lower**	0.875	0.134	**Verified**	**D2 or lower**	0.875	0.119	**Verified**	**D2 or lower**
7	0.792	0.067	**Verified**	**D2 or lower**	0.792	0.117	**Verified**	**D2 or lower**	0.792	0.119	**Verified**	**D2 or lower**
8	0.794	0.067	**Verified**	**D2 or lower**	0.794	0.117	**Verified**	**D2 or lower**	0.794	0.119	**Verified**	**D2 or lower**
9	0.623	0.025	**Verified**	**D0**	0.623	0.030	**Verified**	**D0**	0.623	0.044	**Verified**	**D1**
10	0.521	0.017	**Verified**	**D1**	0.521	0.020	**Verified**	**D1**	0.521	0.030	**Verified**	**D2**
11	0.769	0.065	**Verified**	**D2 or lower**	0.769	0.077	**Verified**	**D2 or lower**	0.769	0.115	**Verified**	**D2 or lower**
12	0.271	0.065	**Verified**	**D2 or lower**	0.271	0.077	**Verified**	**D2 or lower**	0.271	0.115	**Verified**	**D3**
13	0.722	0.067	**Verified**	**D2 or lower**	0.722	0.118	**Verified**	**D2 or lower**	0.722	0.119	**Verified**	**D2 or lower**
14	0.742	0.065	**Verified**	**D2 or lower**	0.742	0.077	**Verified**	**D2 or lower**	0.742	0.115	**Verified**	**D2 or lower**
Mechanism	Probabilistic Tr=475				Probabilistic Tr=975							
	d_u^* (m)	$d_{u\,min}^*$ (m)	Safety	Level of damage	d_u^* (m)	$d_{u\,min}^*$ (m)	Safety	Level of damage				
1	1.736	0.161	**Verified**	**D2 or lower**	1.736	0.179	**Verified**	**D2 or lower**				
2	1.461	0.161	**Verified**	**D2 or lower**	1.461	0.179	**Verified**	**D2 or lower**				
3	0.662	0.161	**Verified**	**D2 or lower**	0.662	0.179	**Verified**	**D2 or lower**				
4	0.791	0.161	**Verified**	**D2 or lower**	0.791	0.179	**Verified**	**D2 or lower**				
5	0.374	0.199	**Verified**	**D3**	0.374	0.221	**Verified**	**D3**				
6	0.875	0.161	**Verified**	**D2 or lower**	0.875	0.179	**Verified**	**D2 or lower**				
7	0.792	0.161	**Verified**	**D2 or lower**	0.792	0.179	**Verified**	**D2 or lower**				
8	0.794	0.161	**Verified**	**D2 or lower**	0.794	0.179	**Verified**	**D2 or lower**				
9	0.623	0.060	**Verified**	**D2**	0.623	0.067	**Verified**	**D2**				
10	0.521	0.040	**Verified**	**D2**	0.521	0.045	**Verified**	**D2**				
11	0.769	0.156	**Verified**	**D2 or lower**	0.769	0.173	**Verified**	**D2 or lower**				
12	0.271	0.156	**Verified**	**D3**	0.271	0.173	**Verified**	**D4**				
13	0.722	0.161	**Verified**	**D2 or lower**	0.722	0.179	**Verified**	**D2 or lower**				
14	0.742	0.157	**Verified**	**D2 or lower**	0.742	0.174	**Verified**	**D2 or lower**				

6. STRENGTHENING

6.1 Introduction

In order to select a possible strengthening solution, it is essential to consider the principles of conservation and the modern criteria for the analysis and restoration of historical structures. These criteria include the well-known requirements for minimum intervention, reversibility, non-invasiveness, durability and compatibility with the original materials and structure. Also it must be known that strengthening normally convey a certain loss of cultural value since they normally involve a certain alteration of the original materials and structures.

Because of reasons reported before, any possible solution must be judged in account of its possible cost and benefit in terms of conservation of the cultural values of the construction.

The intervention has to be done on well known parts of the structure, reducing the number of the operations and, principally, avoiding changing of the original stiffness distribution. Also the ornamental displays are a very important issue when the interventions have to be chosen, because it cannot influence the historical and monumental value of the structure or reduce its artistic merit.

The choice of the interventions is based on the seismic safety evaluations and a good knowledge of the structure. The safety and durability level have to be reached applying minimal operations on the historical manufacture.

The selection of an optimal strengthening technique in order to improve the seismic behaviour of monuments is mostly related to public safety, preventing unacceptable risks to people, and minimizes the possible losses caused by the earthquake. In the case of monuments, the losses to be included are:

- the cultural loss which might be caused by damage or destruction produced by the earthquake;
- the loss that he seismic event may cause in the form of injuries to people or casualties, and in terms of cultural loss in the movable heritage stored inside the building.

The strengthening strategy to be implemented should be oriented to minimize the cost associated with both types of losses.

The effects on monuments caused by an expectable earthquake should be limited to an acceptable amount because of the costs in public safety and cultural heritage.

In order to choose a solution, it has to be taken into account that a level of damage equal to D0 is not recommended because of its cost. Some damages, including deformations and cracks, are accepted.

In general, the damage should be repairable using traditional or historical techniques for repair or maintenance. The cost of loss in immovable cultural value caused by the damage due to earthquake must be smaller that the corresponding cost caused by a more heavy and invasive strengthening designed to prevent this damage.

The solution must respect the structural authenticity of the monument, because it provides an immediate and tangible experience on past construction technologies. Also interventions causing a reduced impact on the original structure are preferred, providing the required safety level. The strengthening mechanical devices must be durable, otherwise, the decay of the material can, in turn, convey damage to the original parts. The strengthening technique must be non-obtrusive, by means, it has not been noticeable and also it must be possible to dismantle them without leaving and lasting alteration or deterioration to the original material and structure. Finally, it must be possible to control the intervention during its execution by monitoring the structure (Rodriguez (2009)).

Therefore, it is accepted for the local mechanisms considered a damage level D2 or lower. Most of them are within this group of damage levels, however higher damage may be expected for mechanisms 5 and 12. Possible solutions to strengthen the corresponding elements are provided in the next section.

6.2 Strengthening solutions

6.2.1 Mechanism 5

Since it is expected that the mechanism 5 will produce significant damage during an earthquake, a strengthening of the corresponding element is recommended. The scheme of the strengthening is presented in Figure 6.1. It is recommended to place steel tendons like schematized in Figure 6.1 (the tendons are highlighted with a darker colour) with a prestress force equal to the one needed in order to reduce the damage level to D2 or, in other words, to reduce the displacement demand to less than 1/8 of the displacement d_0^*. It is recommended to anchor the tendons in the central towers of the façade, on the opposite side from where the mechanism is considered to develop.

The aim of the strengthening is, on a first approach, to reduce the damage when the seismic demand corresponding to the probabilistic approach a return period equal to 975 years is considered, since this is the most demanding seismic action considered in this study. As it is possible to verify in Table 5.8, damage level D3 is expected in this case.

The strengthening is computed as a vertical stabilizing force at the top of the element and at the centre of its thickness. The determination of the vertical force needed, as well as the design of the tendons, is presented on Annex B. Two main conclusions are taken from this calculation: the vertical force is extremely high, being 161% of the self weight of the overturning block; the number of tendons (diameter equal to 15.2mm) needed is 57, which would have be to distributed along a width equal to

2.07m, which means that they would be spaced 3.6cm centre to centre. Because of the high force and the small space between the tendons, this solution is considered to be too invasive to the structure.

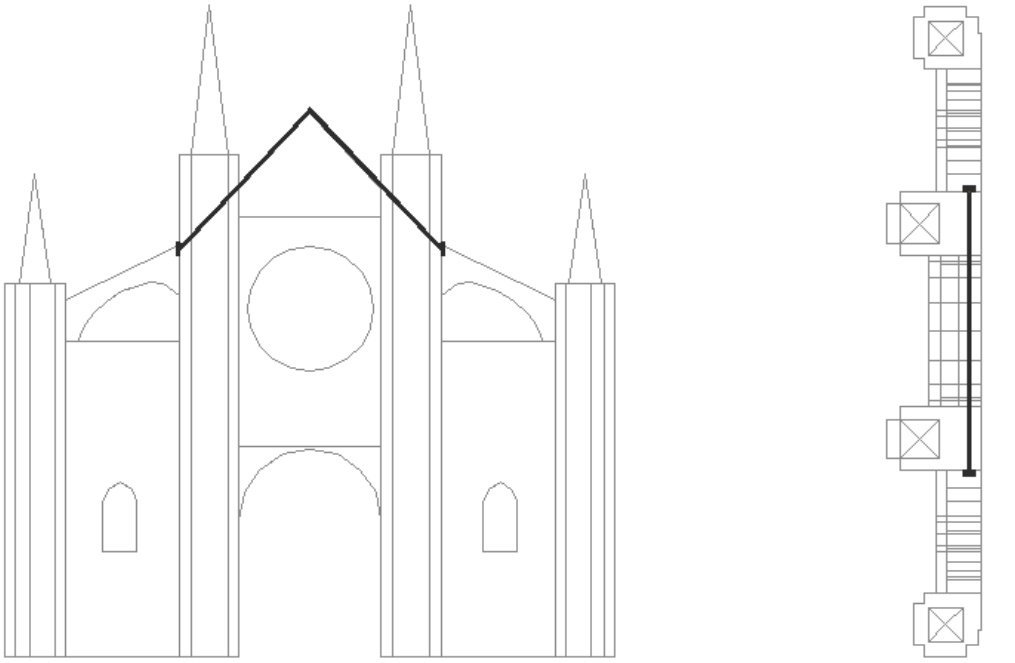

(a) Front view (b) Upper view

Figure 6.1 – Strengthening solution for mechanism 5.

Therefore, and since the safety of the mechanism is assured, less invasive alternatives, with a lower amount of the tendons, are studied in order not to achieve a D2 damage level, but to decrease the damage within the damage level D3.

As the vertical force *V* is increased, the soil seismic response in terms of displacements decreases because of the higher period. However, with the increase of the force *V*, the displacement capacity of the structures is lower, meaning that the value d_0^* decreases. Since this is value is the one compared to the seismic demand in order to get the damage level, it is expected that with the strengthening, the value of the seismic response in terms of displacements decreases in a higher rate than the decrease of d_0^*. As it can be observed in Table 6.1, the latter occurs. However, the seismic demand in this case corresponds to the seismic response of the base of the mechanism that is located at a certain height of the structure. As presented is Table 6.1, for some strengthening solutions proposed, instead of the seismic response of the structure being lower with the increase of the number of tendons, it is higher.

Because of this increase of the seismic response of the structure, the damage level may not be reduced with the strengthening proposed, and in some cases the safety of the mechanism is not assured if the strengthening is considered.

Table 6.1 – Effects of different alternatives of strengthening of mechanism 5.

Number of tendons	Spacing between tendons (m)	F (kN)	V (kN)	d_0^* (m)	T_s (s)	$S_{De}(T_s)$ (m)	$S_{De}(T_s)$ / d_0^*	$d_{u\,min}^*$ (m)	$d_{u\,min}^*$ / d_0^*	Damage level
0	-	0	0	0.934	1.90	0.113	0.121	0.221	0.237	D3
6	0.400	1560	681	0.753	1.58	0.094	0.125	0.280	0.372	D4
11	0.200	2860	1249	0.670	1.40	0.084	0.125	0.351	0.524	Collapse
14	0.150	3640	1589	0.635	1.32	0.079	0.124	0.373	0.588	Collapse
21	0.100	5460	2384	0.576	1.18	0.070	0.122	0.280	0.486	Collapse
42	0.050	10920	4768	0.490	0.93	0.055	0.113	0.091	0.185	D3
57	0.036	14820	6471	0.460	0.82	0.049	0.107	0.057	0.124	D2

The explanation for the increase of the seismic response of the structures is based on Equation (12), which takes into account an amplification factor, designated as A, of the seismic response of the structures at the height of the mechanism's base. This factor is function of the secant period T_s and the natural period of the whole structure in the direction studied T_1, as represented by Equation (23).

$$A = \frac{\left(\frac{T_s}{T_1}\right)^2}{\sqrt{\left(1-\frac{T_s}{T_1}\right)^2 + 0.02 \cdot \frac{T_s}{T_1}}} \tag{23}$$

Knowing from Martinez (2007) that T_1 is equal to 1.28s, the amplification factor is only function of the secant period T_s. This relation is presented on Figure 6.2.

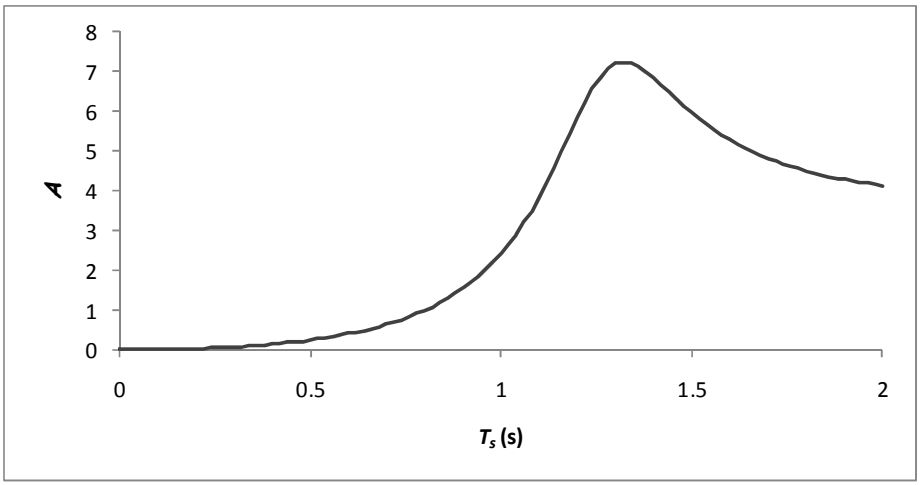

Figure 6.2 – Amplification factor of the seismic response of the structure at a certain height.

Equalizing the derivate of the amplification factor in order to the secant period T_s to zero, its maximum value is obtained and it is equal to 1.32s. Therefore, a solution proposed for the strengthening of this particular mechanism must pay attention to change of the secant period T_s, as it must not be close to 1.32s.

In this case, being the mechanism an intrinsically problematic issue to solve, and since its safety is assured, it is recommended not to proceed to any intervention with strengthening purposes. In order to study a possible solution that would reduce the damage level to D2, a detailed study of the dynamic behaviour of the West façade must be carried out.

6.2.2 Mechanism 12

Also the mechanism 12 is expected to produce significant damage if an earthquake like the one considered on the probabilistic demand corresponding to a return period of 975 years. Thus, it is recommended carrying out a strengthening in order to prevent a damage level equal to D4 and to reduce it to D2. The scheme of the strengthening recommended is presented on Figure 6.3. The solution presented is to place prestressed tendons in the whole width of the façade. The tendons would be placed in the upper part of rose window, in the upper flying arches and would be anchored in the buttresses, on each edge of the façade.

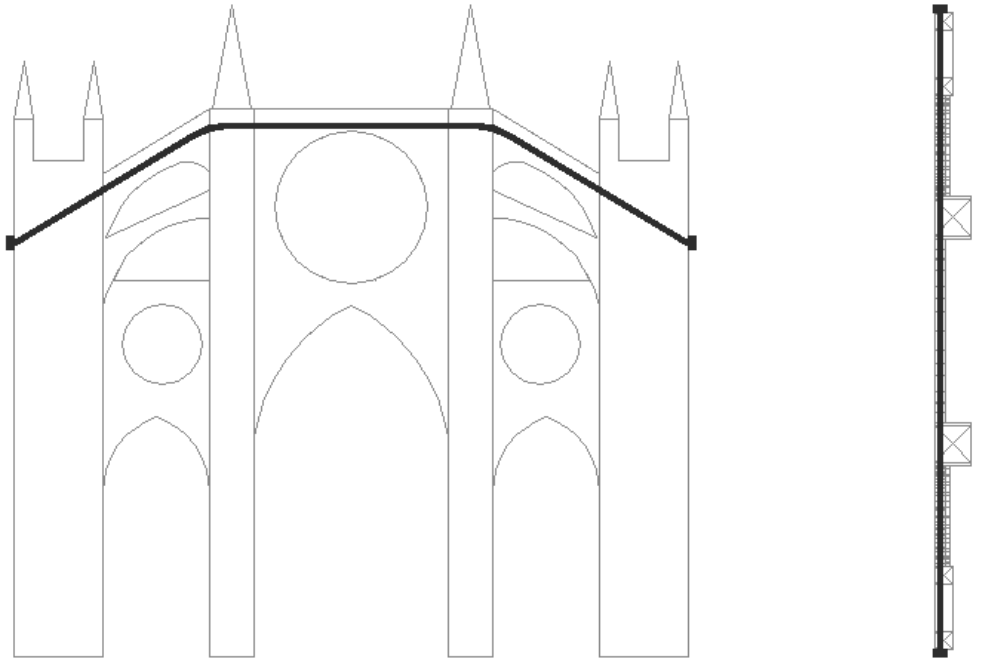

(a) Front view (b) Upper view

Figure 6.3 – Strengthening solution for mechanism 12.

The friction force produced by the prestressed tendons due to the compression on the connection between the buttresses and the upper flying arches stabilizes the overturning mechanism. The

calculation of the horizontal force, transversal to plan of the façade, needed in order to reduce the damage level to D2 is also presented on Annex B.

The number of tendons needed with the solution presented is 3, which is considered a reasonable strengthening solution. It is remarkable that this type of solution doesn't have an influence in the secant period T_s. The effect of the strengthening, as it can be seen in Annex B, is to increase the ultimate displacement d_u^* and the displacement d_0^*.

7. CONCLUSIONS

The main objective of this thesis is the lay-out of the strengthening of Mallorca Cathedral. Historical buildings were usually designed considering static forces, neglecting the seismic action due to its own complexity and due to the complex dynamic behaviour of structures. Therefore it is intended in this thesis to perform a seismic analysis and to propose strengthening solutions so that the safety is assured and the damage is within in an acceptable level if a seismic event occurs.

One important task carried out within the objective of this thesis is the analysis of the previous structural analysis carried out on Mallorca Cathedral. Although several studies about Mallorca Cathedral were presented, they started to be carried out recently when compared to the building's life period. However, these studies had a pioneer nature and significantly contributed to the development and the practical application of structural analysis tools to complex structures.

Several studies are presented in this thesis, comprising from the first ones that used static graphical methods to the most recent ones that used modern technologies in order to perform detailed and complex modelling of the structural behaviour. All the works constitute a valuable starting point for understanding the building itself and, particularly, its structural and seismic behaviour.

In order to carry out a seismic analysis of Mallorca Cathedral or any historical construction, it is important to understand the usual structural response towards seismic events that is characterized by the most common damages: damage in the towers, separations of the main external walls, cracking of the external walls and flattening of vertical elements. Also, from the analysis of previous works about the seismic vulnerability of historical constructions, it was noted that usually the damage is due to local collapse mechanisms that involve only single parts, named macroelements, which are characterized by an almost autonomous structural behaviour of the rest of the building.

Therefore, it is important in the case of Mallorca Cathedral to individualize the local mechanisms that are likely to occur if the building is subjected to a seismic action. Then, these mechanisms must be studied and analyzed separately in order to obtain their seismic behaviour. This is attained by a proper method presented in this thesis that is based on the capacity spectrum method with the capacity curve of each mechanism obtained by limit analysis. As it is mentioned, the common pushover methodologies are not suitable for this type of buildings characterized by rocking mechanisms. The procedure applied herein was developed for the specific case of historical buildings and it is presented on the Italian code.

It is considered the possibility of developing 14 different local mechanisms. Since 2 of them are too complex to be analyzed through limit analysis, the original form of capacity spectrum method is applied. The capacity curves used are taken from previous structural studies on Mallorca Cathedral that carried out detailed finite element modelling of the analyzed macroelements.

Several possibilities for the seismic demand are considered. Two of them are design spectrums taken from the European code EC8 and the Spanish code NSCE-02. However, this type of spectrums is suitable for the design of new buildings. In the case of historical structures it is more accurate of a seismic hazard evaluation of the site is carried out. This was carried out in previous works, where a deterministic and a probabilistic approach were used in order to obtain realistic seismic spectrums, which are also considered in this thesis. It is remarkable that these last seismic spectrums are significantly more demanding than the ones presented in the codes. The more demand spectrum that is considered corresponds to a probabilistic estimation considering a return period equal to 975 years.

The main conclusion arising from the seismic analysis carried out herein is that the structure is safe if subjected to any seismic action that may be expected for the site. However, an undesirable level of damage may be expected if the cathedral is subjected to the most demanding seismic action considered. This damage is due to 2 of the 14 local mechanisms considered. One of them is located in West main façade and the other is located on the East façade. Strengthening solutions for each one of these two mechanisms are proposed.

In the West façade, the damage that is expected to cause significant damage is characterized by the overturning of an almost triangular element located in the centre of the top of the façade. The strengthening solution proposed is to place prestressed tendons along the top of the macroelement and anchor them in the central towers of the façade. This way, the vertical force produced on the top of the macroelement contributes for stabilizing it. However, it is concluded that the amount of tendons needed is too high and therefore this solution is considered to be too invasive to the structure. Less invasive solutions are also analyzed, but due to the dynamic behaviour of the façade the damage is not reduced when compared to the not strengthened situation. Since the main principles and criteria in conservation and restoration of historical structures include minimum intervention and non-invasiveness, it is considered as a good approach not to carry out any strengthening intervention. Moreover, the local mechanism is not expected to collapse since its safety is assured according to the analysis carried out.

The local mechanism that is expected to cause important damage on the East façade is characterized by the overturning of the upper part of the buttresses. The strengthening solution proposed is to place prestressed tendons in the whole width of the façade. The tendons are recommended to be placed in the upper part of the rose window, along the upper flying arches and to be anchored in the outer edge of the buttresses. The number of tendons needed to reduce the damage into an acceptable level is considered to be reasonable.

As a final remark, it is stated that the procedure applied in this thesis for the seismic analysis of Mallorca Cathedral is appropriate for the analysis of historical structures in general. Despite its simplicity, it is possible to get a clear idea of the nonlinear behaviour of each local mechanism. It shall be remarked that the correct individualization of the local mechanisms is of great importance for the accuracy of the final results.

REFERENCES

Ambraseys, N.N., Simpson, K.A., Bommer, J.J. (1996), *Prediction of horizontal response spectra in Europe*, Earthquake Engineering and Structural Dynamics, 25, pp. 371-400.

Casarin, F., Magagna, E. (2001), *Analise strutturale della Catedrale di Palma de Mallorca*, Graduation thesis, Universidad de Padua, Padua.

Clemente, R. (2006), *Análisis estructural de edifícios históricos mediante modelos localizados de fisuración*, Ph. D. dissertation, Universitat Politècnica de Catalunya, Barcelona.

Cuzzilla, R. (2008), *Application of Capacity Spectrum Method to Medieval Constructions*, Master's thesis, Universitat Politècnica de Catalunya, Barcelona.

Das, A. (2008), *Safety assessment of Mallorca cathedral*, Master's thesis, Universistat Politècnica de Catalunya, Barcelona.

EC8 (1998), *Eurocode 8 – Design of structures for earthquake resistance*, CEN, European Standard EN 1998-1, Brussels.

Fajfar, P. (1999), *Capacity spectrum method based on inelastic demand spectra*, Earthquake Engineering and Structural Dynamics, 28, pp. 979-993.

Freeman, S.A. (1998), *Development and use of capacity spectrum method*, 6th U.S. National Conference on Earthquake Engineering, Earthquake Engineering Research Inst, Oakland, California.

Gonzalez, J.L., Roca, P. (2000), *Plan de estudios constructivos-estruturales de la catedral de Palma de Mallorca*, Universitat Politècnica de Catalunya, Barcelona.

González, R., Caballé, F., Domenge, J., Vendrell, M., Giráldez, P., Roca, P., González, J.L. (2008), *Construction process, damage and structural analysis. Two case studies*, Structural Analysis of Historic Construction – Preserving Safety and Significance, CRC Press, Leiden, The Netherlands.

Heyman, J. (1966), *The stone skeleton*, Int. J. Solids Structures, 2, pp. 249-279.

Heyman, J. (1995), *The stone skeleton: Structural engineering of masonry architecture*, Cambridge University Press.

Italian code (2009), *Circolare Ministero delle Infrastrutture e dei trasporti 2 febbraio 2009 n.617 (G.U. b.47 del 26/02/2009 – Suppl. Ordinario n.27)*, Istruzioni per l'apllicazione delle Nuove Norme Tecniche di cui al D.M. 14/01/2008.

Lagomarsino, S. (1998), *A new methodology for the post-earthquake investigation of ancient churches*, 11th European Conference on Earthquake Engineering, Paris.

Lagomarsino, S., Giovinazzi, S., Podestà, S., Resemini, S. (2003), *WP5: Vulnerability assessment of historical and monumental buildings Handbook*, RISK-EU: An advanced approach to earthquake risk scenarios with application to different European towns, Contract: EVKA-CT-2000-00014.

Lagomarisno, S. (2006), *On the vulnerability assessment of monumental buildings*, Bull Earthquake Eng, 4, pp. 445-463.

Mark, R. (1982), *Experiments in Gothic structure*, The Massachusetts Institute of Techonology Press, Massachusetts and London.

Martinez, G. (2007), *Vulnerabilidad sísmica de edifícios históricos de obra de fábrica de mediana y gran luz*, Ph. D. dissertation, Universitat Politècnica de Catalunya, Barcelona.

Maynou, J. (2001), *Estudi estructural del pòrtic tipus de la Catedral de Mallorca mitjançan l'estàtica gràfica*, Graduation thesis, Universitat Politècnica de Catalunya, Barcelona.

Miranda, E., Bertero, V.V. (1994), *Evaluation of strength reduction factors for earthquake resistant design*, Earthequake Spectra, 10, pp. 357-379.

NSCE-02 (2002), *Normativa de construcción sismorresistente española*. Real Decreto 997/2002, Boletin Oficial del Estado Nº. 244 del 11 de Octubre de 2002.

Rodriguez, P. (2009), *Lay-out of seismic strengthening of Mallorca Cathedral*, Master's thesis, Univerisitat Politècnica de Catalunya, Barcelona.

Rubió I Bellver, J. (1912), *Conferencia acerca de los conceptos orgánicos, mecánicos y constructivos de la catedral de Mallorca*, Anuario de la Asociación de Arquitectos de Cataluña, Barcelona, 1912.

Salas, A. (2002), *Estudio estructural de los porticos tipo de la Catedral de Mallorca*, Graduation thesis, Universitat Politècnica de Catalunya, Barcelona.

Ungewitter, G. (1901), *Lehrbuch der Gotischen Konstruktionen*, 4th edition (neu bearbeitet von K. Mohrmann), 2 vols, Leipzig.

Vacas, A. (2009), *Análisis Sísmico de las Catedrales Góticas Mediante el Método del Espectro del Capacidad*, Graduation Thesis, Universitat Politècnica de Catalunya, Barcelona.

ANNEX A: SEISMIC ANALYSIS CALCULATIONS

A.1 Detailed calculations

In order to understand the calculation procedure, the safety verification of the mechanism 11 and the mechanism 9 are detailed here.

- **Mechanism 11**

The mechanism 11 corresponds to the overturning of the whole upper part of the East façade (Figure A.1).

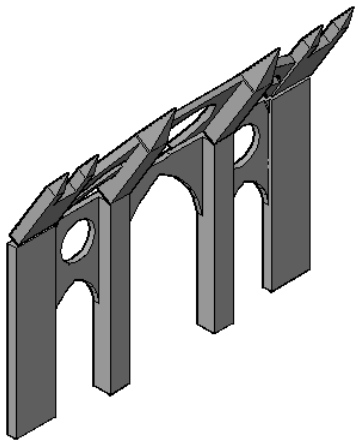

Figure A.1 – Mechanism 11.

The first step to apply the capacity spectrum method through limit analysis is to determine the geometrical properties of the overturning rigid block. In Figure A.2 it is presented the different geometry parameters that are needed to be known.

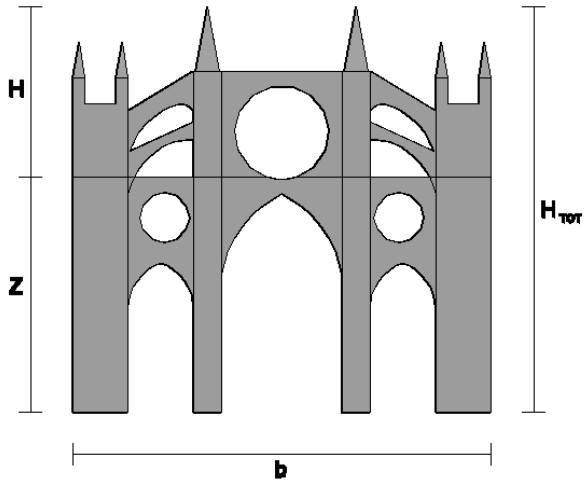

Figure A.2 – Definition of geometrical parameters of local mechanisms.

The values of the geometrical parameters of the mechanism 11 are presented in Table A.1.

Table A.1 – Values of geometrical parameters of mechanism 11.

Z (m)	H (m)	b (m)	H_{TOT} (m)	Volume (m^3)
29.88	21.79	53.40	51.67	782.3

Considering a density of the masonry equal to 21kN/m^3, the forces applied to the overturning rigid block are the ones presented on Table A.2.

Table A.2 – Forces on mechanism 11.

	Force (kN)	Point of application	
		x (m)	y (m)
Self weight P_1	16428.9	1.92	7.29
Vertical thrust from the vault N_1	778.3	2.96	0.72
Horizontal thrust from the vault N_{1H}	198.9	-	4.01

The coordinates of the points of application of the forces are represented in Figure A.3.

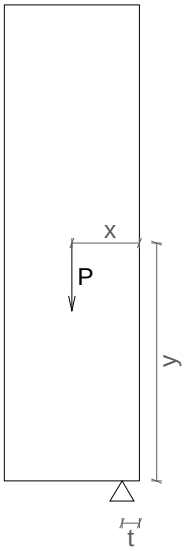

Figure A.3 – Definition of distances within the block.

With these forces, and being the total thickness of the block equal to 3.04m, the distance *t* corresponding to the distance from the edge of the block to the rotation point is calculated through Equation (22) and it is equal to:

$$t = \frac{\sum_i w_i}{2 \cdot b \cdot \sigma_c} = 0.081m$$

Then, the coefficient that activates the mechanism α_0 is obtained imposing the equilibrium between the destabilizing moment M_R and the stabilizing moment M_S:

$$M_S = M_R \Leftrightarrow P_1 \cdot x_{P_1} + N_1 \cdot x_{N_1} = \alpha_0 \cdot \left(P_1 \cdot y_{P_1} + N_1 \cdot y_{N_1}\right) + N_{1H} \cdot y_{N_{1H}} \Leftrightarrow \alpha_0 = 0.279$$

The next step is to compute this coefficient into a spectral acceleration. To calculate the participation mass M^*, it is assumed that the displacement δ_c of a point is equal to the product between the height of this point, H_c, and an infinitesimal rotation θ. It is assumed a unitary displacement of the control point located on the top of the rigid block, which results in an infinitesimal rotation θ equal to:

$$\delta_c = H_c \cdot \theta \Leftrightarrow 1 = H \cdot \theta \Leftrightarrow 1 = 21.79 \cdot \theta \Leftrightarrow \theta = 0.046 rad$$

The displacements δ_i of the points of application of the vertical forces are then the ones presented on Table A.3.

Table A.3 – Displacements of the points of application of the vertical forces.

δ_{P1} (m)	δ_{N1} (m)
0.334	0.033

The participation mass M^* is obtained applying Equation (3):

$$M^* = \frac{\left(P_1 \cdot \delta_{P1} + N_1 \cdot \delta_{N1}\right)^2}{g \cdot \left(P_1 \cdot \delta_{P1}{}^2 + N_1 \cdot \delta_{N1}{}^2\right)} = 1689.7 ton$$

Thus, the value of the fraction of the participation mass e^* is equal to 0.96 and the spectral acceleration a_0^* is obtained by Equation (4):

$$a_0^* = \frac{\alpha_o \cdot g}{e^* \cdot FC} = \frac{0.279 \cdot 9.81}{0.96 \cdot 1.35} = 2.108 m/s^2$$

Although this macroelement is not supported on the soil, the spectral acceleration a_0^* has to be higher than the soil acceleration that is obtained by Equation (8). In Table A.4 it is presented the values of the soil acceleration for the different seismic demand cases.

Table A.4 – Soil acceleration (m/s^2).

EC8	NSCE-02	Deterministic	Probabilistic Tr=475	Probabilistic Tr=975
0.294	0.326	0.520	0.706	0.785

Since the macroelement is not supported on the soil, the spectral acceleration a_0^* has to be also higher than the acceleration of the base of the rigid block that may be higher than the soil acceleration. This is calculated through Equation (9), with T_1 equal to 1.28s according to Martinez (2007), assuming

$\psi(Z)$ to be equal to Z/H_{TOT} and γ equal to $3N/(2N+1)$, where N the number of floors and equal to 1. In Table A.5 the values of the acceleration of the base of the block for the different seismic demand cases are presented.

Table A.5 – Acceleration of the base of the rigid block (m/s^2).

EC8	NSCE-02	Deterministic	Probabilistic Tr=475	Probabilistic Tr=975
0.199	0.236	0.352	0.479	0.532

It is concluded that the soil acceleration is higher than the base acceleration and that the safety is verified through a kinematic linear analysis. However, a kinematic nonlinear analysis was also performed in order to obtain the nonlinear behaviour of the mechanism as well as the damage degree.

For the kinematic nonlinear analysis it is first necessary to determine the finite rotation θ_0 for which the block is in equilibrium without any horizontal acceleration. For that it is necessary to define the angle β_i and the radius R_i of each vertical force. These parameters are schematized on Figure A.4.

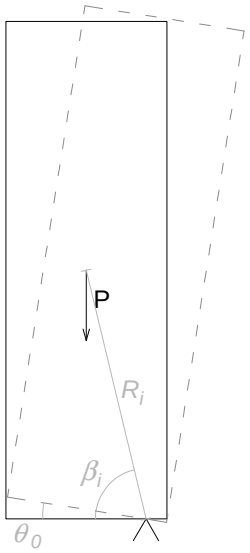

Figure A.4 – Parameters for calculation of the finite rotation θ_0.

The values of these parameters are presented in Table A.6 for each one of the vertical forces applied on the block.

Table A.6 – Values of the parameters for calculation of the finite rotation θ_0.

	β_i (rad)	R_i (m)
P_1	1.313	7.534
N_1	0.239	3.043

Being the stabilizing moment M_S equal to the destabilizing moment M_R, the rotation θ may be defined as function of α. Computing α equal to 0, it is possible to obtain the value of the rotation θ_0:

$$M_S = M_R \Leftrightarrow$$
$$\Leftrightarrow P_1 \cdot R_{P_1} \cdot \cos\left(\beta_{P_1} + \theta_0\right) + N_1 \cdot R_{N_1} \cdot \cos\left(\beta_{N_1} + \theta_0\right) =$$
$$= \alpha \cdot \left[P_1 \cdot R_{P_1} \cdot \cos\left(\beta_{P_1} + \theta_0\right) + N_1 \cdot R_{N_1} \cdot \cos\left(\beta_{N_1} + \theta_0\right)\right] + N_{1H} \cdot y_{1H} \Leftrightarrow$$
$$\Leftrightarrow \theta_0 = 0.268\,rad$$

To determine the ultimate displacement d_u^*, first the height of the barycentre of the block h_{bar} is determined:

$$h_{bar} = \frac{P_1 \cdot y_{P_1} + N_1 \cdot y_{N_1}}{P_1 + N_1} = 6.99\,m$$

Assuming this point as the control point of the block, it is necessary to determine its displacement corresponding to the annulment of the coefficient α:

$$d_{k,0} = h_{bar} \cdot \sin\left(\theta_0\right) = 1.851 m$$

It is also necessary to calculate the virtual horizontal displacement of the same point of control $\delta_{x,0}$:

$$\delta_{x,0} = h_{bar} \cdot \theta = 0.424\,m$$

Then, the equivalent spectral displacement of the displacement $d_{k,0}$ is obtained:

$$d_0^* = d_{k,0} \cdot \frac{P_1 \cdot {\delta_{P1}}^2 + N_1 \cdot {\delta_{N1}}^2}{\delta_{x,0} \cdot \left(P_1 \cdot \delta_{P1} + N_1 \cdot \delta_{N1}\right)} = 1.922 m$$

Consequently, the ultimate displacement d_u^* is equal to:

$$d_u^* = 0.4 \cdot d_0^* = 0.769\,m$$

This displacement must be compared to the demand displacement obtained for the secant period T_s. The displacement d_s^* is first calculated:

$$d_s^* = 0.4 \cdot d_u^* = 0.307\,m$$

Also, the corresponding acceleration:

$$a_s^* = a_0^* \cdot \left(1 - \frac{d_s^*}{d_0^*}\right) = 1.770\,m/s^2$$

Then, it is possible to obtain the secant period T_s:

$$T_s = 2 \cdot \pi \cdot \sqrt{\frac{d_s^*}{a_s^*}} = 2.62\,s$$

In Figure A.5 the capacity curve of the mechanism, the line corresponding to the secant period T_s and the several demand spectrums are presented. In Figure A.5 is possible to evaluate the performance point considering each seismic demand.

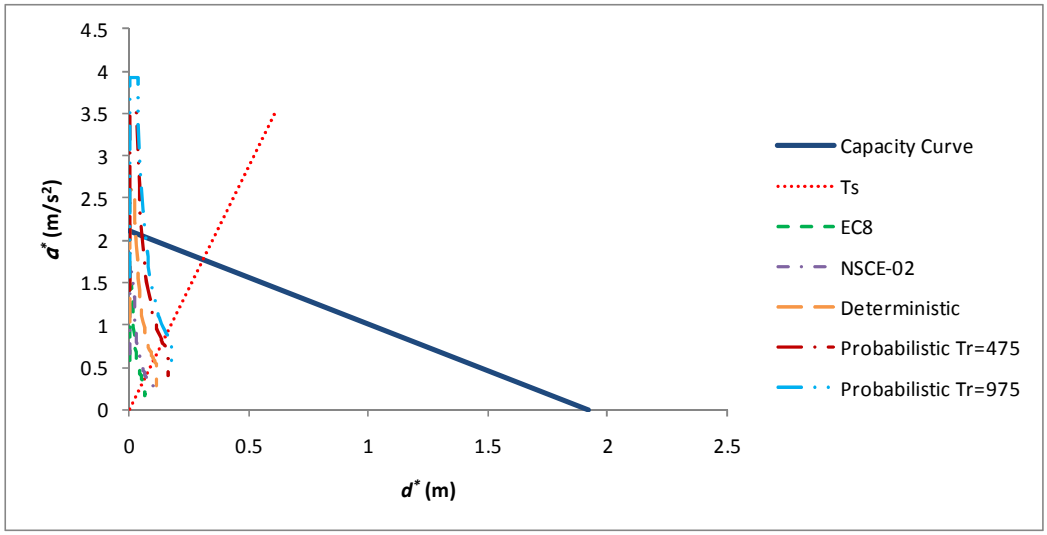

Figure A.5 – Capacity curve and demand spectrums of mechanism 11.

The elastic spectral response in terms of displacements corresponding to the period T_s, $S_{de}(T_s)$, for the different seismic demands considered are presented on Table A.7.

Table A.7 – Spectral response in terms of displacements of the soil (m).

EC8	NSCE-02	Deterministic	Probabilistic Tr=475	Probabilistic Tr=975
0.059	0.069	0.103	0.141	0.156

Also it must be considered the response spectrum in terms of displacements of the building at the height which this kinematic mechanism is developed. These values are calculated through Equation (12) and they are presented on Table A.8.

Table A.8 – Spectral response in terms of displacements of the building at the height which the kinematic mechanism is developed (m).

EC8	NSCE-02	Deterministic	Probabilistic Tr=475	Probabilistic Tr=975
0.065	0.077	0.115	0.156	0.173

It is possible to verify that the ultimate displacement d_u^* is higher than all the displacements obtained for the different seismic demands and for both the soil response and the building response at the height of the macroelement. Therefore, the safety of the mechanism is assured for the considered seismic actions.

In order to evaluate the damage level, the spectral responses in terms of displacements of the building at the height in which the mechanism is developed are considered since they are higher that the soil spectral responses. In Table A.9 it is presented the ratio between the demand displacement and the displacement d_0^*. Since all the values obtained for the different seismic demands are lower than 1/8, the corresponding damage level is D2 or lower than that.

Table A.9 – Damage levels.

	EC8	NSCE-02	Deterministic	Probabilistic Tr=475	Probabilistic Tr=975
$d_{u\ min}^* / d_0^*$	0.034	0.040	0.060	0.081	0.090
Damage level	D2 or lower	D2 or lower	D2 or lower	D2 or lower	D2 or lower

- **Mechanism 9**

The mechanism 9 corresponds to the transversal action on a typical bay of Mallorca Cathedral and it is study in this work through the results of the finite element modelling carried out by Martinez (2007) (Figure A.6).

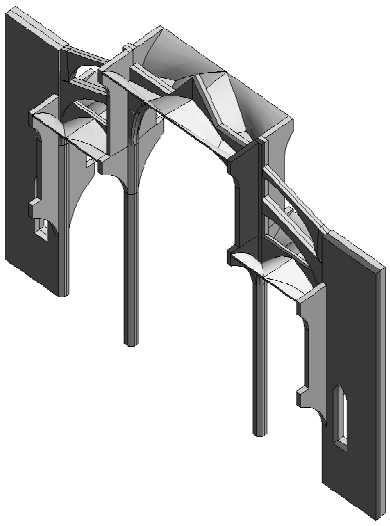

Figure A.6 – Modelling of the macroelement corresponding to a typical bay by Martinez (2007).

In Table A.10 are presented the values for the yielding and the ultimate points of the bilinear capacity curve obtained by Martinez (2007) for the equivalent single degree of freedom (SDOF) system of this macroelement.

Table A.10 – Values of the bilinear capacity curve of the typical bay obtained by Martinez (2007).

Yielding point		Ultimate point	
d_y (m)	a_y (g)	d_u (m)	a_u (m)
0.05	0.161	0.623	0.193

The bilinear capacity curve is also presented on Figure A.7.

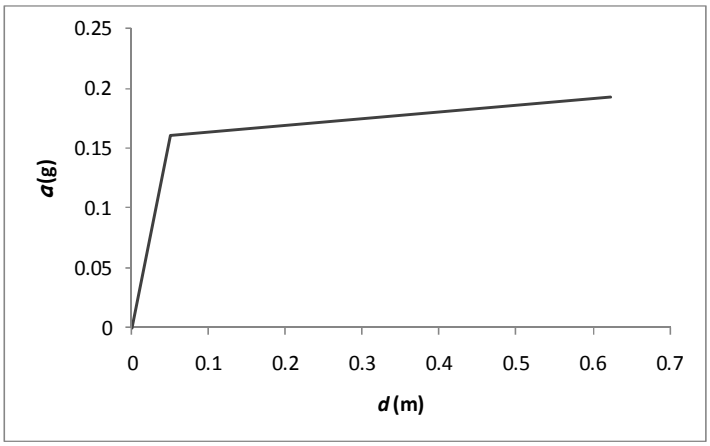

Figure A.7 – Bilinear capacity curve of the SDOF equivalent system of the typical bay.

The pushover analysis carried out for this mechanism and for mechanism 10 is based on the proposal by Fajfar (1999) where an idealized acceleration-displacement relation of the equivalent SDOF system has to be considered in an elastic-perfectly plastic form. This is because the graphical procedure requires the post yield stiffness to be equal to zero, since the reduction factor R_μ is defined as the ratio of the required elastic strength to the yield strength. This curve is presented in Figure A.8.

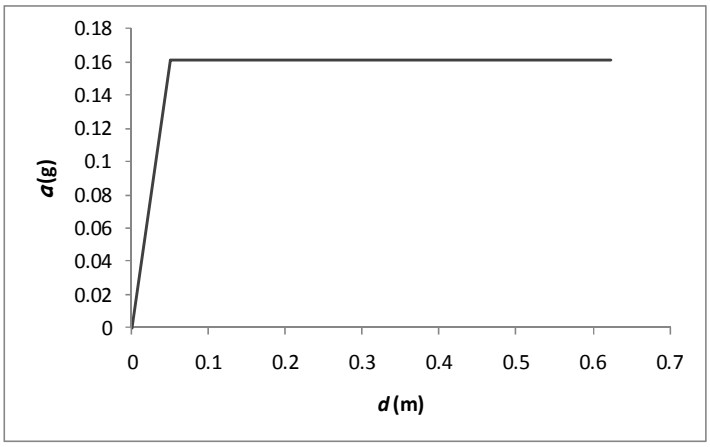

Figure A.8 – Bilinear capacity curve of the SDOF equivalent system of the typical bay with zero post yield stiffness.

For the inelastic SDOF system, the acceleration spectral response (S_a) and the displacement spectral response (S_d) can be obtained as expressed in Equation (A.1) and Equation (A.2), respectively. In these equations μ is the ductility factor defined as the ration between the maximum displacement and the yield displacement and S_{ae}, S_{de} and T are the elastic acceleration spectrum, elastic displacement spectrum and elastic period, respectively.

$$S_a = \frac{S_{ae}}{R_\mu} \tag{A.2}$$

$$S_d = \frac{\mu}{R_\mu} \cdot S_{de} = \frac{\mu}{R_\mu} \cdot \frac{T^2}{4 \cdot \pi^2} \cdot S_{ae} = \mu \cdot \frac{T^2}{4 \cdot \pi^2} \cdot S_a \tag{A.2}$$

Several proposals have been made for the reduction factor R_μ, applied due to ductility or, in other words, due to the hysteric dissipation of ductile structures. In this work, the proposal by Miranda and Bertero (1994) will be applied. The determination of R_μ is carried out through the Equation (A.3) and the Equation (A.4), where T_c is the characteristic period of the ground motion and Is defined as the transition period where the constant acceleration segment of the response spectrum passes to the constant velocity segment of the spectrum.

$$T \leq T_c \qquad R_\mu = (\mu - 1) \cdot \frac{T}{T_c} + 1 \tag{A.3}$$

$$T \geq T_C \qquad R_\mu = \mu \tag{A.4}$$

Therefore the first step is to determine the elastic period of the SDOF equivalent system that is given by Equation (A.5) and results equal to 1.12s.

$$T = 2 \cdot \pi \cdot \sqrt{\frac{d_y}{a_y}} \tag{A.5}$$

The elastic responses for the several seismic demand spectrums are presented in Table A.11.

Table A.11 – Values of elastic spectral responses.

	EC8	NSCE-02	Deterministic	Probabilistic Tr=475	Probabilistic Tr=975
S_{de} (m)	0.025	0.030	0.044	0.060	0.067
S_{ae} (g)	0.081	0.095	0.142	0.193	0.215

If the elastic response is the elastic range of the bilinear capacity curve, the elastic spectrum is used. If it is in the inelastic range, the Equation (A.3) and Equation (A.4) are used. It may be observed that only the elastic responses corresponding to both the probabilistic demands are in the inelastic range of the bilinear capacity curve.

In Figure A.9 it is presented the elastic or inelastic spectrum corresponding to each seismic demand case, as well as the bilinear capacity curve, so that the performance points can be evaluated.

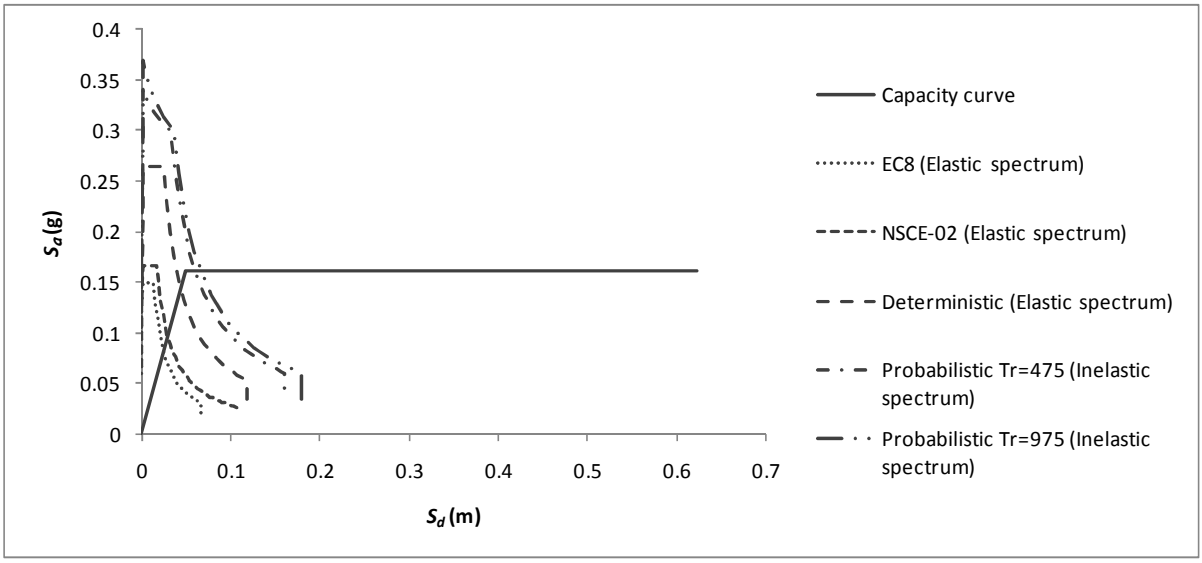

Figure A.9 – Intersection of the bilinear capacity curve with the demand spectrums.

The values of the performances points obtained are presented in Table A.12.

Table A.12 – Values of the inelastic spectral responses.

	EC8	NSCE-02	Deterministic	Probabilistic Tr=475	Probabilistic Tr=975
S_{de} (m)	0.025	0.030	0.044	0.060	0.067
S_{ae} (g)	0.081	0.095	0.142	0.161	0.161

It is remarkable that the elastic and inelastic responses in the case of the probabilistic seismic demand spectrums are the same in terms of displacements, being the differences related to the lower acceleration obtained when considering the inelastic response.

In Table A.13 is presented the safety as well as the damage levels that are defined in the same way as it was presented for the capacity curves obtained by limit analysis, being d_0^* equal to du in this case.

Table A.13 – Safety verification and damage levels of the mechanism 9.

	EC8	NSCE-02	Deterministic	Probabilistic Tr=475	Probabilistic Tr=975
S_d (m)	0.025	0.030	0.044	0.060	0.067
d_u (m)	0.623	0.623	0.623	0.623	0.623
Safety verification	Verified	Verified	Verified	Verified	Verified
Damage level	D0	D0	D1	D2	D2

A.2 Summary of the calculation procedure

In this section, the summary of the calculation procedure for all the other mechanisms is presented.

- **Mechanism 1**

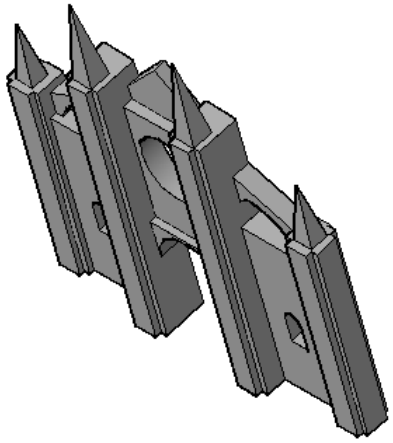

Figure A.10 – Mechanism 1.

Table A.14 – Values of geometrical parameters of mechanism 1.

Z (m)	H (m)	b (m)	H_{TOT} (m)	Volume (m^3)
0	64.52	60.4	64.52	11364.1

Table A.15 – Forces on mechanism 1.

	Force (kN)	Point of application	
		x (m)	y (m)
P_1	238646.7	4.45	22.65
N_1	692.8	7.58	30.22
N_2	691.4	7.58	22.80
N_{1H}	177.0	-	33.35
N_{2H}	176.7	-	24.69

Table A.16 – Value of spectral acceleration corresponding to the activation of the mechanism 1.

α_0	M^* (ton)	a_0^* (m/s^2)
0.197	24460.1	1.429

Table A.17 – Acceleration of the base of mechanism 1 (m/s^2).

	EC8	NSCE-02	Deterministic	Probabilistic Tr=475	Probabilistic Tr=975
Soil	0.294	0.326	0.520	0.706	0.785
Structure	-	-	-	-	-
Safety (linear analysis)	Verified	Verified	Verified	Verified	Verified

Table A.18 – Values of ultimate displacement and secant period of the mechanism 1.

d_0^* (m)	d_u^* (m)	T_s (s)
4.339	1.736	4.78

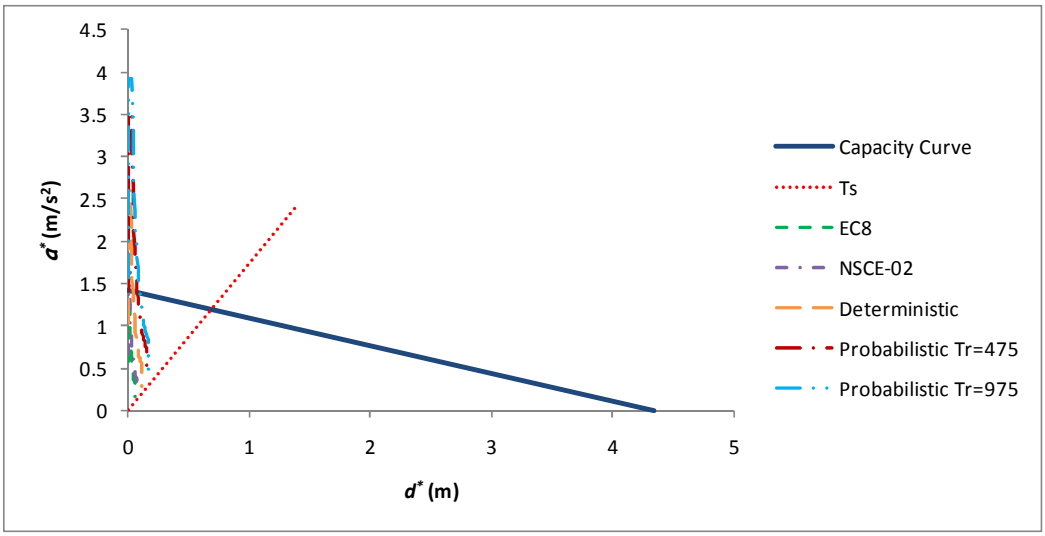

Figure A.11 – Capacity curve and demand spectrums of mechanism 1.

Table A.19 – Spectral response in terms of displacements of mechanism 1 (m).

	EC8	NSCE-02	Deterministic	Probabilistic Tr=475	Probabilistic Tr=975
Soil	0.067	0.126	0.119	0.161	0.179
Structure	-	-	-	-	-
Safety (nonlinear analysis)	Verified	Verified	Verified	Verified	Verified
Damage level	D2 or lower	D2 or lower	D2 or lower	D2 or lower	D2 or lower

- **Mechanism 2**

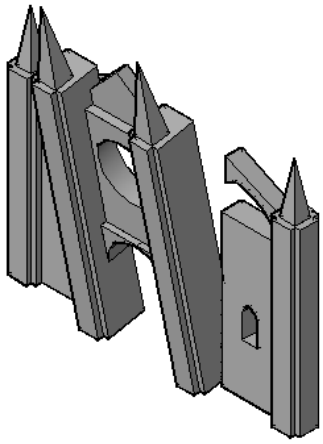

Figure A.12 – Mechanism 2.

Table A.20 – Values of geometrical parameters of mechanism 2.

Z (m)	H (m)	b (m)	H_{TOT} (m)	Volume (m^3)
0	64.52	25.87	64.52	5952.3

Table A.21 – Forces on mechanism 2.

	Force (kN)	Point of application	
		x (m)	y (m)
P_1	124997.3	3.64	26.83
N_1	692.8	7.35	30.22
N_2	345.7	7.35	22.80
N_{1H}	177.0	-	33.35
N_{2H}	88.3	-	24.69

Table A.22 – Value of spectral acceleration corresponding to the activation of the mechanism 2.

α_0	M^* (ton)	a_0^* (m/s^2)
0.137	12845.8	0.992

Table A.23 – Acceleration of the base of mechanism 2 (m/s^2).

	EC8	NSCE-02	Deterministic	Probabilistic Tr=475	Probabilistic Tr=975
Soil	0.294	0.326	0.520	0.706	0.785
Structure	-	-	-	-	-
Safety (linear analysis)	Verified	Verified	Verified	Verified	Verified

Table A.24 – Values of ultimate displacement and secant period of the mechanism 2.

d_0^* (m)	d_u^* (m)	T_s (s)
3.652	1.461	5.26

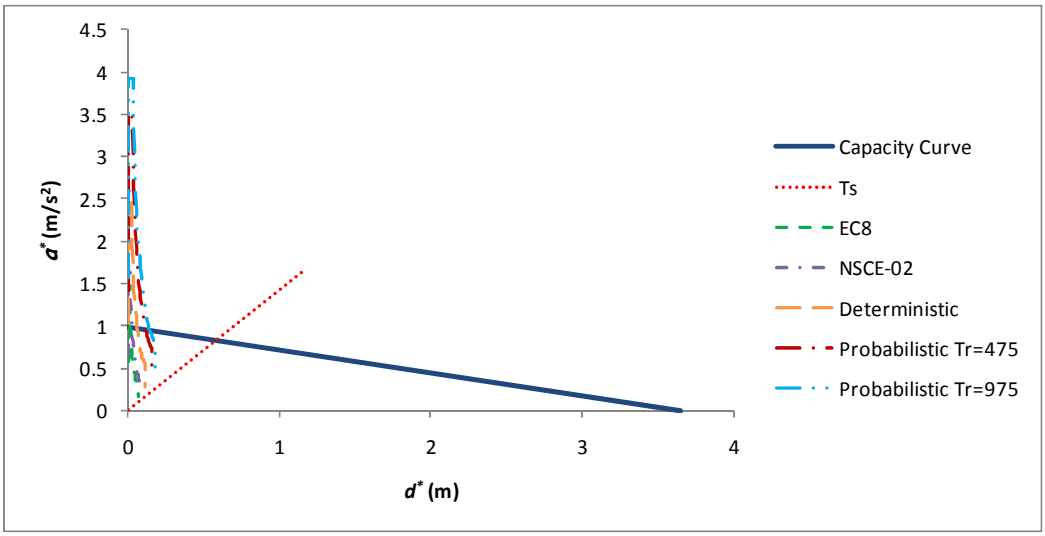

Figure A.13 – Capacity curve and demand spectrums of mechanism 2.

Table A.25 – Spectral response in terms of displacements of mechanism 2 (m).

	EC8	NSCE-02	Deterministic	Probabilistic Tr=475	Probabilistic Tr=975
Soil	0.067	0.139	0.119	0.161	0.179
Structure	-	-	-	-	-
Safety (nonlinear analysis)	Verified	Verified	Verified	Verified	Verified
Damage level	D2 or lower	D2 or lower	D2 or lower	D2 or lower	D2 or lower

- **Mechanism 3**

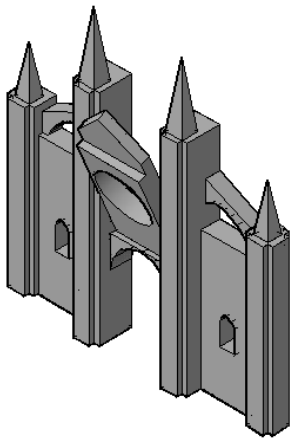

Figure A.14 – Mechanism 3.

Table A.26 – Values of geometrical parameters of mechanism 3.

Z (m)	H (m)	b (m)	H_{TOT} (m)	Volume (m^3)
20.88	32.97	14.09	64.52	920.8

Table A.27 – Forces on mechanism 3.

	Force (kN)	Point of application	
		x (m)	y (m)
P_1	19337.0	1.67	13.38

Table A.28 – Value of spectral acceleration corresponding to the activation of the mechanism 3.

α_0	M^* (ton)	a_0^* (m/s^2)
0.125	1971.2	0.905

Table A.29 – Acceleration of the base of mechanism 3 (m/s^2).

	EC8	NSCE-02	Deterministic	Probabilistic Tr=475	Probabilistic Tr=975
Soil	0.294	0.326	0.520	0.706	0.785
Structure	0.112	0.132	0.197	0.268	0.298
Safety (linear analysis)	Verified	Verified	Verified	Verified	Verified

Table A.30 – Values of ultimate displacement and secant period of the mechanism 3.

d_0^* (m)	d_u^* (m)	T_s (s)
1.654	0.662	3.71

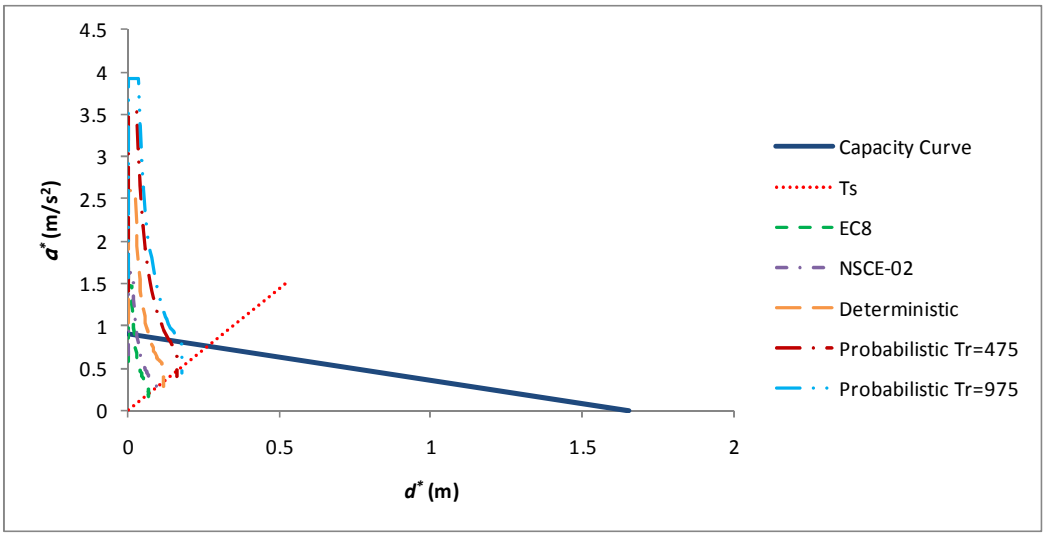

Figure A.15 – Capacity curve and demand spectrums of mechanism 3.

Table A.31 – Spectral response in terms of displacements of mechanism 3 (m).

	EC8	NSCE-02	Deterministic	Probabilistic Tr=475	Probabilistic Tr=975
Soil	0.067	0.098	0.119	0.161	0.179
Structure	0.041	0.048	0.072	0.098	0.108
Safety (nonlinear analysis)	Verified	Verified	Verified	Verified	Verified
Damage level	D2 or lower	D2 or lower	D2 or lower	D2 or lower	D2 or lower

- **Mechanism 4**

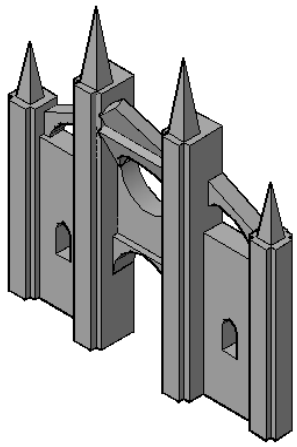

Figure A.16 – Mechanism 4.

Table A.32 – Values of geometrical parameters of mechanism 4.

Z (m)	H (m)	b (m)	H_{TOT} (m)	Volume (m^3)
34.46	19.4	14.09	64.52	440.9

Table A.33 – Forces on mechanism 4.

	Force (kN)	Point of application	
		x (m)	y (m)
P_1	9258.3	2.03	9.09

Table A.34 – Value of spectral acceleration corresponding to the activation of the mechanism 4.

α_0	M^* (ton)	a_0^* (m/s^2)
0.223	943.8	1.619

Table A.35 – Acceleration of the base of mechanism 4 (m/s^2).

	EC8	NSCE-02	Deterministic	Probabilistic Tr=475	Probabilistic Tr=975
Soil	0.294	0.326	0.520	0.706	0.785
Structure	0.184	0.218	0.325	0.442	0.491
Safety (linear analysis)	Verified	Verified	Verified	Verified	Verified

Table A.36 – Values of ultimate displacement and secant period of the mechanism 4.

d_0^* (m)	d_u^* (m)	T_s (s)
1.977	0.791	3.03

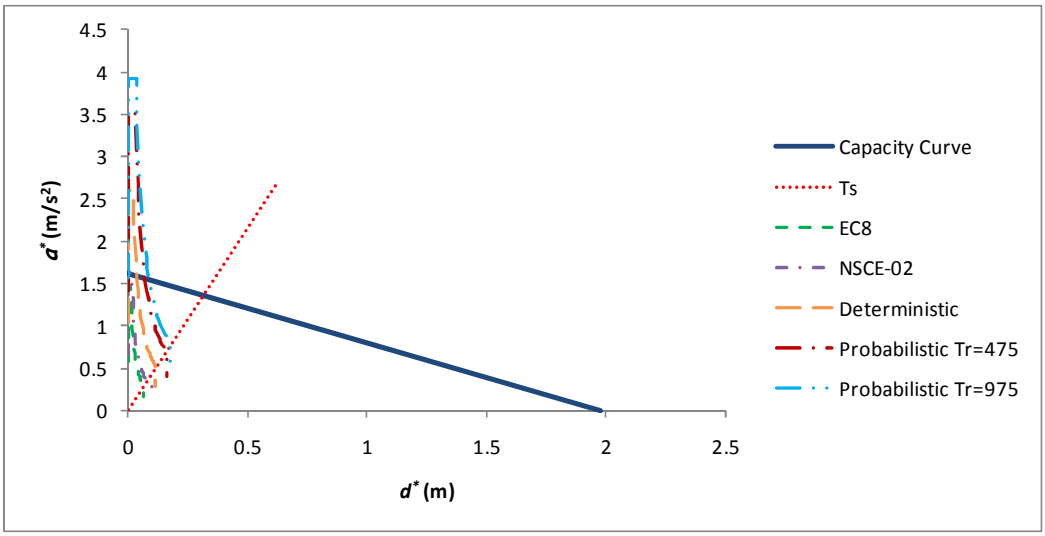

Figure A.17 – Capacity curve and demand spectrums of mechanism 4.

Table A.37 – Spectral response in terms of displacements of mechanism 4 (m).

	EC8	NSCE-02	Deterministic	Probabilistic Tr=475	Probabilistic Tr=975
Soil	0.067	0.080	0.119	0.161	0.179
Structure	0.062	0.073	0.109	0.149	0.165
Safety (nonlinear analysis)	Verified	Verified	Verified	Verified	Verified
Damage level	D2 or lower	D2 or lower	D2 or lower	D2 or lower	D2 or lower

- **Mechanism 5**

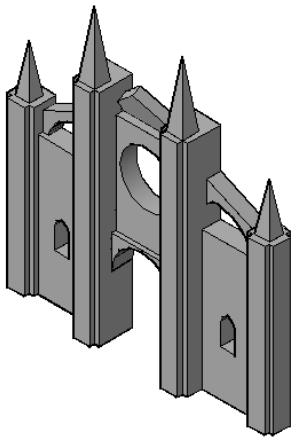

Figure A.18 – Mechanism 5.

Table A.38 – Values of geometrical parameters of mechanism 5.

Z (m)	H (m)	b (m)	H_{TOT} (m)	Volume (m^3)
43.62	10.24	14.09	64.52	190.1

Table A.39 – Forces on mechanism 5.

	Force (kN)	Point of application	
		x (m)	y (m)
P_1	3991.1	0.97	3.61

Table A.40 – Value of spectral acceleration corresponding to the activation of the mechanism 5.

α_0	M^* (ton)	a_0^* (m/s^2)
0.268	406.8	1.951

Table A.41 – Acceleration of the base of mechanism 5 (m/s^2).

	EC8	NSCE-02	Deterministic	Probabilistic Tr=475	Probabilistic Tr=975
Soil	0.294	0.326	0.520	0.706	0.785
Structure	0.233	0.276	0.412	0.560	0.622
Safety (linear analysis)	Verified	Verified	Verified	Verified	Verified

Table A.42 – Values of ultimate displacement and secant period of the mechanism 5.

d_0^* (m)	d_u^* (m)	T_s (s)
0.936	0.374	1.90

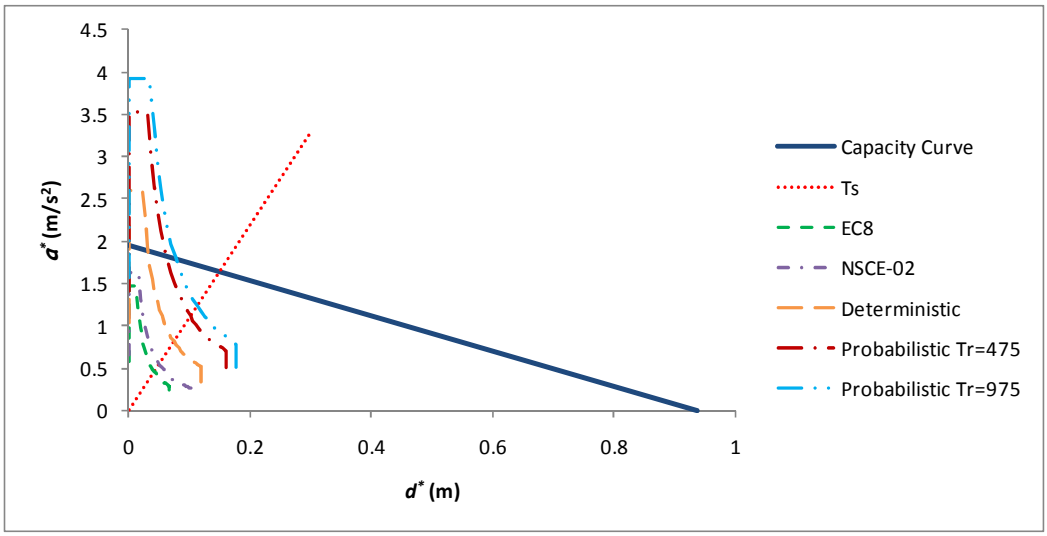

Figure A.19 – Capacity curve and demand spectrums of mechanism 5.

Table A.43 – Spectral response in terms of displacements of mechanism 5 (m).

	EC8	NSCE-02	Deterministic	Probabilistic Tr=475	Probabilistic Tr=975
Soil	0.042	0.050	0.075	0.102	0.113
Structure	0.083	0.098	0.147	0.199	0.221
Safety (nonlinear analysis)	Verified	Verified	Verified	Verified	Verified
Damage level	D2 or lower	D2 or lower	D3	D3	D3

- **Mechanism 6**

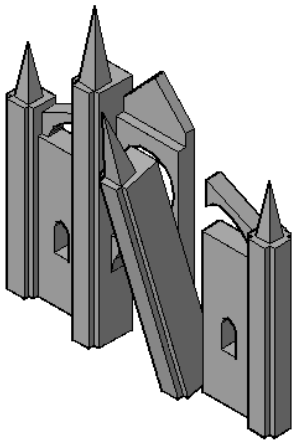

Figure A.20 – Mechanism 6.

Table A.44 – Values of geometrical parameters of mechanism 6.

Z (m)	H (m)	b (m)	H_{TOT} (m)	Volume (m^3)
0	64.52	5.89	64.52	2450.5

Table A.45 – Forces on mechanism 6.

	Force (kN)	Point of application	
		x (m)	y (m)
P_1	51461.3	2.23	25.64
N_1	346.4	6.36	30.22
N_2	172.8	6.36	22.80
N_{1H}	88.5	-	33.35
N_{2H}	44.2	-	24.69

Table A.46 – Value of spectral acceleration corresponding to the activation of the mechanism 6.

α_0	M^* (ton)	a_0^* (m/s^2)
0.088	5297.4	0.642

Table A.47 – Acceleration of the base of mechanism 6 (m/s^2).

	EC8	NSCE-02	Deterministic	Probabilistic Tr=475	Probabilistic Tr=975
Soil	0.294	0.326	0.520	0.706	0.785
Structure	-	-	-	-	-
Safety (linear analysis)	Verified	Verified	Verified	Not verified	Not verified

Table A.48 – Values of ultimate displacement and secant period of the mechanism 6.

d_0^* (m)	d_u^* (m)	T_s (s)
2.187	0.875	5.06

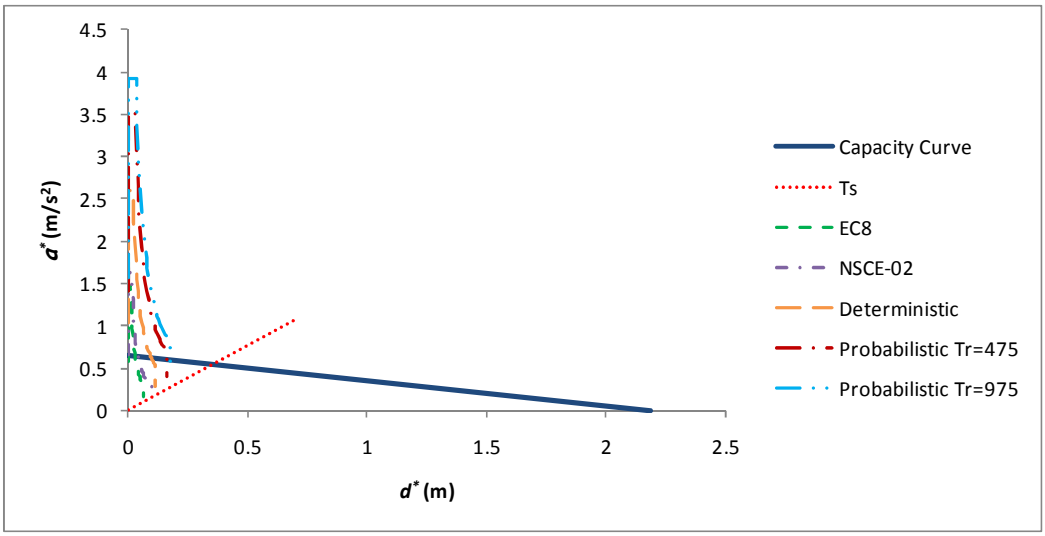

Figure A.21 – Capacity curve and demand spectrums of mechanism 6.

Table A.49 – Spectral response in terms of displacements of mechanism 6 (m).

	EC8	NSCE-02	Deterministic	Probabilistic Tr=475	Probabilistic Tr=975
Soil	0.067	0.134	0.119	0.161	0.179
Structure	-	-	-	-	-
Safety (nonlinear analysis)	Verified	Verified	Verified	Verified	Verified
Damage level	D2 or lower	D2 or lower	D2 or lower	D2 or lower	D2 or lower

- **Mechanism 7**

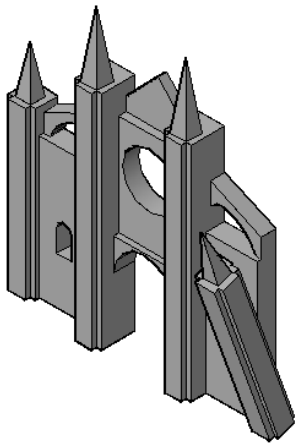

Figure A.22 – Mechanism 7.

Table A.50 – Values of geometrical parameters of mechanism 7.

Z (m)	H (m)	b (m)	H_{TOT} (m)	Volume (m^3)
0	47.74	5.89	64.52	1232.1

Table A.51 – Forces on mechanism 7.

	Force (kN)	Point of application	
		x (m)	y (m)
P_1	25874.3	1.99	19.10

Table A.52 – Value of spectral acceleration corresponding to the activation of the mechanism 7.

α_0	M^* (ton)	a_0^* (m/s^2)
0.104	2637.5	0.758

Table A.53 – Acceleration of the base of mechanism 7 (m/s^2).

	EC8	NSCE-02	Deterministic	Probabilistic Tr=475	Probabilistic Tr=975
Soil	0.294	0.326	0.520	0.706	0.785
Structure	-	-	-	-	-
Safety (linear analysis)	Verified	Verified	Verified	Verified	Not verified

Table A.54 – Values of ultimate displacement and secant period of the mechanism 7.

d_0^* (m)	d_u^* (m)	T_s (s)
1.981	0.792	4.43

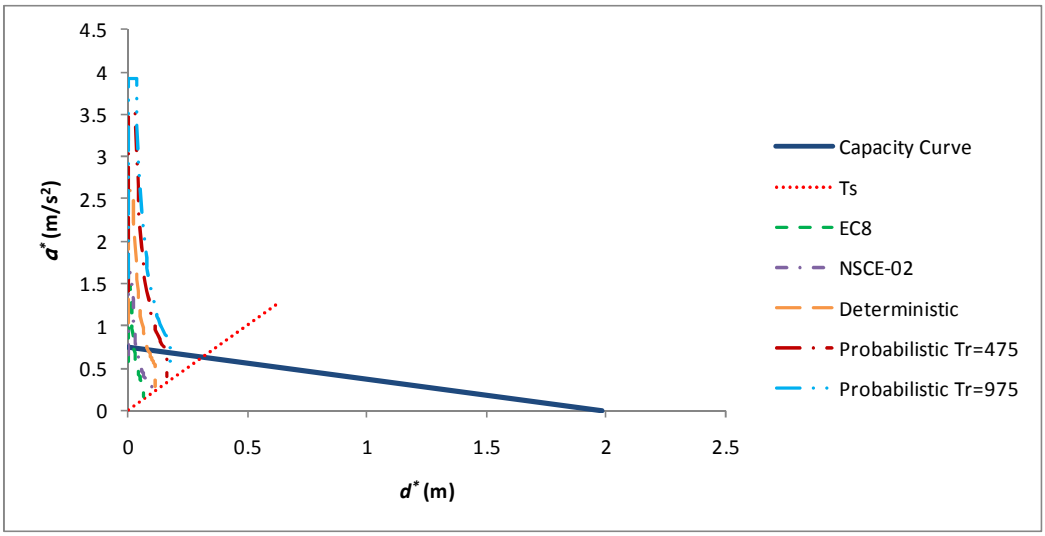

Figure A.23 – Capacity curve and demand spectrums of mechanism 7.

Table A.55 – Spectral response in terms of displacements of mechanism 7 (m).

	EC8	NSCE-02	Deterministic	Probabilistic Tr=475	Probabilistic Tr=975
Soil	0.067	0.117	0.119	0.161	0.179
Structure	-	-	-	-	-
Safety (nonlinear analysis)	Verified	Verified	Verified	Verified	Verified
Damage level	D2 or lower	D2 or lower	D2 or lower	D2 or lower	D2 or lower

- **Mechanism 8**

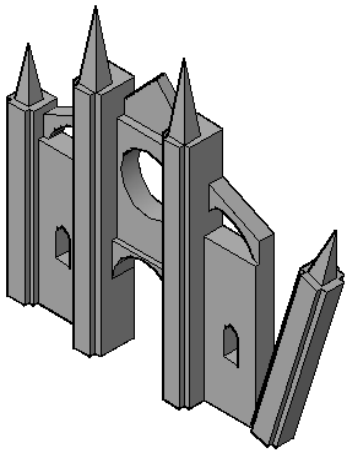

Figure A.24 – Mechanism 8.

Table A.56 – Values of geometrical parameters of mechanism 8.

Z (m)	H (m)	b (m)	H_{TOT} (m)	Volume (m^3)
0	47.74	6.14	64.52	1232.1

Table A.57 – Forces on mechanism 8.

	Force (kN)	Point of application	
		x (m)	y (m)
P_1	25874.3	2.00	19.10

Table A.58 – Value of spectral acceleration corresponding to the activation of the mechanism 8.

α_0	M^* (ton)	a_0^* (m/s^2)
0.105	2637.5	0.760

Table A.59 – Acceleration of the base of mechanism 8 (m/s^2).

	EC8	NSCE-02	Deterministic	Probabilistic Tr=475	Probabilistic Tr=975
Soil	0.294	0.326	0.520	0.706	0.785
Structure	-	-	-	-	-
Safety (linear analysis)	Verified	Verified	Verified	Verified	Not verified

Table A.60 – Values of ultimate displacement and secant period of the mechanism 8.

d_0^* (m)	d_u^* (m)	T_s (s)
1.986	0.794	4.43

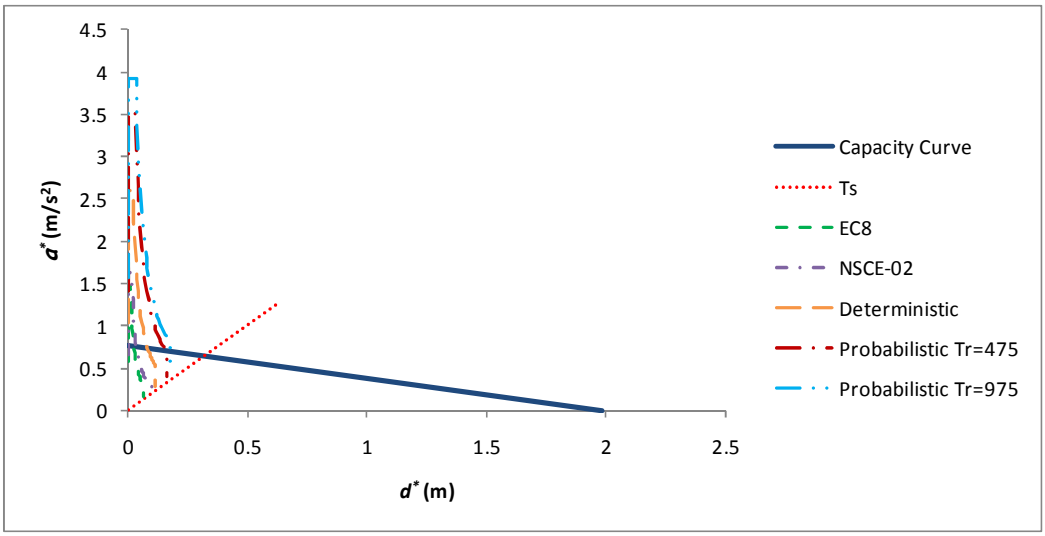

Figure A.25 – Capacity curve and demand spectrums of mechanism 8.

Table A.61 – Spectral response in terms of displacements of mechanism 8 (m).

	EC8	NSCE-02	Deterministic	Probabilistic Tr=475	Probabilistic Tr=975
Soil	0.067	0.117	0.119	0.161	0.179
Structure	-	-	-	-	-
Safety (nonlinear analysis)	Verified	Verified	Verified	Verified	Verified
Damage level	D2 or lower	D2 or lower	D2 or lower	D2 or lower	D2 or lower

- **Mechanism 10**

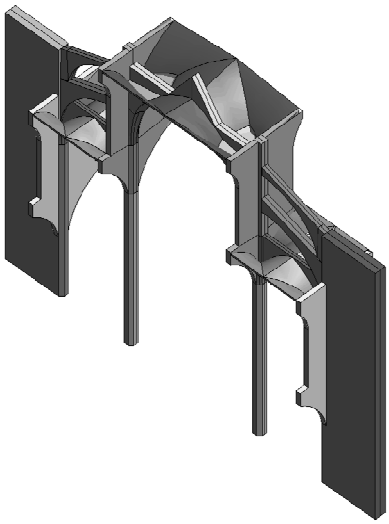

Figure A.26 – Modelling of the macroelement corresponding to the transept by Martinez (2007).

Table A.62 – Values of the bilinear capacity curve of the typical bay obtained by Martinez (2007).

Yielding point		Ultimate point	
d_y (m)	a_y (g)	d_u (m)	a_u (m)
0.021	0.150	0.521	0.190

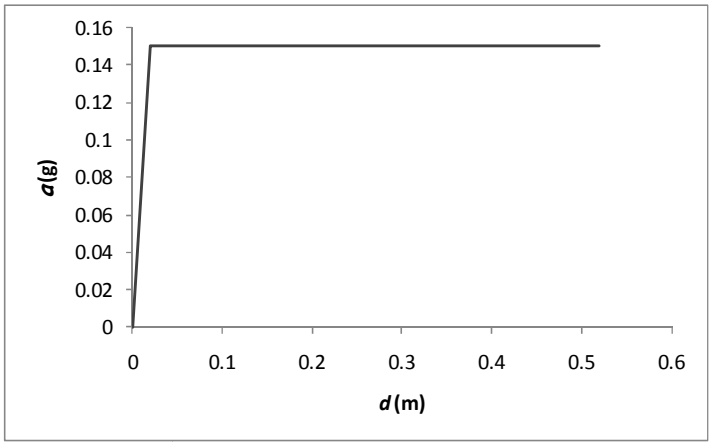

Figure A.27 – Bilinear capacity curve of the mechanism 10 SDOF equivalent system.

Table A.63 – Values of elastic spectral responses of mechanism 10.

	EC8	NSCE-02	Deterministic	Probabilistic Tr=475	Probabilistic Tr=975
S_{de} (m)	0.017	0.020	0.030	0.040	0.044
S_{ae} (g)	0.120	0.142	0.212	0.288	0.320

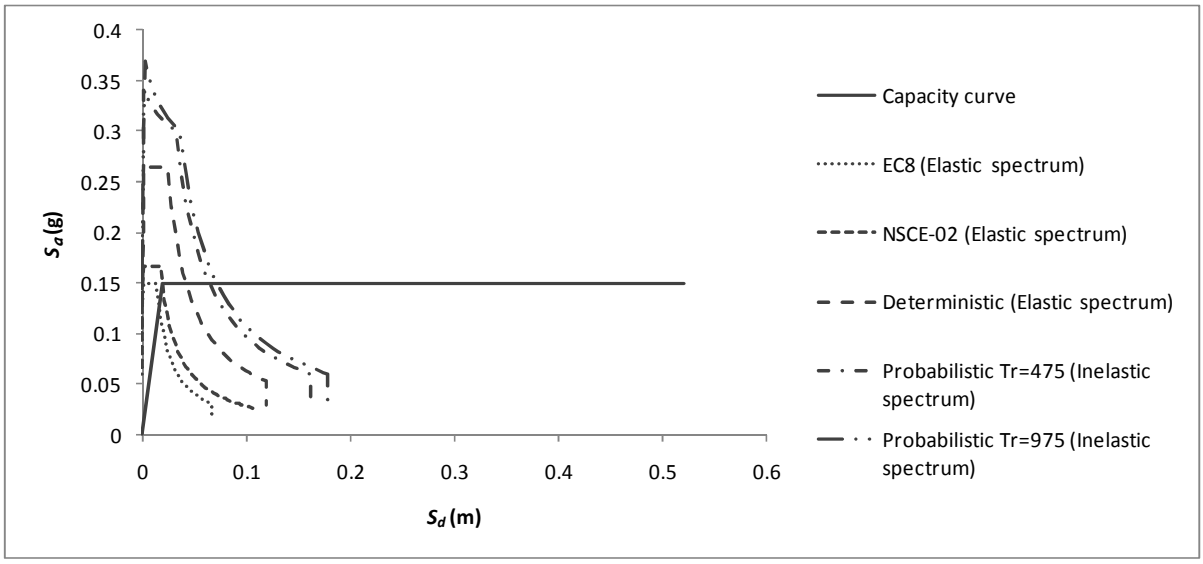

Figure A.28 – Intersection of the bilinear capacity curve of mechanism 10 with the inelastic demand spectrums.

Table A.64 – Safety verification and damage levels of the mechanism 10.

	EC8	NSCE-02	Deterministic	Probabilistic Tr=475	Probabilistic Tr=975
S_d (m)	0.017	0.020	0.030	0.040	0.045
d_u (m)	0.521	0.521	0.521	0.521	0.521
Safety verification	Verified	Verified	Verified	Verified	Verified
Damage level	D1	D1	D2	D2	D2

- **Mechanism 12**

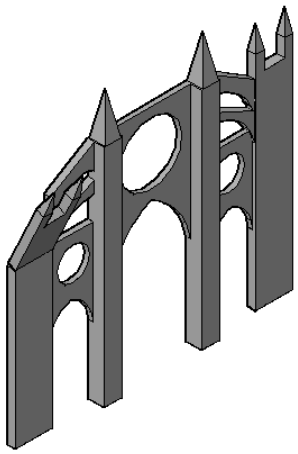

Figure A.29 – Mechanism 12.

Table A.65 – Values of geometrical parameters of mechanism 12.

Z (m)	H (m)	b (m)	H_{TOT} (m)	Volume (m^3)
29.8777	17.2703	7.0405	51.6706	126.0

Table A.66 – Forces on mechanism 12.

	Force (kN)	Point of application	
		x (m)	y (m)
P_1	2646.9	0.68	6.05

Table A.67 – Value of spectral acceleration corresponding to the activation of the mechanism 12.

α_0	M^* (ton)	a_0^* (m/s^2)
0.113	269.8	0.818

Table A.68 – Acceleration of the base of mechanism 12 (m/s^2).

	EC8	NSCE-02	Deterministic	Probabilistic Tr=475	Probabilistic Tr=975
Soil	0.294	0.326	0.520	0.706	0.785
Structure	0.199	0.236	0.352	0.479	0.532
Safety (linear analysis)	Verified	Verified	Verified	Verified	Verified

Table A.69 – Values of ultimate displacement and secant period of the mechanism 12.

d_0^* (m)	d_u^* (m)	T_s (s)
0.676	0.271	2.49

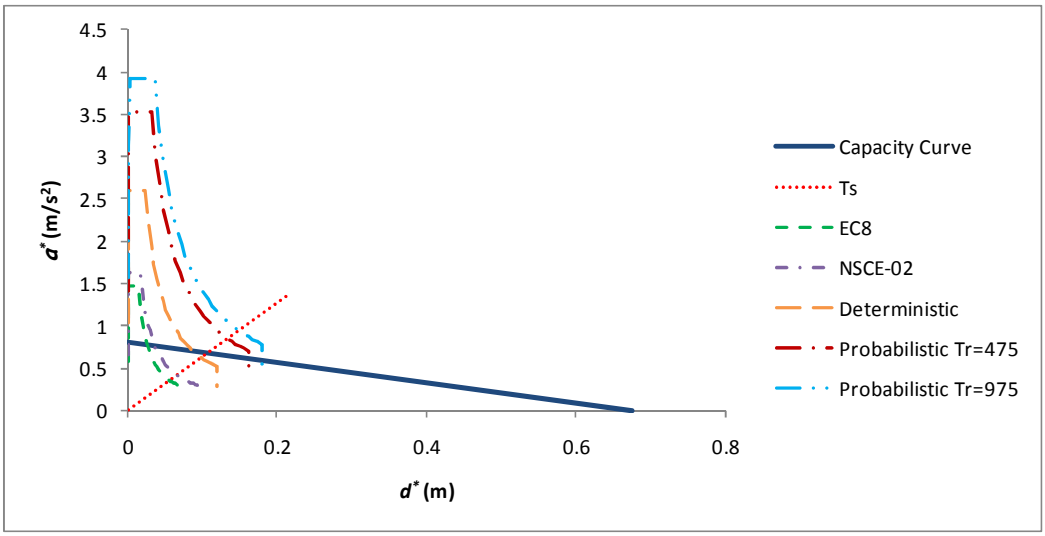

Figure A.30 – Capacity curve and demand spectrums of mechanism 12.

Table A.70 – Spectral response in terms of displacements of mechanism 12 (m).

	EC8	NSCE-02	Deterministic	Probabilistic Tr=475	Probabilistic Tr=975
Soil	0.056	0.066	0.099	0.134	0.149
Structure	0.065	0.077	0.115	0.156	0.173
Safety (nonlinear analysis)	Verified	Verified	Verified	Verified	Verified
Damage level	D2 or lower	D2 or lower	D3	D3	D4

- **Mechanism 13**

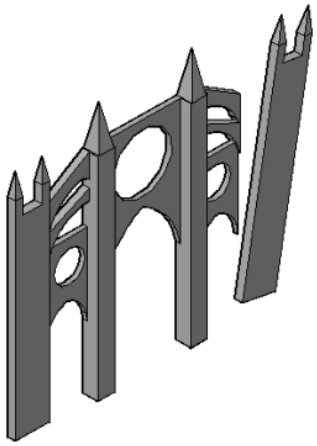

Figure A.31 – Mechanism 13.

Table A.71 – Values of geometrical parameters of mechanism 13.

Z (m)	H (m)	b (m)	H_{TOT} (m)	Volume (m^3)
0	47.148	1.5491	51.6706	451.9

Table A.72 – Forces on mechanism 13.

	Force (kN)	Point of application	
		x (m)	y (m)
P_1	9490.0	1.96	20.79
N_1	195.0	2.98	22.15
N_{1H}	65.0	-	24.35

Table A.73 – Value of spectral acceleration corresponding to the activation of the mechanism 13.

α_0	M^* (ton)	a_0^* (m/s^2)
0.094	987.2	0.685

Table A.74 – Acceleration of the base of mechanism 13 (m/s^2).

	EC8	NSCE-02	Deterministic	Probabilistic Tr=475	Probabilistic Tr=975
Soil	0.294	0.326	0.520	0.706	0.785
Structure	-	-	-	-	-
Safety (linear analysis)	Verified	Verified	Verified	Not verified	Not verified

Table A.75 – Values of ultimate displacement and secant period of the mechanism 13.

d_0^* (m)	d_u^* (m)	T_s (s)
1.806	0.722	4.45

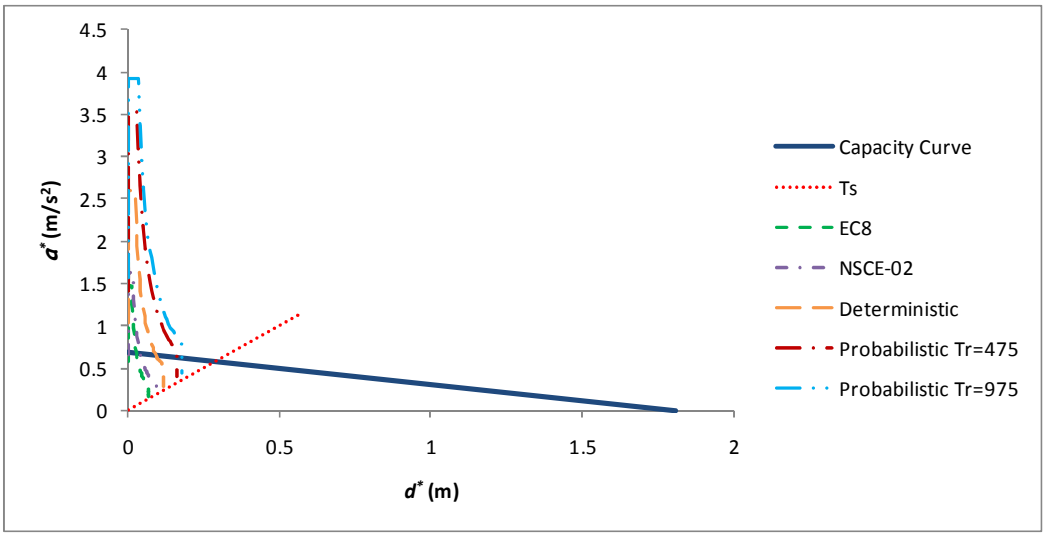

Figure A.32 – Capacity curve and demand spectrums of mechanism 13.

Table A.76 – Spectral response in terms of displacements of mechanism 13 (m).

	EC8	NSCE-02	Deterministic	Probabilistic Tr=475	Probabilistic Tr=975
Soil	0.067	0.118	0.119	0.161	0.179
Structure	-	-	-	-	-
Safety (nonlinear analysis)	Verified	Verified	Verified	Verified	Verified
Damage level	D2 or lower	D2 or lower	D2 or lower	D2 or lower	D2 or lower

- **Mechanism 14**

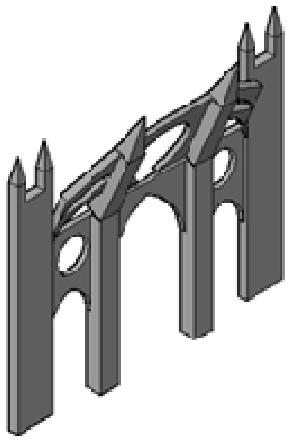

Figure A.33 – Mechanism 14.

Table A.77 – Values of geometrical parameters of mechanism 14.

Z (m)	H (m)	b (m)	H_{TOT} (m)	Volume (m^3)
29.8777	21.7929	39.3152	51.6706	530.2

Table A.78 – Forces on mechanism 14.

	Force (kN)	Point of application	
		x (m)	y (m)
P_1	11135.1	1.80	7.87
N_1	778.3	2.96	0.72
N_{1H}	198.9	-	4.01

Table A.79 – Value of spectral acceleration corresponding to the activation of the mechanism 14.

α_0	M^* (ton)	a_0^* (m/s^2)
0.251	1149.0	1.926

Table A.80 – Acceleration of the base of mechanism 14 (m/s^2).

	EC8	NSCE-02	Deterministic	Probabilistic Tr=475	Probabilistic Tr=975
Soil	0.294	0.326	0.520	0.706	0.785
Structure	0.199	0.236	0.352	0.479	0.532
Safety (linear analysis)	Verified	Verified	Verified	Verified	Verified

Table A.81 – Values of ultimate displacement and secant period of the mechanism 14.

d_0^* (m)	d_u^* (m)	T_s (s)
1.856	0.742	2.69

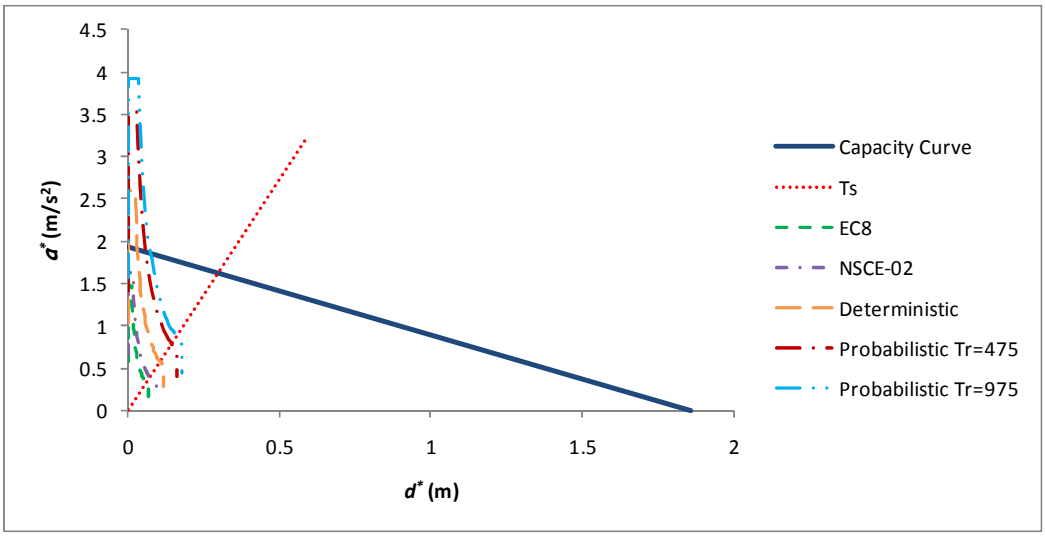

Figure A.34 – Capacity curve and demand spectrums of mechanism 14.

Table A.82 – Spectral response in terms of displacements of mechanism 14 (m).

	EC8	NSCE-02	Deterministic	Probabilistic Tr=475	Probabilistic Tr=975
Soil	0.060	0.071	0.106	0.144	0.161
Structure	0.065	0.077	0.115	0.157	0.174
Safety (nonlinear analysis)	Verified	Verified	Verified	Verified	Verified
Damage level	D2 or lower	D2 or lower	D2 or lower	D2 or lower	D2 or lower

ANNEX B: STRENGTHENING CALCULATIONS

B.1 Mechanism 5

The proposal for a solution to strengthen local mechanism 5 is to adopt the solution schematized in Figure B.1, so that the stabilizing vertical produced by the prestress reduces to the damage to a value corresponding to damage level D2.

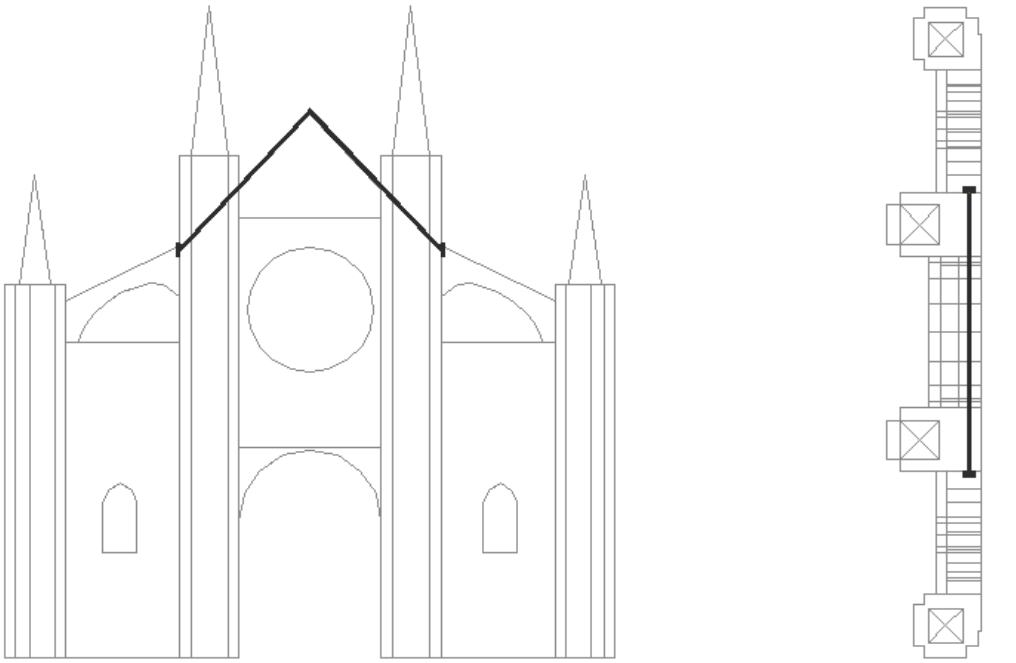

(a) Front view (b) Upper view

Figure B.1 – Strengthening solution for mechanism 5.

The introduction of a vertical stabilizing force, designated as *V*, has influence in both the acceleration that activates the mechanism as in the displacement for which the horizontal multiplier is equal to zero. The first step must be to define the position of the force with respect to the rotation point. It should be noticed that the thickness *t* remains the same. In Table B.1 it is presented the horizontal and vertical distances of the point of application of the forces to the rotation point, designated as distances x_V and y_V, respectively.

Table B.1 – Distance between the rotation point and the point of application of the vertical force *V*.

x_V (m)	y_V (m)
0.96	9.95

Using the force P_1 and the distance x_{P1} defined in Annex A for mechanism 5, the coefficient that activates the mechanism α_0 is obtained by:

$$M_S = M_R \Leftrightarrow P_1 \cdot x_{P_1} + V \cdot x_V = \alpha_0 \cdot \left(P_1 \cdot y_{P_1}\right)$$

Then, the same procedure presented in Annex A is applied in order to obtain the corresponding the spectral acceleration a_0^*.

To determine the finite rotation θ_0 for which the block is in equilibrium without any horizontal acceleration, it is necessary to define the angle β_V and the radius R_V of the vertical force V (as defined in Annex A in Figure A.4), that are presented on Table B.2.

Table B.2 – Values of the parameters for calculation of the finite rotation θ_0.

β_V (rad)	R_V (m)
1.47	10.00

Being the stabilizing moment M_S equal to the destabilizing moment M_R, the rotation θ may be defined as function of α. Computing α equal to 0, it is possible to obtain the value of the rotation θ_0:

$$M_S = M_R \Leftrightarrow P_1 \cdot R_{P_1} \cdot \cos\left(\beta_{P_1} + \theta\right) + V \cdot R_V \cdot \cos\left(\beta_V + \theta\right) = \alpha \cdot P_1 \cdot R_{P_1} \cdot \cos\left(\beta_{P_1} + \theta\right)$$

The next steps are the same that are presented in Annex A for the mechanisms without strengthening.

Applying an iterative procedure in order to find the lowest force V that results in a damage level D2 or in a demand in terms of displacements lower than 1/8 of $d_{k,0}$., a value equal to 6435kN in obtained. The corresponding capacity curve, the secant period T_s and the demand spectrum corresponding to the probabilistic approach with a return period of 975 years are presented in Figure B.2. In the same figure is also possible to compare the obtained capacity curve with the one corresponding to the situation with no strengthening.

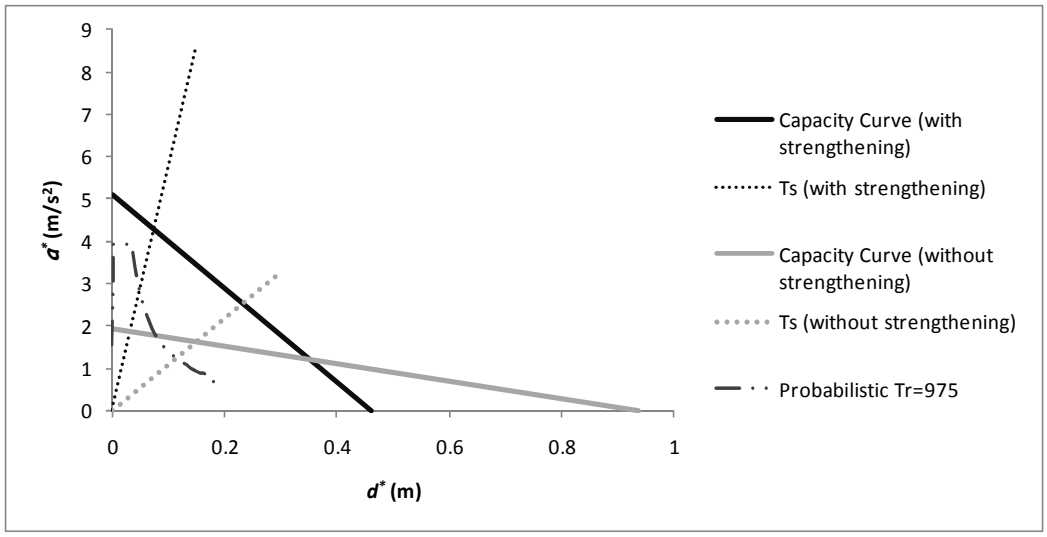

Figure B.2 – Effect of the first solution for strengthening of mechanism 5 in the capacity curve.

The damage level and the value of the displacement demand are presented on Table B.3, for both the strengthened and the not strengthened case. In the same table, the displacement demand is compared with the displacement d_0^*.

Table B.3 – Demand displacement and damage level of mechanism 5 with the solution proposed for strengthening.

	$d_{u\,min}^*$ (m)	d_0^* (m)	$d_{u\,min}^*/d_0^*$ (m)	Damage level
Not strengthened	0.221	0.936	0.236	D3
Strengthened	0.058	0.460	0.125	D2 or lower

Considering the vertical force V in the direction of the tendon (the angle between them is equal to 43.3º) and considering and effective force equal to 60% of the prestress, the prestress force F needed to reduce the damage level to D2 is equal to 14736.7kN. Considering the use of tendons from the Spanish company MK4 with a diameter equal to 15.2mm (rupture force F_{pK} equal to 260kN), 57 tendons are needed. They have to be placed on a width equal to 2.07m (the thickness of the overturning block), which means that the spacing between the tendons is equal to 3.6cm centre to centre.

B.2 Mechanism 12

The proposal for a solution to strengthen local mechanism 12 is to place tendons like presented in the schematic drawing presented on Figure B.3. The horizontal friction force produced by the prestressed tendons, designated as force *T*, due to the compression of the connection between the buttresses and the upper flying arches is expected to reduce the damage level to D2.

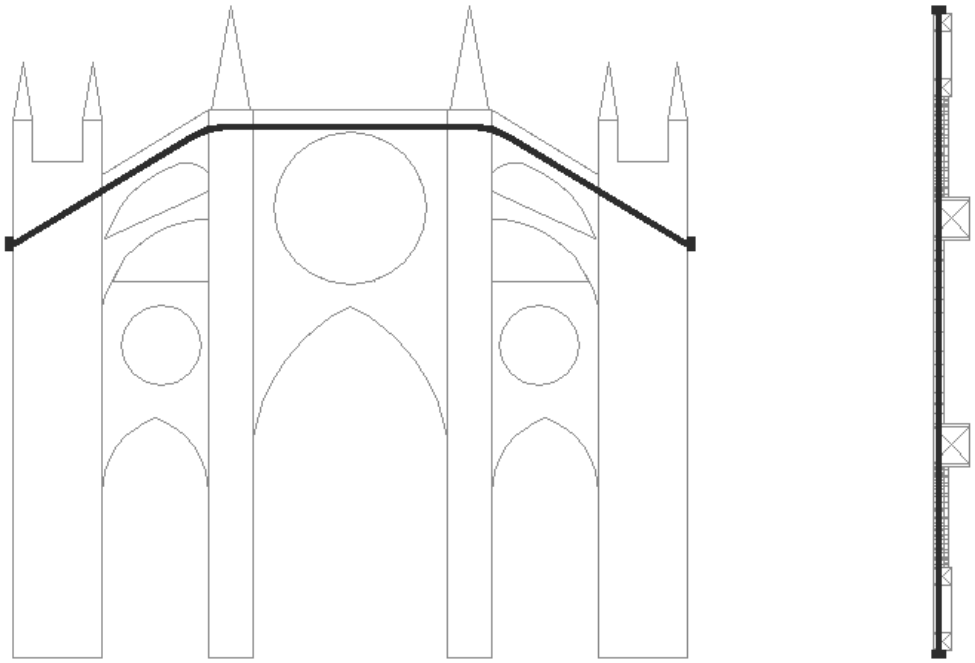

(a) Front view (b) Upper view

Figure B.3 – Strengthening solution for mechanism 12.

Adopting the same iterative procedure presented above for mechanism 5 in order to find the lowest force *T* that results in a damage level D2, a value equal to 270kN is obtained.

In Table B.4 it is presented the horizontal and vertical distances of the point of application of the forces to the rotation point, designated as distances x_T and y_T, respectively.

Table B.4 – Distance between the rotation point and the point of application of the vertical force *T*.

x_T (m)	y_T (m)
0.52	7.16

Using the force P_1 and the distance x_{P1} defined in Annex A for mechanism 12, the coefficient that activates the mechanism α_0 is obtained by:

$$M_S = M_R \Leftrightarrow P_1 \cdot x_{P_1} + T \cdot x_T = \alpha_0 \cdot \left(P_1 \cdot y_{P_1}\right) \Leftrightarrow \alpha_0 = 0.233$$

Then, the same procedure presented in Annex A is applied in order to obtain the corresponding the spectral acceleration a_0^*, that in this case is equal results equal to 1.695m/s^2.

To determine the finite rotation θ_0 for which the block is in equilibrium without any horizontal acceleration, it is necessary to define the angle β_T and the radius R_T of the horizontal force T (as defined in Annex A in Figure A.4), that are presented on Table B.5.

Table B.5 – Values of the parameters for calculation of the finite rotation θ_0.

θ_T (rad)	R_T (m)
1.50	7.18

Computing α equal to 0 in the equation obtained when the stabilizing and destabilizing moments are equalized, it is possible to obtain the value of the rotation θ_0:

$$M_S = M_R \Leftrightarrow P_1 \cdot R_{P_1} \cdot \cos(\beta_{P_1} + \theta) + T \cdot R_T \cdot \cos(\beta_T + \theta) = \alpha \cdot P_1 \cdot R_{P_1} \cdot \cos(\beta_{P_1} + \theta)$$
$$\Leftrightarrow \theta_0 = 0.230\,rad$$

The corresponding capacity curve, the secant period T_s and the demand spectrum corresponding to the probabilistic approach with a return period of 975 years are presented in Figure B.4. In the same figure is also possible to compare the obtained capacity curve with the one corresponding to the situation with no strengthening.

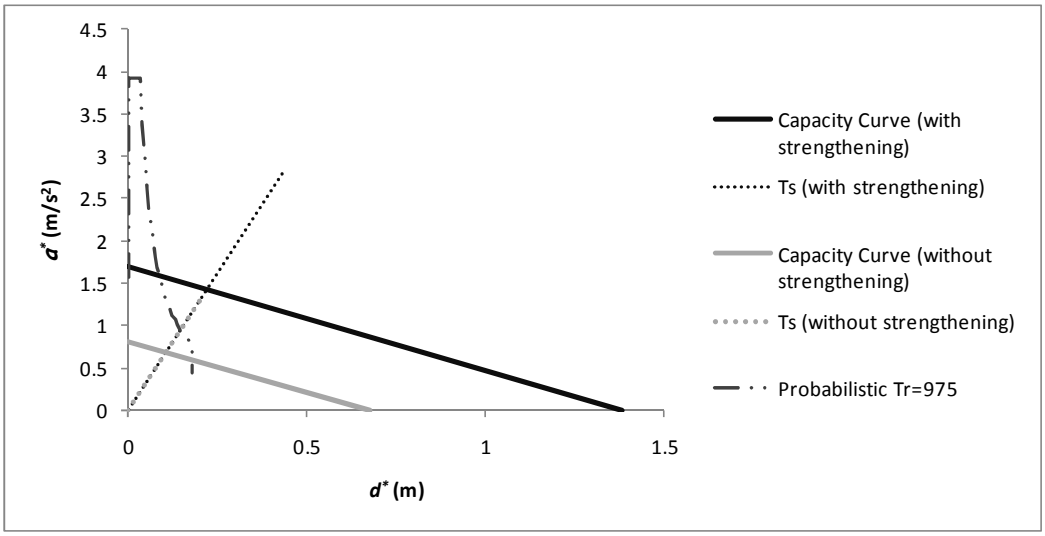

Figure B.4 – Effect of the first solution for strengthening of mechanism 12 in the capacity curve.

The damage level and the value of the displacement demand are presented on Table B.6, for both the strengthened and the not strengthened case. In the same table, the displacement demand is compared with the displacement d_0^*.

Table B.6 – Demand displacement and damage level of mechanism 12 with the solution proposed for strengthening.

	$d_u^*{}_{min}$ (m)	d_0^* (m)	$d_u^*{}_{min}/d_0^*$ (m)	Damage level
Not strengthened	0.173	0.676	0.256	D4
Strengthened	0.173	1.384	0.125	D2 or lower

To calculate the effective force of the prestress, a friction coefficient μ equal to 0.6 is considered. It is also considered that the effective force is 60% of the prestress applied to the tendons, which leads to a prestress force F equal to 750kN. Using 15.2mm diameter tendons from the Spanish company MK4, 3 tendons are needed.